E-20-E45
#1

AN INVESTIGATION OF FIBER REINFORCED RECYCLED PLASTIC/COMPOSITE RAILROAD CROSSTIES

Georgia Institute of Technology
September, 2001

TABLE OF CONTENTS

LIST OF FIGURES

LIST OF TABLES

CHAPTER I

INTRODUCTION

Purpose and Objectives

The purpose of this research was to examine experimentally the stiffness of recycled plastic beams reinforced with fiber reinforced composites and to determine experimentally the flexural modulus of elasticity of recycled plastics using small scale flexural tests. The specific objectives of this thesis included:

1) establishing the effectiveness of two different diameters of E-glass fiber reinforcing bars in full-scale, Seatimber® recycled plastic ties;

2) finding the modulus of elasticity of different formulations of recycled plastics using small scale flexural tests;

3) establishing the effectiveness of externally applied E-glass, carbon, and stainless steel fabrics in reinforcing recycled plastic beams; and

4) confirming the use of simple strength of material formulas for predicting the flexural behavior of recycled plastic beams.

Scope

Ninety-six unreinforced small-scale beams, of which 94 were 1.5-inch square and two were 4.25-inch square, were made of different formulations of recycled plastics. Each beam was tested in a three point bending configuration to determine its flexural stiffness and its flexural modulus of elasticity. Eight small-scale recycled plastic beams (1.5-inch square) were reinforced: two were externally reinforced with E-glass FRP fabric tape, two were externally reinforced with carbon FRP fabric tape, two were externally reinforced with stainless steel FRP fabric tape, and two were internally reinforced with E-glass tape.

Fourteen full-scale beams were tested in three-point bending configuration. One wood tie was tested for comparison. Three beams were recycled plastic Duratie® crossties: two were tested without reinforcement, and one was reinforced with externally applied carbon fiber reinforced polymer fabric. Eight beams were recycled plastic Seatimber® ties: two were unreinforced, two were reinforced with 1.25-inch diameter E-glass fiber bars, three were reinforced with 0.5-inch diameter E-glass fiber bars, and one was reinforced with externally applied carbon fiber reinforced polymer fabric.

The experimental results were compared with those obtained from a simple transformed section bending analysis.

Background

Wood has been the most commonly used material for railway crossties in North America due to the large abundance of trees and forests. More than 99.7% of crossties are wood (Chopin, 1983). The future use of wood crossties is uncertain due to mounting environmental concerns. The wood crosstie is impregnated with creosote to increase its service-life, but creosote is harmful to the environment. Creosote is carcinogenic and can leech into the ground water table and contaminate ground water (Anonymous, 1995). Every year there are over 12 million wooden crossties replaced with an estimated cost of 500 million dollars (Zarembski, 1989). The typical life span of the most common impregnated oak timber is 25 years (Profillidis, 1995).

The first railways were established in the seventeenth and eighteenth century in quarries, where trains of carts would be pulled by horses over wooden or stone rails (Bonnet, 1996). In the nineteenth century, steel rails supported by wooden cross ties (crossties) made up the typical railway. The railroad crosstie is designed to distribute the load from the steel rails to the ground (ballast). The ties also maintain the correct gage length between the rails and resist lateral loads. Between the rails and the crossties are tie plates. The tie plates reduce both the pressure of the rail load on the crosstie and mechanical wear. Fasteners are incorporated with the tie plates to hold the rail at the correct gauge distance and to resist lateral loadings in railway curves. The crossties need to resist the pull out and lateral shifting of the fastener. A typical railway cross section is shown in Figure 1.1.

While wood has been the most common crosstie material, concrete and steel crossties have been used in railways, and new polymeric based crossties are currently being developed and tested. Wood, concrete, steel and polymeric crossties are reviewed in the following sections.

All cross section and mechanical properties which could be found in the literature for wood, concrete, and steel crossties as well as some of the polymeric based crossties are shown in Table 1.1.

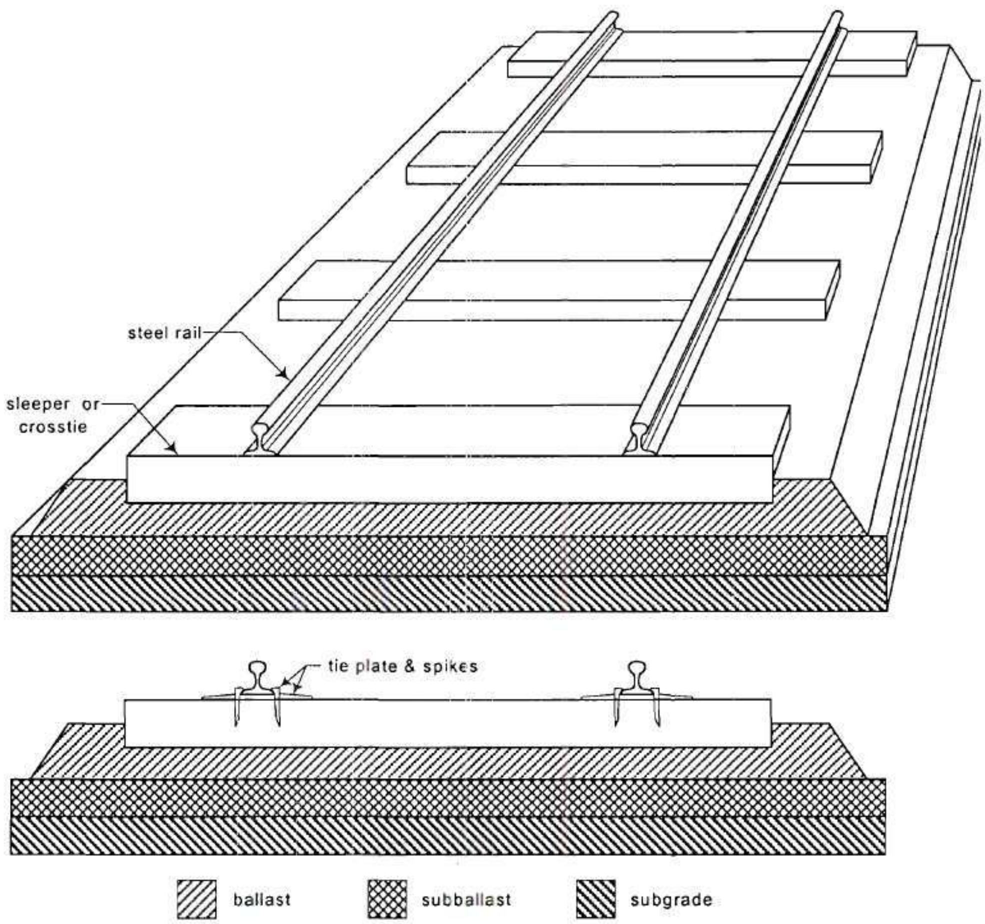

Figure 1.1: Typical railway cross section

Table 1.1: Railroad tie properties

Railroad Tie Type	Cross sectional Area (in^2)	weight (lbs) 8.5ft long	$I_z^{(a)}$ (in^4)	$E_a^{(b)}$ (ksi)	$D_z^{(c)}$ (kip-in^2)
Wood[(d)]	57.38	250[(e)]	217.85	1,679	365,800
Parallam® PSL wood tie	63.0	152	257.25	2,000	514,500
Azobe wood tie[(f)]	63.0	260	257.25	2,466	634,400
Concrete [(g)]	77.3[(h)]	560[(i)]	225[(h)]	3,120[(j)]	703,500
T&TS - HH 14 steel tie	7.84	227	18.80	29,000	545,200
NARSTCO H 14 steel tie	7.91	229	19.06	29,000	552,900
Primix tie	63.0	320	257.25	200 - 250	51,500 - 64,300
Duratie®[(k)]	63.0 +/-0.0156		257.25	>300[(l)]	>77,200
Tested Duratie®[(m)]	67.18		299.37	261.5	78,300

a. I_z is the moment if inertia about the z-axis
b. E_a is the flexural modulus of elasticity
c. D_z is the stiffness about the z-axis (weak axis)
d. Values are from Chapter 3 specimen 1 data
e. (Chopin, 1983)
f. Properties based on a 7 inch x 9 inch cross section (Springfellow, 2001).
g. Data from typical concrete monoblock shown in Figure 1.3.
h. Based on a 175 mm x 210 mm cross section
i. Based on average cross section of 193 mm x 210 mm w_c = 145 pcf
j. $E_c = 57000\sqrt{f'_c}$, where f'_c=3000 psi
k. Information from U.S. Plastic Lumber Corp.
l. Tested @ a 6 foot span.
m. Values are from Chapter 3 specimens 2 & 3 data.

Wood Crossties

Douglas fir and oak are the typical species of wood used for timber crossties. Before a timber can be used as a railway tie, it is milled to the correct dimensions, dried, and impregnated with a petroleum based preservative such as coal tar creosote. The tested wood specimen was a 9-inch x 7-inch red oak wood railroad tie having dressed dimensions of 8.5 inches x 6.75 inches as shown in Figure 1.2.

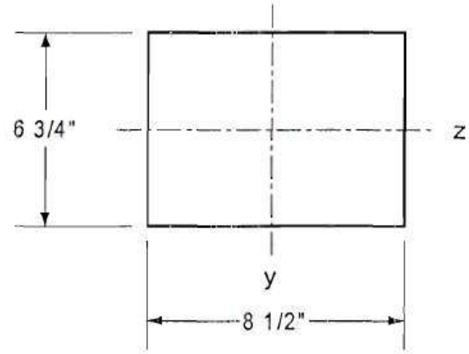

Figure 1.2: Typical 7 inches x 9 inches wood cross section

Wood deteriorates while in service by splitting. The ends of the wood crossties dry faster than the rest of the crosstie. This causes the crosstie's ends to split early in the service life. The split ends allow moisture to infiltrate the crosstie. Since the creosote does not penetrate throughout the whole crosstie, moisture on the interior of the crosstie accelerates decay.

Mechanical damage of the crosstie also occurs while the crosstie is in service by means of rail plate cutting and spike killing. Rail plate cutting occurs when the edges of the rail plate score into the wood from the dynamic loads of the passing train and from thermal expansion and contraction. Today's rail plates do reduce this abrasive action but do not eliminate the problem. Spike killing, which is the deterioration of a crosstie at the location of a removed spike, occurs when the spikes are unable to hold the steel rail in place adequately. A hole, left from a removed spike, collects water and accelerates the decay of the crosstie. Spike killing can be reduced if the holes are specified to be prebored before the creosote process. This preboring of the holes allows the wood preservative to protect the holes from decay when a spike is replaced. These, and many other innovations have reduced the mechanical deterioration of the wood cross tie. However, the life span of the wood cross tie is still the one of the shortest of all railway crossties.

There are more dense woods, such as Azobé, which is a natural wood from moist forests and freshwater swamps. Its naturally moist habitat produces a higher density wood. Azobé has a density of 70 pcf (Springfellow, 2001), which is over twice the density of the common ash, red oak, and douglas fir. It also has a typical gross weight of 260 lbs for an 8.5-foot crosstie. The modulus of elasticity in compression is 2,466 ksi, (Springfellow, 2001). The service-life of a non-impregnated Azobé tie is 40 years and 45 years for the impregnated Azobé tie (Profillidis, 1995).

The 'Parallam® PSL'[1] tie is another type of wood crosstie which uses recycled wood or wood chips in its manufacture. This tie is a composite wood tie made similar to that of a glued laminated beam. It is typically used for wooden rail bridges and switches because of the ability to produce longer pieces. These pieces are straight and true along the length of the tie. The modulus of elasticity is 2,000 ksi and the tie has a density of 41 pcf. Therefore, a 7 inches x 9 inches x 8.5 foot crosstie would weigh 152 lbs. (Trus Jois MacMillan®, 1998)

Concrete Ties

There are two major types of concrete ties: the monoblock tie and the twin block tie. The monoblock tie was first constructed with conventional reinforcement. After years of improvements the concrete monoblock crosstie is now prestressed. The prestressed concrete tie should never crack in tension. The typical cross section dimensions of a British monoblock is shown in Figure 1.3. The gross weight of a monoblock tie is over 600 lbs.

---

1. Parallam® is a registered trademark of Trus Joist MacMillian a limited partnership, Boise, Idaho.

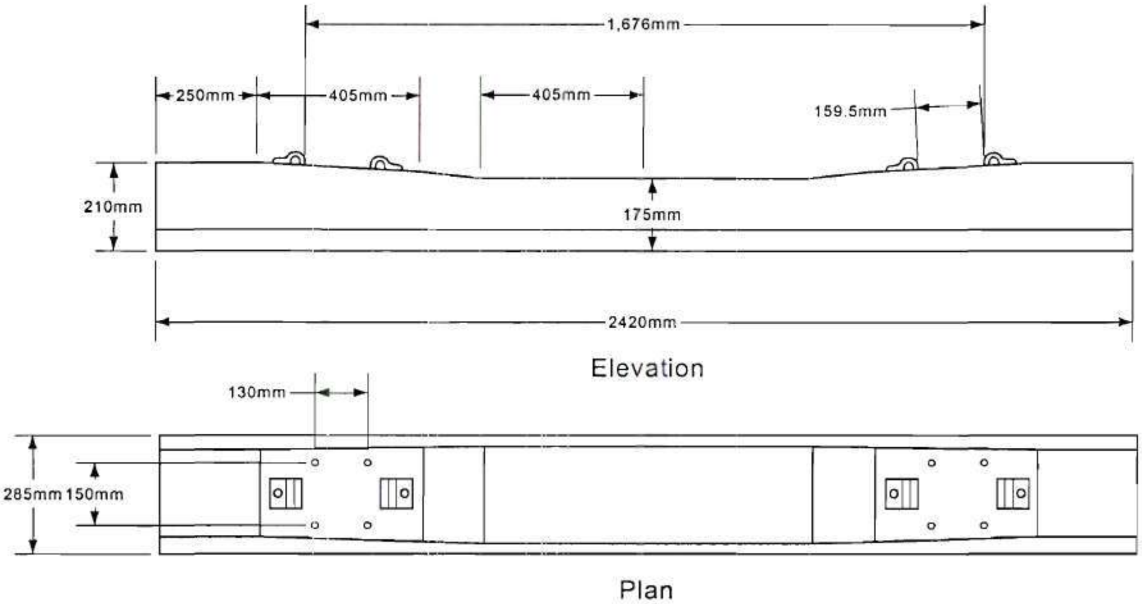

Figure 1.3: British railways concrete monoblock crosstie (Profillidis, 1995)

The twin block tie is made up of two conventionally reinforced concrete blocks connected by a steel bar, which is embedded into both blocks. The twin block tie weighs 150 lbs. This is 450 lbs lighter than the monoblock concrete tie. The dimensions of a U31 French twin block tie are shown in Figure 1.4.

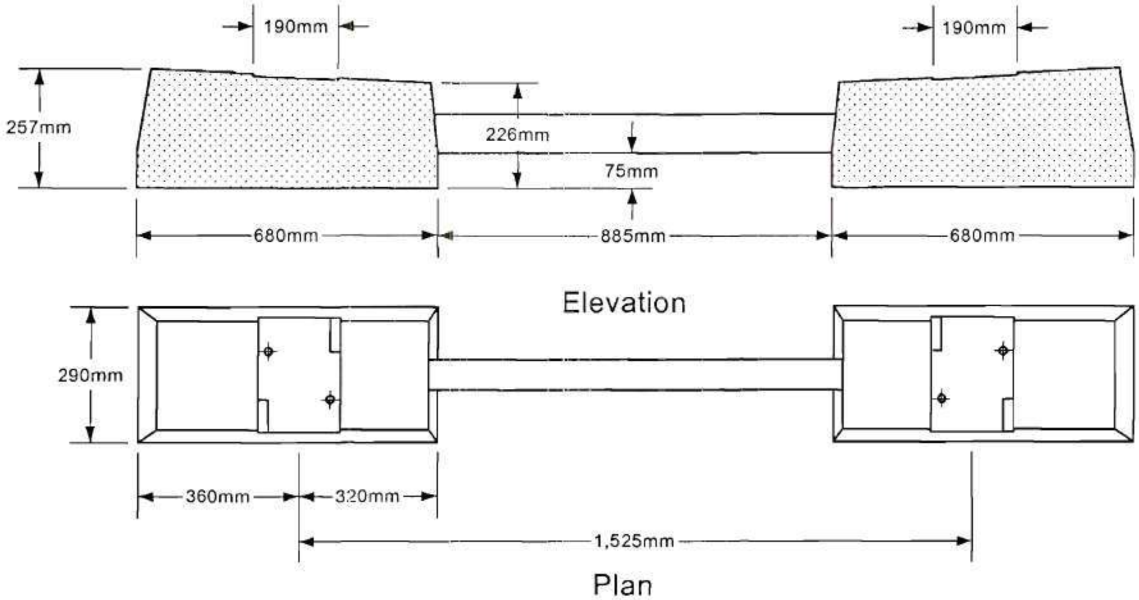

Figure 1.4: French railways concrete twin block cross tie U31 (Profillidis, 1995)

Concrete ties can be cost effective if installed in a new railway line where the most effective space can be used. Concrete ties have cracked and prematurely deteriorated not from the design, but from bad concrete mixes (Roe, 1996). The service life of a concrete tie can be 50 years (Roe, 1996). As for wood crosstie replacement, concrete crossties are not desired since wood ties are spaced closer. Another disadvantage of the concrete crossties are its high gross weight, which make placement difficult. The cast-in-place fasteners require low tolerances. The ballast material is also important to the performance of the concrete ties. A thicker ballast, with better mechanical characteristics than a wood crosstie, are required for a concrete crosstie (Pruase, 1978).

Steel Ties

Steel ties make-up only one percent of the ties used in the United States (Roe, 1996). Railways with steel cross ties are known to be very noisy. Steel cross ties are very light and would seem to be easier to place. However the geometry of the steel cross tie causes positioning difficulty, and the electrical conductivity of steel causes problems with railway track signaling. Steel ties are not desirable near industrial or coastal areas where the crossties are susceptible to sulfur attack and high corrosion. The maintenance of steel ties is also difficult. (Profillidis, 1995) Two commonly used steel crossties are the Tie & Track Systems (TT&S) and NARSTCO crossties described below.

Tie & Track Systems' Steel Railroad Tie

The steel HH14 Tie, available from Tie & Track Systems, TTS, shown in Figure 1.5, has a moment of inertia of 18.80 in^4 and a cross sectional area of 7.839 in^2, and the apparent stiffness (D_z=EI_z) of the HH14 steel tie is 545,200 k-in^2 (E = 29,000ksi). The section weight is 26.67 lbs per linear foot. Therefore, an 8.5-foot tie would weigh approximately 228 lbs. (TTS, 2001)

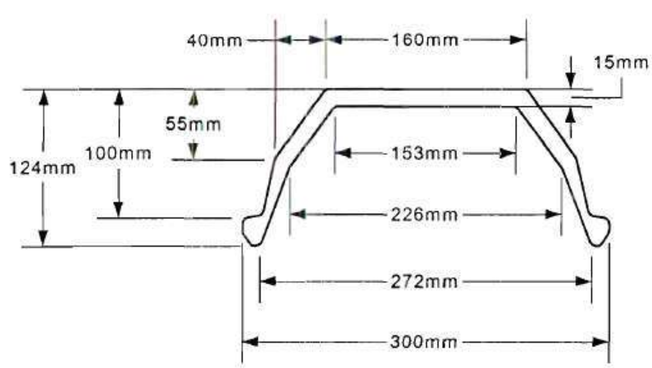

Figure 1.5: TTS steel railroad tie cross section

NARSTCO Steel Railroad Tie

The NARSTCO H14 steel tie has a moment of inertia of 19.06 in^4 and a cross sectional area of 7.919 in^2. The apparent stiffness ($D_z=EI_z$) of the H14 steel tie from NARSTCO is 552,869 k-in^2 (E = 29,000 ksi). The section weight is 26.941 lbs per linear foot. Therefore, an 8.5-foot tie would weigh approximately 229 lbs. Cross section dimensions could not be found for the NARSTO H14 but the H14 is very similar to the TTS HH 14 shown in Figure 1.5. (NARSTCO, 1996)

Polymeric Based Crossties

Polymeric based crossties are made from recycled and virgin plastics, as well as FRP composites. With the plastic/composite technology of today and the possibility of a FRP composite crosstie having a service-life twice that of a typical wood tie, the polymeric crosstie has generated considerable interest in the railway industry. Several current polymeric based ties are the following:

- Duratie® Crosstie (U.S. Plastic Lumber Corporation)
- Polywood Crosstie (Polywood Incorporated)
- Primix Crossties (Primix Corporation)
- TieTek Ties, North American Technologies Group Inc. (NATK)

A description of the polymeric crossties listed above is presented below.

'DURATIE®'

Since 1994, Rutgers University's Plastics and Composites Group, Earth Care product (US Plastic Lumber), Conrail, Norfolk Southern and the U.S. Army Corps of Engineers have been collaborating to develop and continue to study recycled plastic railway crossties. This alliance has tested recycled plastic crossties, installed plastic ties and is monitoring and adding more ties to in-use railways.

The plastic ties were tested under a four point bending configuration, with the distance between the two central loads spaced 6 inches and centered on a 60-inch span as shown in Figure 1.6. (Gillespie et al., 1997)

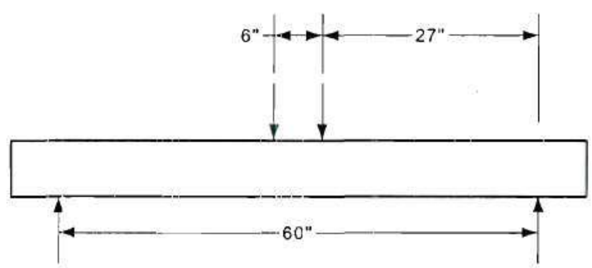

Figure 1.6: Elevation of Norfolk Southern bending test (Gillespie et al., 1997)

The results from this paper show the ultimate strength of the crossties greater than 4,000 psi (27.59 MPa) and flexural modulus greater than 300 ksi (2,068.97 MPa) (Nosker et al., 1998). The ultimate strength was calculated from an elementary strength of materials flexural approach.

Ten of the plastic Duratie® crossties were installed in October 1995 at Rose Yard in Altoona, Pennsylvania. No signs of weathering or damage were visible after 2 years and 13 million gross tons (MGT) at speeds less than 15 mph (Gillespie et al., 1997). The crossties were visually checked periodically, and six geometric measurements (see Figure 1.7) were monitored. As of 1997, not one measurement had changed (Nosker et al., 1998).

Ties also have been installed in 5 and 6 degree curves on higher speed rails of 40 mph and 35 mph, respectively. No damage or noticeable change has been seen (Nosker et al., 1998).

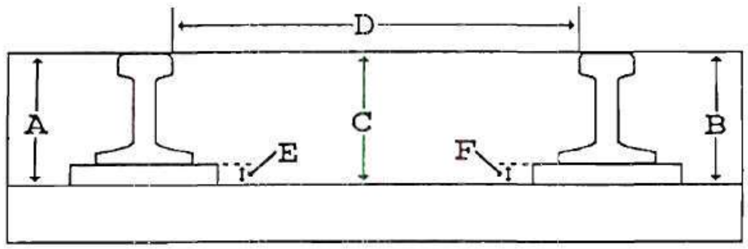

Figure 1.7: Six monitored Duratie® measurements (Nosker et al., 1998)

Polywood

Polywood Inc. manufactures a plastic crosstie, but no information was publicly available.

Primix

The Primix railroad tie is a composite railway tie with a reinforced concrete inner structural core that is encased with a high-density polyethylene and recycled rubber jacket (RT&S, 2000). An installed Primix tie is shown next to an existing wooden tie in Figure 1.8. The cross section of the Primix tie is 7 inches x 9 inches and the 8.5 foot tie weighs 320 lbs. The reported flexural modulus of elasticity was between 200 ksi and 250 ksi (Primix, 2001). Also, the Primix tie has been reported to have a service-life expectancy of 60 years. The ultimate strength of the Primix Crosstie tested under a 5 foot span was reported to be between 24 kips and 72 kips at 1 inch deflection. (Primix, 2001) The Primix cross section is shown in Figure 1.9. No technical data related to the tests performed were available in the literature.

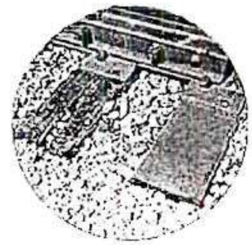

Figure 1.8: Installed Primix tie to the right of a wooden tie (Primix, 2001)

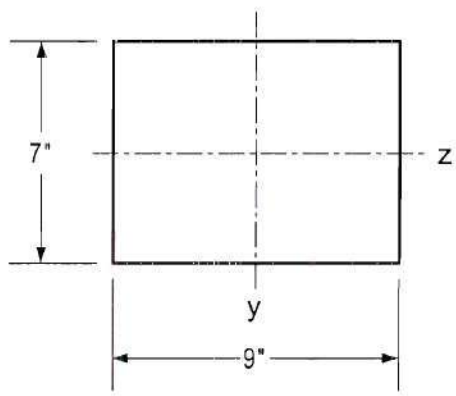

Figure 1.9: Primix tie cross section

TieTek

Research and development of the TieTek crosstie began in 1994. The crosstie is made from 75% recycled materials. Since the first installation in 1996, the manufacturer has installed over 3000 crossties. The TieTek tie can be spiked just like wood. The manufacture states that the TieTek tie will not check or split like wood, and is resilient to insects and decay. The TieTek can be installed using the same equipment used to handle wood ties, and can be incorporated along with existing wood ties. Also, the TieTek tie requires no environmental hazardous preservatives and hardwood trees are saved (NATK, 2001). Technical details concerning the performance of the TieTek crosstie were not available in the literature.

GFRP-Reinforced Wood Crosstie

At West Virginia University, Davalos et al. (1999) studied wood railway ties reinforced with glass fiber fabrics. There were four groups of ten samples. Each sample had the dimensions of 1.75 inches x 1.75 inches x 36 inches. Two of the four groups were not reinforced, with one group having a 12% moisture content (MC) and one with a 31% MC, which is considered saturated. The other two groups were reinforced externally with glass composites using a filament winding process. One group had the wood at a 13% MC while the other group was soaked for 63 days to achieve saturation of wood and fiber wrap. The target thickness of the GFRP was 0.07" with a +/- 45 degree angle lay-up and an estimated 50% fiber volume fraction. The tests were carried out in a four point bending configuration with three equal spans as shown in Figure 1.10.

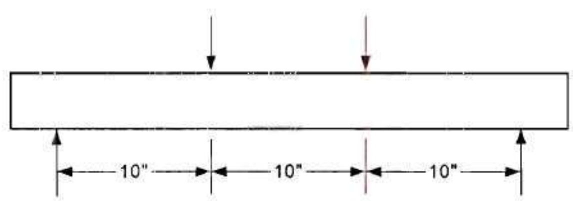

Figure 1.10: GFRP sample span (Davalos et al., 1999)

The results of the tests found that the application of the GRFP to the wood sections had increased the stiffness and ultimate load. The ultimate load of the 13% MC (dry) GRFP group reinforced with glass fiber composites increased by 28%. The ultimate load of the saturated (wet) GRFP group reinforced with glass fiber composites increased by 70%. The mid-span deflection of the 13% MC (dry) GRFP group reinforced with glass fiber composites decreased by 21%. The mid-span deflection of the saturated (wet) GRFP group reinforced with glass fiber composites decreased by 25%.

Recycled Plastic Lumber

Lampo (1996) summarizes the work of an alliance between Rutgers University and the U.S. Corps of Engineers' Construction Research Laboratory.

Plastic lumber has been reported to have equal strength to that of softwoods. Douglas Fir-Larch compression strength is 1,700 psi (11.7 MPa), and its tensile strength is 1,000 psi (6.89 MPa). Plastic Lumber's compressive strength ranges from 1740 psi to 3,500 psi (12.0 MPa to 24.1 MPa), and its tensile strength ranges from 1,250 psi to 3,500 psi (8.62 MPa to 24.1 MPa) (Lampo et al., 1996).

The compression modulus of plastic lumber is an order of magnitude less than the compressive modulus of a typical softwood. The compressive modulus of wood is an average of 1,200 ksi (8,270 MPa) with the compressive modulus of Douglas Fir-Larch being 1,700 ksi (11,720 MPa). The compressive modulus of plastic lumber ranges from 60 ksi to 180 ksi (410 MPa to 1,420 MPa) with an average of about 130 ksi (900 Mpa) (Lampo et al., 1996).

Plastic lumber also has been found to withstand a bending strain of 600-800%. This is much greater than the typical fracture strain of wood of 0.7% (Lampo et al., 1996).

Another concern is the excessive creep under a load bearing application. Due to the viscoelastic properties of plastic lumber, sag occurs under a sustained load and creep results in extreme deflections. (Lampo et al., 1996)

CHAPTER II

SMALL-SCALE RECYCLE PLASTIC (RP) BEAMS

This chapter presents the results of testing of small scale recycled beams made of different formulations of recycled plastics that were tested in order to determine the apparent stiffness and apparent modulus of different formulations of recycled plastics, fibers, and filler materials. Two different groups of small-scale specimens of different dimensions were tested. The first group consisted of 92 specimens each of which had cross sectional dimensions of 1.5 inches x 1.5 inches as shown in Figure 2.1. The second group consisted of two specimens each of which had dimensions of 4.25 inches x 4.25 inches as shown in Figure 2.2. The specimens were tested in three point bending to determine the individual stiffness and flexural modulus of each type of material "matrix" composition.

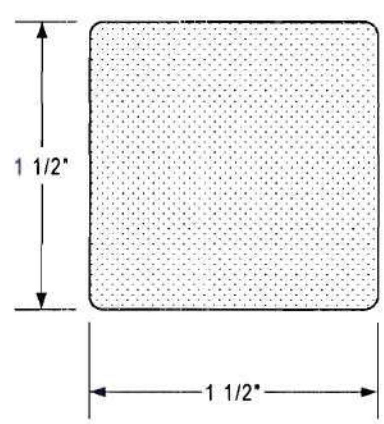

Figure 2.1: 1.5-inch x 1.5-inch small-scale specimen cross section

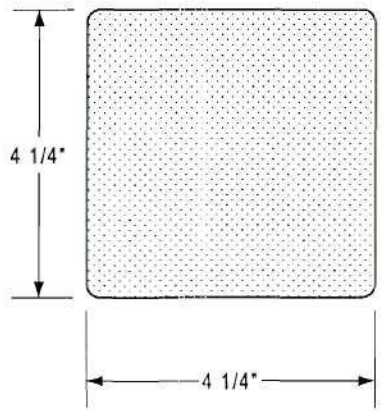

Figure 2.2: 4.25-inch x 4.25-inch small-scale specimen cross section

Test Set-up of 1.5-inch x 1.5-inch Small-scale Recycled Plastic (RP) Specimens

All small-scale specimens, manufactured by Seaward International, were tested in a three-point bending configuration following the guidelines of ASTM D 790-96a "Standard Methods for Flexural Properties of Unreinforced and Reinforced Plastics and Electrical Insulating Materials". The boundary conditions consisted of knife-edge supports centered on a two-inch bearing length. The two-inch steel bearing pads were used at the knife edge supports to prevent any localized bearing deformations. A 0.5-inch diameter steel rod was used to transfer the load to the beam as shown in Figure 2.3. The load was applied at the mid-span with a displacement rate of 0.0625 in/min.

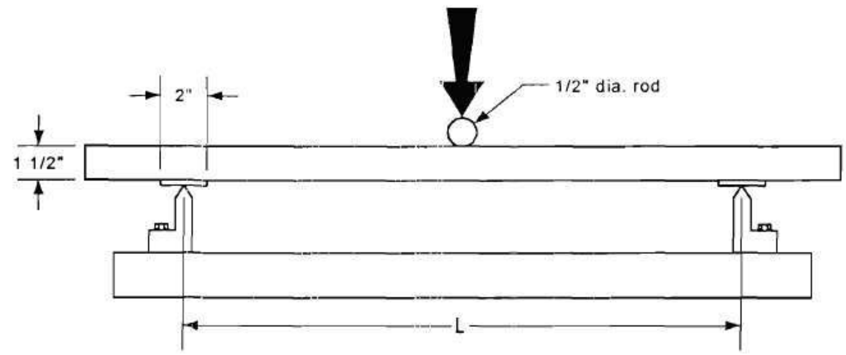

Figure 2.3: Set-up, elevation view

The test span for specimen RP1 to RP18 was 14 inches (span to depth ratio of 9.33:1). The test span for specimens RP2-1 to RP2-74 was 24 inches (span to depth ratio of 16:1). The load was applied by a 50 kip MTS close-looped hydraulic system, and data were recorded with a Megadac data acquisition system at the rate of two readings per second for specimens RP1 through RP22. For specimens RP2-1 through RP2-74 the load was applied by a 22 kip screw driven press, and data were recorded by Partner software accompanying the Instrom Press at a rate of five readings per second.

The apparent flexural stiffness (D_z) was computed from a linear regression performed on the load - deflection data corresponding to the deflection values between the limits of 0.0 inches < δ < 0.125 inches:

$$D_z = \frac{P}{\delta}\frac{L^3}{48} \tag{1}$$

where L is the span length in inches and δ is the deflection at mid-span. The apparent flexural modulus (E_a) was computed from the following equation:

$$E_a = \frac{D_z}{I_z} \qquad (2)$$

where I_z is the moment of inertia of the specimen.

Results of 1.5-inch Small-scale Specimens

Material descriptions, percentages of polymer, fibers, and filler materials, apparent flexural stiffness (D_z) and apparent flexural modulus (E_a) for specimens RP 1 through RP 18 are given in Table 2.1.

Table 2.1: Material description and D_z and E_a of RP1 - RP18

Specimen No.	Seaward ID No.	Material Description	Polymer %	Fiber %	Filler %	D_z (lbs-in^2)	E_a (lbs/in^2)
RP1	6-16-99 001B	HMW T.93 HDPE	100	0	0	4,473	10,600
RP2	6-16-99 002C	HDPE first state	100	0	0	55,980	132,700
RP3	6-16-99 003C	MDPE plastic revs.	100	0	0	18,353	43,500
RP4	7-12-99 001C	HDPE recycled TV cable	100	0	0	53,637	127,100
RP5	7-12-99 002C	HDPE masterbatch	50	50	0	365,049	865,300
RP6	7-12-99 003C	masterbatch & polymer	75	25	0	218,868	518,800
RP7	7-15-99 201 001B	junk plastic/carpet 50/50	100	0	0	142,031	336,700
RP8	7-15-99 202 002B	junk plastic/carpet 50/50	100	0	0	104,369	247,400
RP9	7-15-99 206 003B	HMW MD EP uf junk LD	100	0	0	53,535	126,900
RP10	7-15-99 402 010B	carpet w/ reinf.	45	25	30	233,760	554,100
RP11	7-15-99 406 012B	HMW MD EP uf junk LD	45	30	25	125,012	296,300
RP12	7-15-99 409 013B	HMW MD diaper junk LD	30	40	30	202,822	480,800
RP13	7-22-99 001D	313-0	70	30	0	227,066	538,200
RP14	7-22-99 002B	313-1	60	35	0	381,633	904,600
RP15	7-22-99 003B	LLDPE	100	0	0	54,685	129,600
RP16	7-26-99 001D	LDPE plastics group	100	0	0	28,944	68,600
RP17	7-26-99 002D	PP/PE mixed monoflo scrap	100	0	0	73,882	175,100
RP18	7-26-99 003C	carpet edge trim PP/PA	100	0	0	124,915	296,100

Secant modulus values for RP 2-1 through RP 2-32 were calculated at 0.125 inch deflection intervals up to a deflection of 1.25 inches; these values are reported in Table 2.2. The secant modulus values for RP 2-33 through RP 2-74 were calculated at 0.125 inch deflection intervals up to a deflection of 0.50 inches; these values are reported in Table 2.3. The secant modulus was computed by equation (3):

$$E_{ai} = \frac{(P_i - P_{(i-1)})}{(\delta_i - \delta_{(i-1)})} \frac{L^3}{48I} \tag{3}$$

Figure B-1 through Figure B-26 of Appendix B show the load - deflection curves for each individual batch. Figure C-1 through Figure C-26 in Appendix C show the relationship between the mid-span load and the apparent flexural modulus for each batch.

Table 2.2: Moduli of small-scale specimens

Specimen No.	Seaward ID No.	E_a (ksi)	$E_{.25}$ (ksi)	$E_{.375}$ (ksi)	$E_{.50}$ (ksi)	$E_{.625}$ (ksi)	$E_{.75}$ (ksi)	$E_{.875}$ (ksi)	$E_{1.0}$ (ksi)	$E_{1.125}$ (ksi)	$E_{1.25}$ (ksi)
RP 2-1	300-02-01-02	358	246	175	131	104	71	71	49	49	38
RP 2-2	300-02-01-04	522	317	213	153	98	76	60	49	38	33
RP 2-3	300-02-01-06	545	371	240	158	109	76	60	38	33	27
RP 2-4	300-02-02-02	756	628	442	279	-	-	-	-	-	-
RP 2-5	300-02-04-02	296	235	180	153	126	98	87	71	60	49
RP 2-6	300-02-04-04	294	229	186	142	126	98	82	66	60	49
RP 2-7	300-02-04-06	291	229	169	147	120	98	82	71	55	49
RP 2-8	300-02-05-03	389	306	240	191	147	109	104	49	55	44
RP 2-9	300-02-05-05	383	311	251	197	147	115	87	60	49	38
RP 2-10	300-02-05-07	384	311	257	202	147	120	87	66	49	38
RP 2-11	300-02-06-03	248	180	137	115	82	76	60	55	44	38
RP 2-12	300-02-06-05	248	186	142	109	93	76	71	49	44	38
RP 2-13	300-02-06-07	246	175	142	109	87	76	66	49	44	38
RP 2-14	300-02-07-01	268	197	153	104	76	55	33	16	0	0
RP 2-15	300-02-07-03	251	180	142	104	76	55	33	22	5	5
RP 2-16	300-02-08-02	254	208	169	142	126	93	82	71	55	49
RP 2-17	300-02-08-04	250	202	175	153	131	109	93	76	71	49
RP 2-18	300-02-08-06	251	202	175	153	131	115	87	76	66	49
RP 2-19	300-02-12-03	140	98	87	71	55	44	38	33	27	27
RP 2-20	300-02-12-05	118	93	76	66	60	49	38	38	33	22

Table 2.2: Moduli of small-scale specimens

Specimen No.	Seaward ID No.	E_a (ksi)	$E_{.25}$ (ksi)	$E_{.375}$ (ksi)	$E_{.50}$ (ksi)	$E_{.625}$ (ksi)	$E_{.75}$ (ksi)	$E_{.875}$ (ksi)	$E_{1.0}$ (ksi)	$E_{1.125}$ (ksi)	$E_{1.25}$ (ksi)
RP 2-21	300-02-12-07	110	87	76	60	60	49	38	3338	33	27
RP 2-22	300-02-13-02	342	273	208	158	126	98	76	66	55	44
RP 2-23	300-02-13-04	317	262	218	175	131	109	82	66	55	44
RP 2-24	300-02-13-06	315	262	208	180	137	104	82	71	55	44
RP 2-25	300-02-15-02	136	104	93	82	66	60	44	49	33	33
RP 2-26	300-02-15-04	133	104	87	76	66	49	49	44	33	22
RP 2-27	300-02-15-06	133	104	87	76	60	60	44	44	33	33
RP 2-28	300-02-16-03	363	251	175	120	93	71	55	49	33	33
RP 2-29	300-02-16-05	374	251	175	126	104	66	60	44	33	27
RP 2-30	300-02-16-07	376	268	186	137	104	87	60	49	38	33
RP 2-31	300-02-06-04	214	188	167	152	139	128	119	110	103	97
RP 2-32	300-02-06-07b	212	186	162	146	133	122	113	106	99	93

Table 2.3: Moduli of augmented small-scale specimens

Specimen No.	Seaward ID No.	E_a (ksi)	$E_{.25}$ (ksi)	$E_{.375}$ (ksi)	$E_{.50}$ (ksi)
RP 2-33	300-02-01-05 AUG	420	284	202	142
RP 2-34	300-02-01-07 AUG	416	295	202	147
RP 2-35	300-02-01-09 AUG	415	295	208	147
RP 2-36	300-02-04-03 AUG	298	235	180	153
RP 2-37	300-02-04-05 AUG	295	229	180	153
RP 2-38	300-02-04-07 AUG	293	224	180	153
RP 2-39	300-02-05-04 AUG	341	268	218	180
RP 2-40	300-02-05-06 AUG	344	279	235	197
RP 2-41	300-02-05-08 AUG	345	284	229	197
RP 2-42	300-02-06-03 AUG	299	224	175	142
RP 2-43	300-02-06-05 AUG	286	224	180	153
RP 2-44	300-02-06-07 AUG	287	218	175	153
RP 2-45	300-02-07-03 AUG	273	213	175	147
RP 2-46	300-02-07-07 AUG	293	229	186	153
RP 2-47	300-02-07-09 AUG	293	229	180	164
RP 2-48	300-02-08-03 AUG	226	186	164	142
RP 2-49	300-02-08-05 AUG	223	186	158	137
RP 2-50	300-02-08-07 AUG	223	191	164	137
RP 2-51	300-02-09-05 AUG	238	202	180	158
RP 2-52	300-02-09-07 AUG	241	208	180	158

Table 2.3: Moduli of augmented small-scale specimens

Specimen No.	Seaward ID No.	E_a (ksi)	$E_{.25}$ (ksi)	$E_{.375}$ (ksi)	$E_{.50}$ (ksi)
RP 2-53	300-02-09-09 AUG	245	202	180	158
RP 2-54	300-02-12-05 AUG	146	109	98	87
RP 2-55	300-02-12-07 AUG	145	115	98	82
RP 2-56	300-02-12-09 AUG	142	115	93	87
RP 2-57	300-02-12-03 AUG	307	257	218	191
RP 2-58	300-02-13-07 AUG	311	257	224	186
RP 2-59	300-02-13-09 AUG	303	257	213	191
RP 2-60	300-02-15-03 AUG	186	153	126	191
RP 2-61	300-02-15-05 AUG	187	147	126	115
RP 2-62	300-02-15-07 AUG	182	142	126	104
RP 2-63	300-02-16-03 AUG	365	273	208	164
RP 2-64	300-02-16-05 AUG	363	273	202	153
RP 2-65	300-02-16-07 AUG	355	257	202	142
RP 2-66	300-02-17-03 AUG	155	126	109	98
RP 2-67	300-02-17-05 AUG	158	120	115	104
RP 2-68	300-02-17-07 AUG	157	126	109	98
RP 2-69	300-02-18-03 AUG	550	437	355	284
RP 2-70	300-02-18-05 AUG	668	541	448	371
RP 2-71	300-02-18-07 AUG	726	601	470	360
RP 2-72	300-02-19-03 AUG	209	175	147	131
RP 2-73	300-02-19-05 AUG	206	175	147	131
RP 2-74	300-02-19-07 AUG	211	175	147	126

Test Set-up of 4.25 inches x 4.25 inches (RP) Specimens

Two 4.25 inches x 4.25 inches recycled plastic beams (Figure 2.2) labeled RP 2-75 and RP 2-76 were also tested. The recycled plastic specimen RP 2-75 was formulated from batch 6 and RP 2-76 was formulated from batch 16.

The tests were performed in a three point bending configuration with a span of 60 inches (span to depth ratio of 14.1:1) as shown in Figure 2.4. The boundary conditions consisted of four-inch long steel bearing pads centered on knife edge supports. A 1.5-inch diameter rod was used to transfer the load to the beam. The beams were loaded to a 0.25 inch deflection. The load was measured from a 1 kip load cell. Deflection at mid-span was measured with a 2-inch LVDT. Data were recorded by a Megadac data acquisition system at a rate of three readings per second. The beams were not loaded to failure.

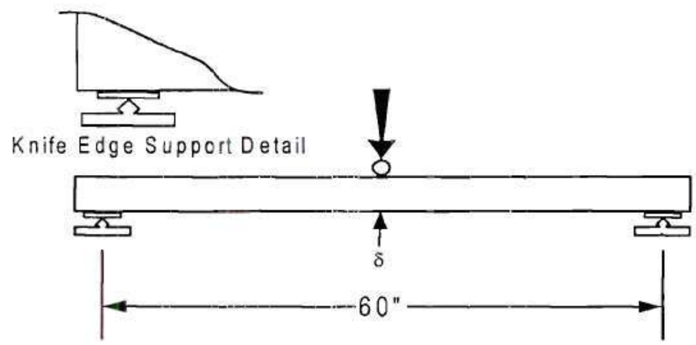

Figure 2.4: Elevation of 4.25-inch specimen test set-up

The apparent flexural stiffness (D_z) was computed using equation (1) from a linear regression performed on the load - deflection data corresponding to the deflection values between the limits of 0.0 inches < δ < 0.125 inches:

The apparent flexural modulus (E_a) was computed from equation (2). Table 2.4 shows the unreinforced apparent stiffness (D_z^u) and the apparent modulus (E_a^u) of the two recycled plastic beams. The initial load - deflection curves are shown in Figure 2.5.

Table 2.4: Apparent stiffness and modulus results of the 4.25-inch beam specimens

Specimen No.	Slope (lbs/in)	D_z^u (lbs-in^2)	E_a^u (lbs/in^2)
RP 2-75	641.48	2,886,660	106,200

Table 2.4: Apparent stiffness and modulus results of the 4.25-inch beam specimens

Specimen No.	Slope (lbs/in)	D_z^u (lbs-in^2)	E_a^u (lbs/in^2)
RP 2-76	738.24	3,322,080	122,200

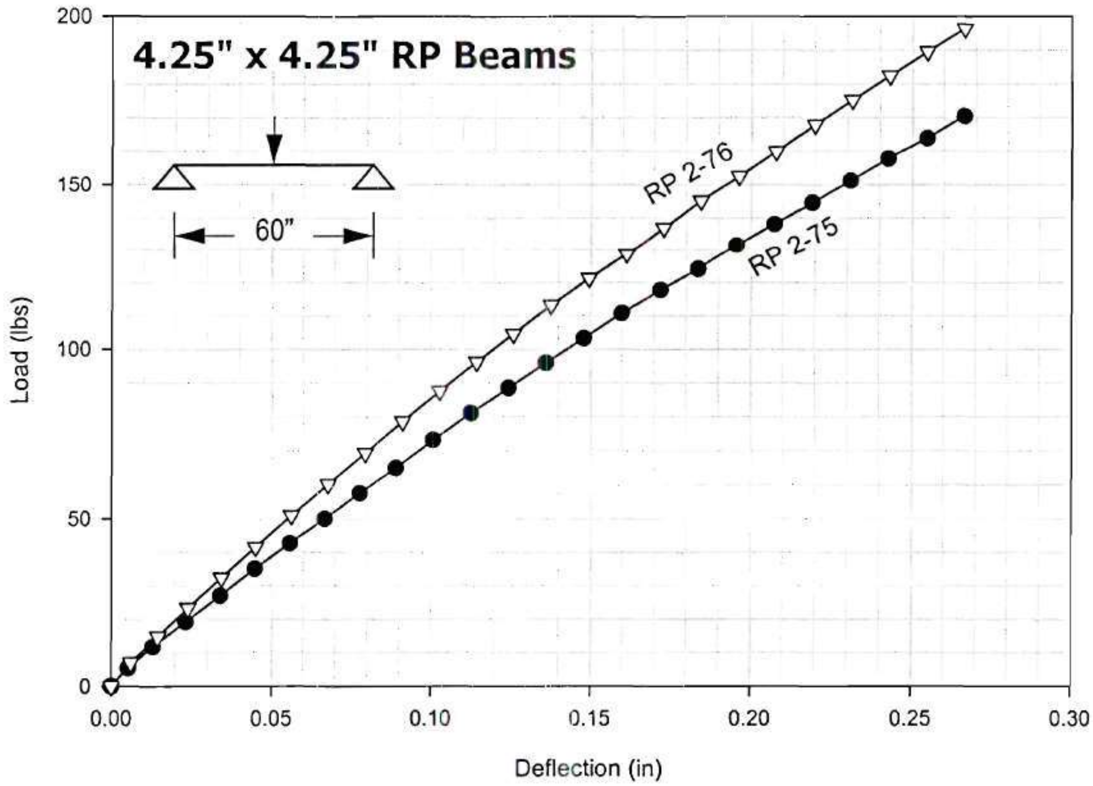

Figure 2.5: Load - deflection curves of the 4.25" square beam specimens

Eastpoint (2001) reported average flexural modulus values of High Density Polyethylene (HDPE), Low Density Polyethylene (LDPE), and Low Linear Density Polyethylene (LLDPE) as 120 ksi, 22 ksi, and 70 ksi, respectively. Specimens RP1, RP2, RP4 and

RP5 all contain some form of HDPE within the formulation of the beam specimen. The E_a of RP2 and RP4 was 133 ksi and 127 ksi, respectively, and these values averaged 8% greater than that given by Eastpoint. RP1 and RP5 had E_a values of 10.6 ksi and 8.65 ksi, respectively, and these values averaged 92% lower then that given by Eastpoint. The E_a of specimen RP15, which was made up of a LLDPE material, was 130 ksi, 86% greater then the value given by Eastpoint. The E_a of RP16, made of LDPE, was 68.6 ksi, and this value is 310% greater then that given by Eastpoint.

The actual material composition properties of the specimens RP2-1 through RP2-74 are proprietary to Seaward International; therefore, no comparisons except the listing of the initial stiffness, initial moduli and plots of the load - deflection and moduli - load curves were presented.

CHAPTER III

SMALL-SCALE RECYCLED PLASTIC (RP) BEAMS REINFORCED WITH POLYMER COMPOSITES

Introduction

This chapter presents the experimental results concerning the flexural response of small-scale recycled plastic (RP) beams reinforced with three different thermoplastic reinforcing tape systems containing E-glass, carbon, and stainless steel fiber, respectably. Tensile coupon tests were performed on the reinforcement tape systems to determine their moduli and strengths. The reinforced beams were tested in a three-point bending configuration to determine the flexural response of the recycled plastic beams externally reinforced.

Description of Reinforcing Systems

The three reinforcing systems are polypropylene thermoplastic E-glass, carbon and stainless steel systems. The average dimensions and fiber contents for each reinforcing system is shown in Table 3.1.

Table 3.1: Physical properties of reinforcing systems

Reinforcing System	Fiber[(a)] Content (by weight)	Number of Coupons	Average Thickness (inches)	Average Width (inches)
E-Glass	75%	10	0.0436	.4859
Carbon	37%	10	0.0128	.4926
Stainless Steel	60%	6	0.0182	.5010

a. Manufactures values.

Preparation and test set-up of the reinforcing systems

In preparing the three polypropylene thermoplastic E-glass, carbon, and stainless steel systems, each tensile specimen's thickness was measured at the center and at the ends of the six inch gauge length. The average of the three measurements was used for the representative width of each specimen. Twenty width measurements were taken from each reinforcing system, and the average for each system was used for each tensile specimen. The average measurements and fiber content as reported by the supplier are given in Table 3.1. Grips with surface area of 0.5 inches x 2 inches were cut from fiberglass electrical boards and were adhered to the specimen with 2500 psi "Devcon" Epoxy. Unwanted hardened epoxy was sanded off the grip surface. The layout of the grips on the tensile specimen is shown in Figure 3.1.

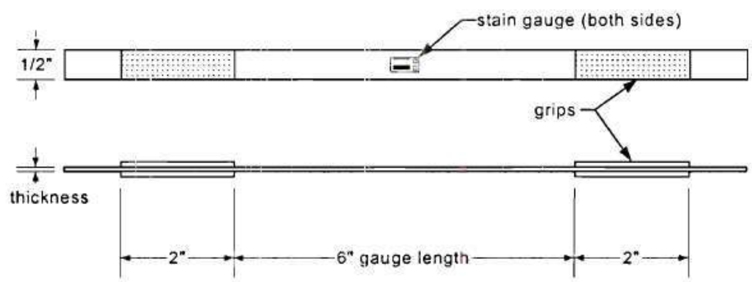

Figure 3.1: Tensile specimen

The tensile tests were conducted using a 50 kip MTS close-looped hydraulic system with hydraulic grips in accordance with the ASTM standard D 3039 / D 3039M-95a "Standard Test Method for Tensile Properties of Polymer Matrix Composite Materials". The specimen was loaded in displacement control at the rate of 0.03 in/min. An extensometer with a 1-inch gauge length was used to obtain the strain. Electrical resistance strain gauges were applied back to back on tensile specimens C1, C2, E1 and E2. The electrical resistance strain gauges were used to measure the strain at failure and to verify the calibration of the extensometer. Data were recorded with a Megadac data acquisition system at the rate of one reading per second. The stress - strain curve from each test was used to compute the tensile chord modulus of each reinforcing system within the ASTM 3039 guidelines.

Description of Reinforced RP Specimens

The previously mentioned reinforcing system was added externally to six previously tested 1.5 inches x 1.5 inches recycled plastic beams. Recycled plastic specimens RP23 through RP28 were first tested without the external reinforcement to determine the unreinforced apparent modulus (E_a^u). Then, the reinforcing systems were applied, and specimens were retested to measure the increase in flexural stiffness. The material composition of specimens RP23 through RP25 used a Banbury mixed material (mix 314.1), and specimens RP26 through RP28 used fiberglass masterbatch (mix320.0). The mix description and percentages of polymer, fibers and filler material is given in Table 3.2. The reinforcing system was applied on the top and bottom of each specimen with Magnolia 56 epoxy. Figure 3.2 presents the dimensions of the cross section along and the locations of the external reinforcement.

Table 3.2: Material description of 1.5 inches x 1.5 inches RP specimens

Specimen No.	Seaward No.	Material Description	Polymer%	Fiber%	Filler%
RP23	6-05-00 002	mix 314.1	47	40	13
RP24	6-05-00 003	mix 314.1	47	40	13
RP25	6-05-00 004	mix 314.1	47	40	13
RP26	6-05-00 005	mix 320.0	65	35	0
RP27	6-05-00 007	mix 320.0	65	35	0
RP28	6-05-00 008	mix 320.0	65	35	0

The stainless steel reinforcing system had a geometric defect (in-plane curvature) which made it impossible to apply the reinforcement longitudinally down the specimen without the two strips of reinforcement overlapping at the mid-span. At the supports, the two strips are lined up next to each other.

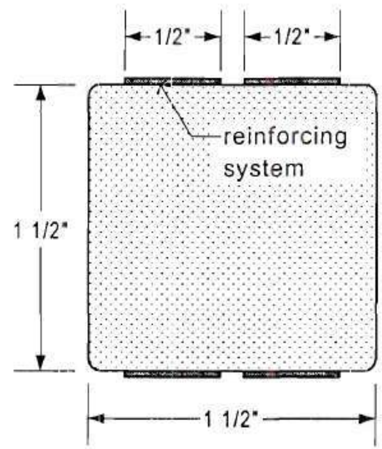

Figure 3.2: Cross section of RP beam with reinforcing system applied externally

Preparation and test set-up of recycled plastic beams

All reinforced plastic beam specimens, manufactured by Seaward International, were tested in three-point bending following the guidelines of ASTM D 790-96a "Standard Methods for Flexural Properties of Unreinforced and Reinforced Plastics and Electrical Insulating Materials". The boundary conditions consisted of knife-edge supports centered on a 2-inch steel bearing plate. The knife edges were used to simulate free rotation at the supports. Two-inch bearing pads were used to prevent any localized bearing deformations. A 0.5-inch diameter steel rod was used to transfer the load to the beam as shown in Figure 3.3. The load was applied to the 1.5 inches x 1.5 inches beams with a displacement rate of 0.0625 in/min.

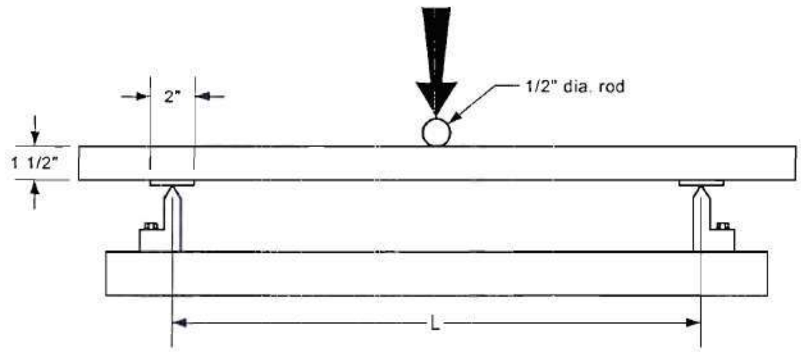

Figure 3.3: Set-up, elevation view

The beams were tested using a 24-inch span (span to depth ratio of 16:1). An Instron 22-kip testing machine was used to apply the load, and data were recorded at a rate of five readings per second.

The apparent flexural stiffness (D_z) was computed from a linear regression performed on the load - deflection data corresponding to the deflection values between the limits of 0.0 inches < δ < 0.125 inches:

$$D_z = \frac{P}{\delta}\frac{L^3}{48} \tag{4}$$

where L is the span length in inches and δ is the deflection at mid-span. The apparent flexural modulus (E_a) was computed from the following equation:

$$E_a = \frac{D_z}{I_z} \tag{5}$$

where I_z is the moment of inertia of the specimen.

Results of the Reinforcing Systems

Figure 3.4, Figure 3.5 and Figure 3.6 show the stress-strain curves for each test coupon for each respective reinforcing system: E-glass, carbon and stainless steel. Figure 3.7 presents the average load-strain curves for the three reinforcing systems. Figure 3.8 presents the average stress - strain curve for the three reinforcing systems. The ultimate load and modulus were used to calculate the ultimate strain. Table 3.3 lists moduli and strengths of the three reinforcing systems. Table 3.4, Table 3.5 and Table 3.6 list the properties for each E-glass, carbon and stainless steel coupon, respectively. The stress (σ) values was calculated from this equation:

$$\sigma = \frac{P}{A} \tag{6}$$

where P is the load and A is the cross sectional area. The Modulus of the reinforcing system is of the combined system and not just the fiber alone.

The carbon and E-glass performed as expected. However, the stainless steel epoxy specimen all failed at the grips. The stainless steel/epoxy tape, with a 60 percent fiber content, should have a modulus of least 16,000 ksi if a modulus of the stainless steel is assumed to be 28,000 ksi. The stainless system had a manufacture flaw in that the tape was not straight and linear. All of the failures occurred at the grip in a tearing fashion suggests that the tensile load was not uniform across the tape system.

Table 3.3: Reinforcing system's average stress strain properties

Reinforcing System	Number of Coupons	Average Ultimate Strength (lbs)	Average E_r (ksi)	Average Ultimate Tensile Stress (ksi)	Average Ultimate Tensile Strain (%)[(a)]
E-Glass	10	1,802	4,727	82.74	1.75
Carbon	10	980.2	11,411[(b)]	153.4	1.41[b]
Stainless Steel	6	131.3	2,991	14.72	0.481

a. Calculated from a linear relationship between the ultimate stress and the E_{chord}.
b. Average excludes coupon C3.

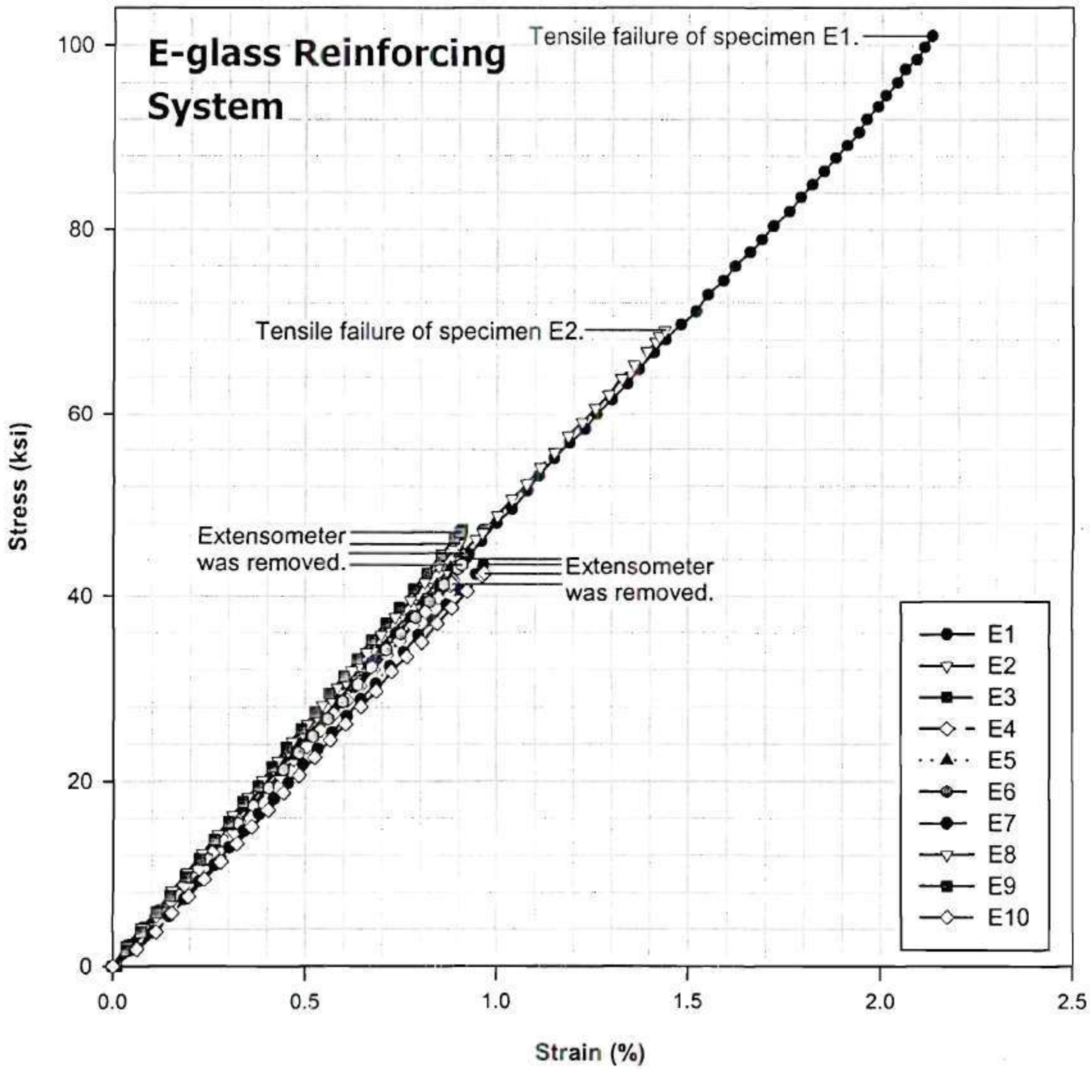

Figure 3.4: Stress - strain data for the E-glass reinforcing system

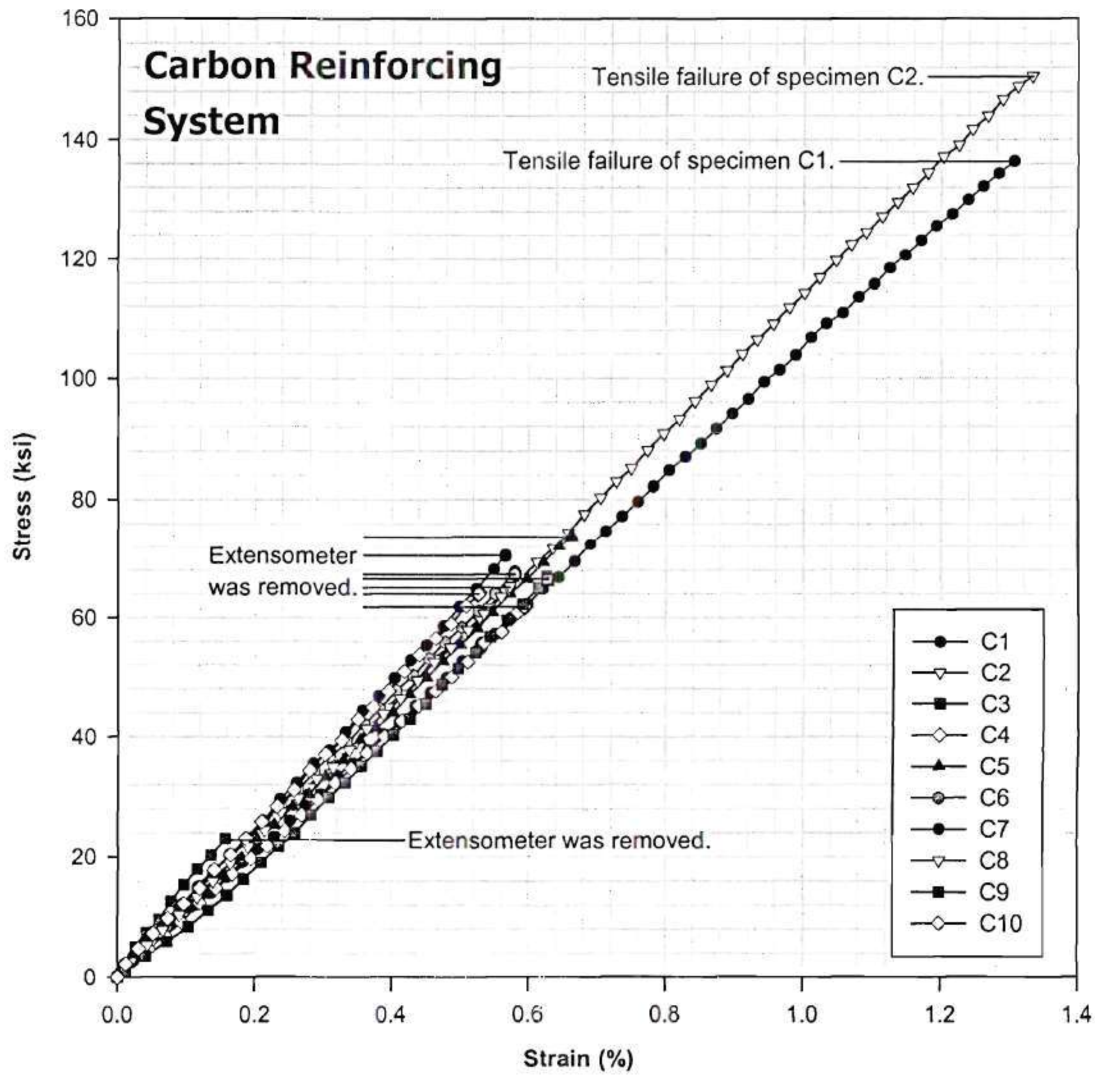

Figure 3.5: Stress - strain data for the carbon reinforcing system

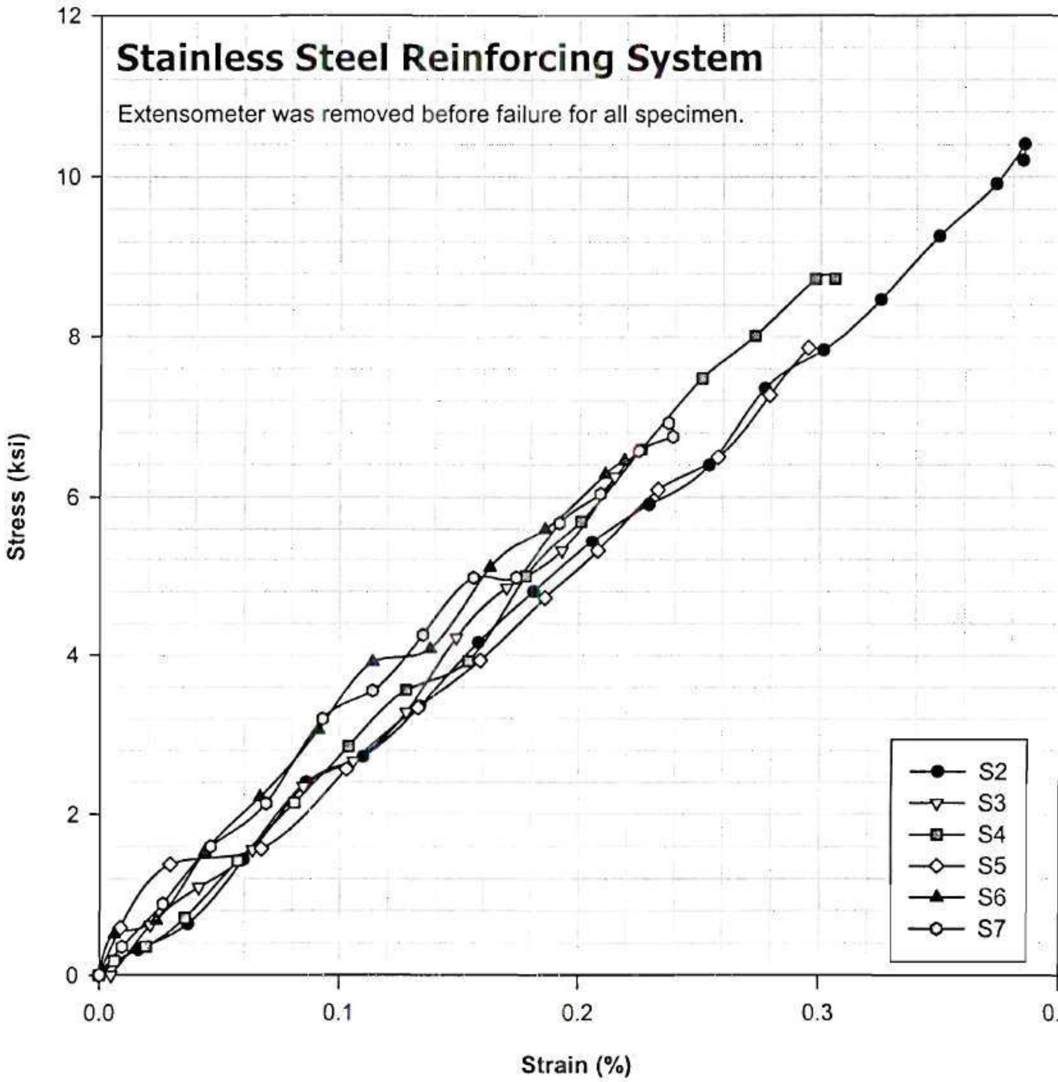

Figure 3.6: Stress - strain data for the stainless steel reinforcing system

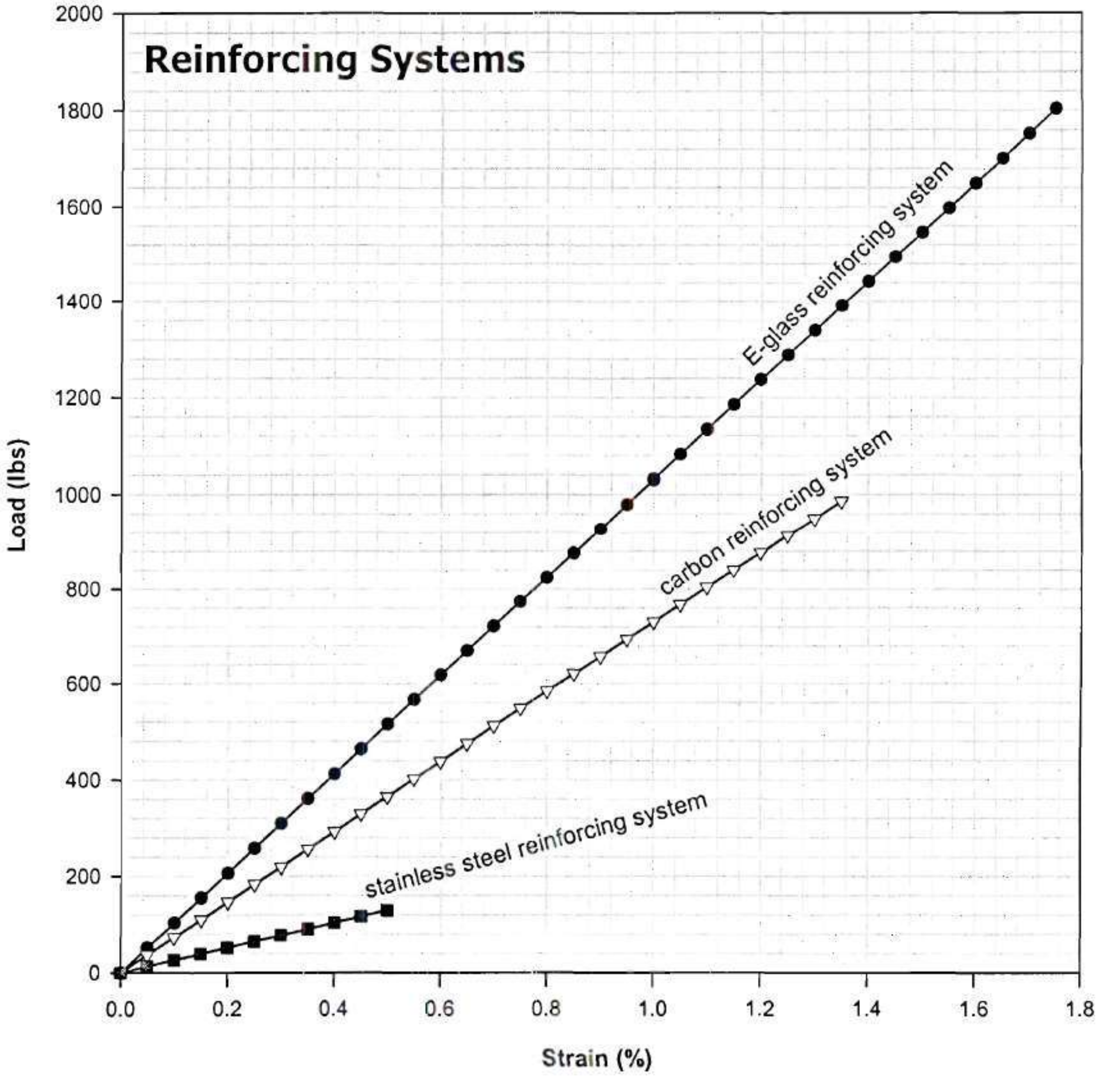

Figure 3.7: Average load - strain curves of the three reinforcing systems

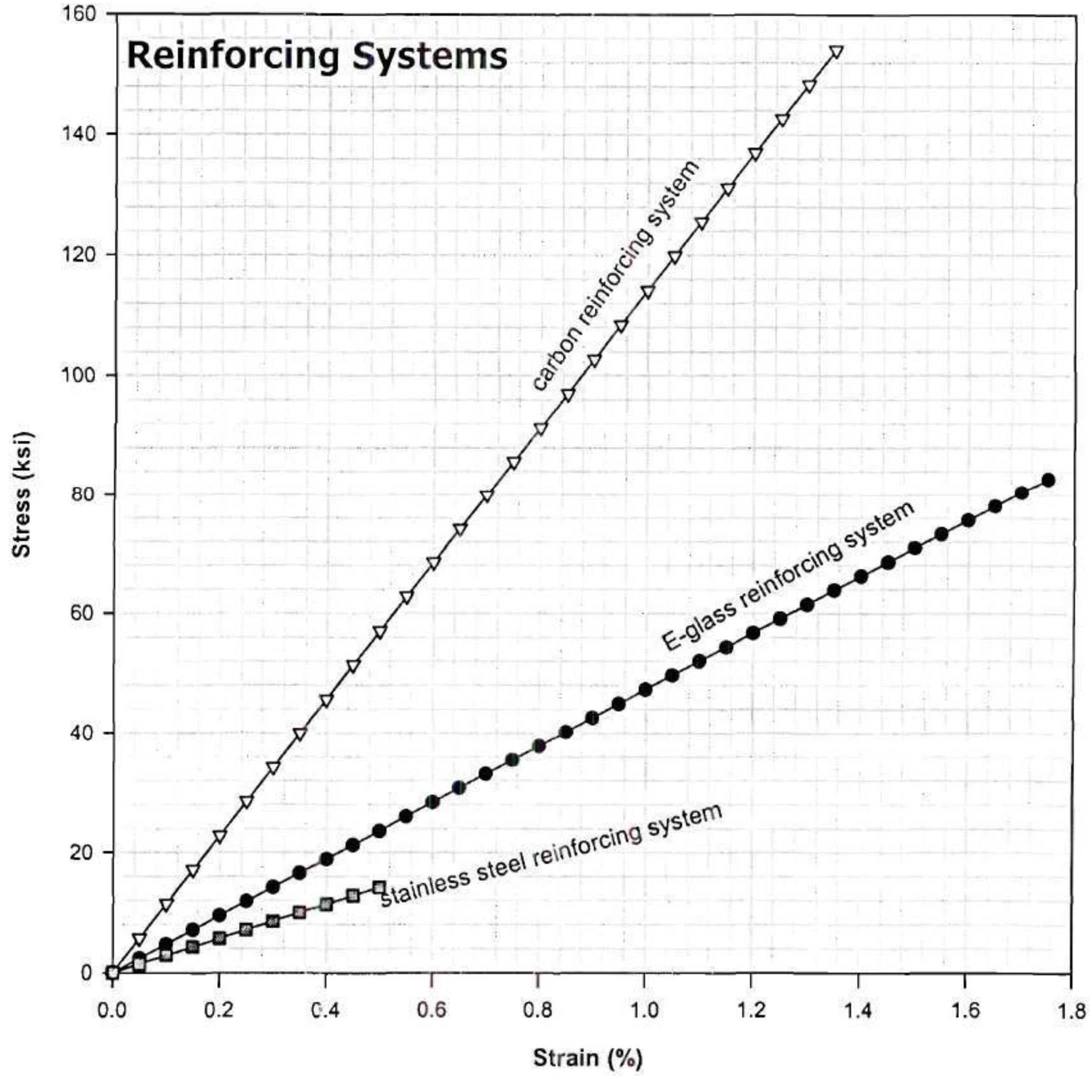

Figure 3.8: Average stress - strain curves of the three reinforcing systems

Table 3.4: Tensile properties of the E-glass reinforcing system

E-Glass Specimen	Average Thickness (in)	Average Width (in)	Ultimate Tensile Strength (lbs)	Modulus "E_{chord}" (ksi)	Ultimate Tensile Stress (ksi)	Ultimate Tensile Strain (%)[a]
E1	0.04305	0.04859	2,109	4,948.6	100.84	2.04
E2	0.04320	0.04859	1,447	4,907.5	68.93	1.40
E3	0.04335	0.4859	1,995	4,901.6	94.73	1.93
E4	0.04560	0.4859	1,638	4,746.5	73.90	1.56
E5	0.04310	0.4859	1,677	4,997.6	80.06	1.60
E6	0.04380	0.4859	1,936	4,803.8	90.96	1.89
E7	0.04575	0.4859	2,011	4,609.1	90.46	1.96
E8	0.04170	0.4859	1,758	4,119.5	86.75	1.69
E9	0.04130	0.4859	1,494	5,232.7	74.44	1.42
E10	0.04465	0.4859	1,959	4,478.1	90.31	2.02
Average	0.04355	0.4859	1,802	4,874.5	85.14	1.75
Standard Deviation	0.00139	0.0039	220.0	214.42	9.80	0.233
Coeff. of Variation	3.2%	.80%	12.2%	4.4%	11.5%	13.3%

a. Calculated from a linear relationship between the ultimate stress and the E_{chord}.

Table 3.5: Tensile properties of the carbon reinforcing system

Carbon Specimen	Average Thickness (in)	Average Width (in)	Ultimate Tensile Strength (lbs)	Modulus "E_{chord}" (ksi)	Ultimate Tensile Stress (ksi)	Ultimate Tensile Strain (%)[(a)]
C1	0.01430	0.4926	969	10,789.0	137.6	1.28
C2	0.01306	0.4926	986	10,580.1	153.2	1.45
C3	0.01255	0.4926	994	-	160.7	-
C4	0.01355	0.4926	934	10,366.9	140.0	1.35
C5	0.01255	0.4926	989	10,813.7	160.0	1.48
C6	0.01245	0.4926	966	11,210.1	157.4	1.40
C7	0.01160	0.4926	959	12,168.2	167.9	1.38
C8	0.01260	0.4926	997	10,813.5	160.6	1.49
C9	0.01285	0.4926	998	10,357.2	157.7	1.52
C10	0.01265	0.4926	1,009	11,922.8	162.0	1.36
Average	0.01282	0.4926	980.2	11,002.4	155.7	1.41
Standard Deviation	0.00068	0.0036	21.52	611.4	9.20	0.0746
Coeff. of Variation	5.3%	0.73%	2.2%	5.6%	5.9%	5.3%

a. Calculated from a linear relationship between the ultimate stress and the E_{chord}.

Table 3.6: Tensile properties of the stainless steel reinforcing system

Stainless Steel Specimen	Average Thickness (in)	Average Width (in)	Ultimate Tensile Strength (lbs)	Modulus "E_{chord}" (ksi)	Ultimate Tensile Stress (ksi)	Ultimate Tensile Strain (%)[(a)]
S2	0.01955	0.5010	148	3,731.8	15.18	.407
S3	0.02000	0.5010	178	2,886.3	17.81	.617
S4	0.01755	0.5010	134	3,063.6	15.32	0.500
S5	0.01590	0.5010	127	2,740.6	15.92	0.581
S6	0.01840	0.5010	125	2,890.8	13.59	0.470
S7	0.01760	0.5010	72	2,633.0	8.18	0.311
Average	0.01817	0.5010	131.3	2,991.0	14.72	0.481
Standard Deviation	.00136	0.0055	29.47	357.3	2.95	0.103
Coeff. of Variation	7.5%	1.1%	22.4%	12.0%	20.0%	21.4%

a. Calculated from ultimate stress and E_{chord}, a linear relationship.

Results of Reinforced RP Specimens

The average apparent modulus (E_a) for specimens RP 23 - RP 28 increased in stiffness with the addition of the reinforcement. Results are shown in Table 3.7. Specimens RP23, RP24 and RP25 load - deflection curves are shown in Figure 3.9. Specimens RP26, RP27 and RP28 have relatively equal unreinforced apparent moduli. Therefore, Figure 3.10 best illustrates the difference in the three reinforcing systems' performance under a flexural load. Figure 3.11 through Figure 3.16 are the individual load - deflection curves of the reinforced RP specimens.

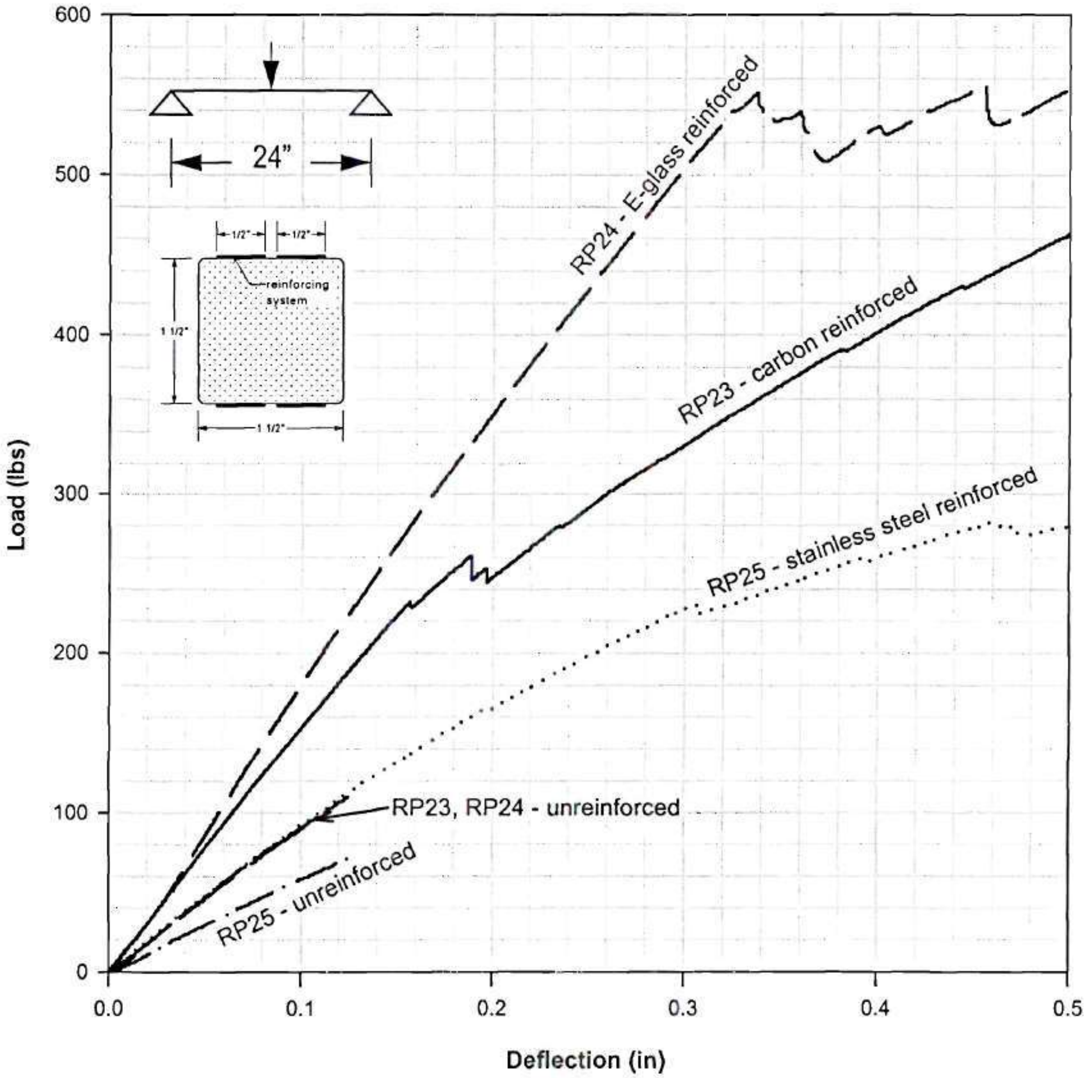

Figure 3.9: Load - deflection curves of specimens RP23, RP24 & RP25

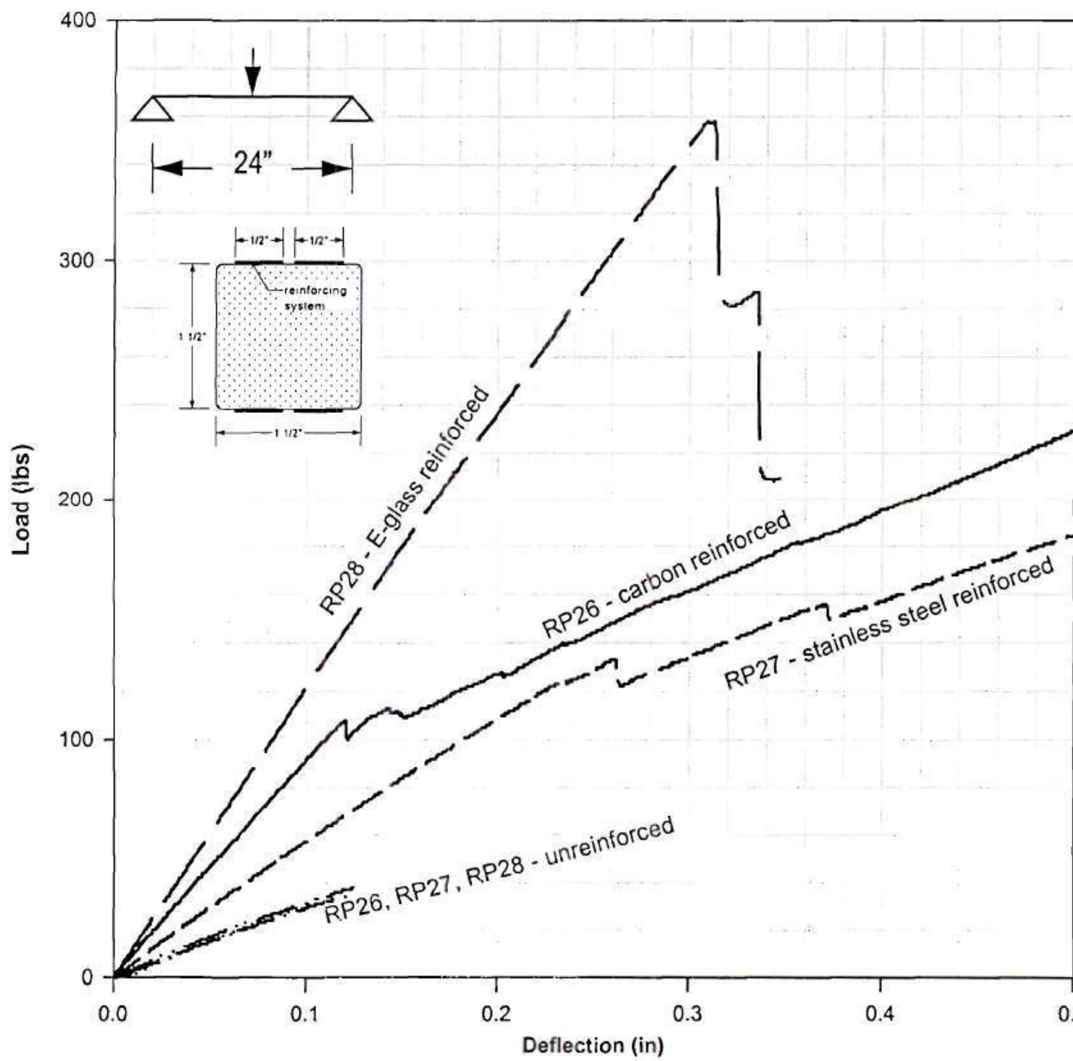

Figure 3.10: Load - deflection curves of specimens RP26, RP27 & RP28

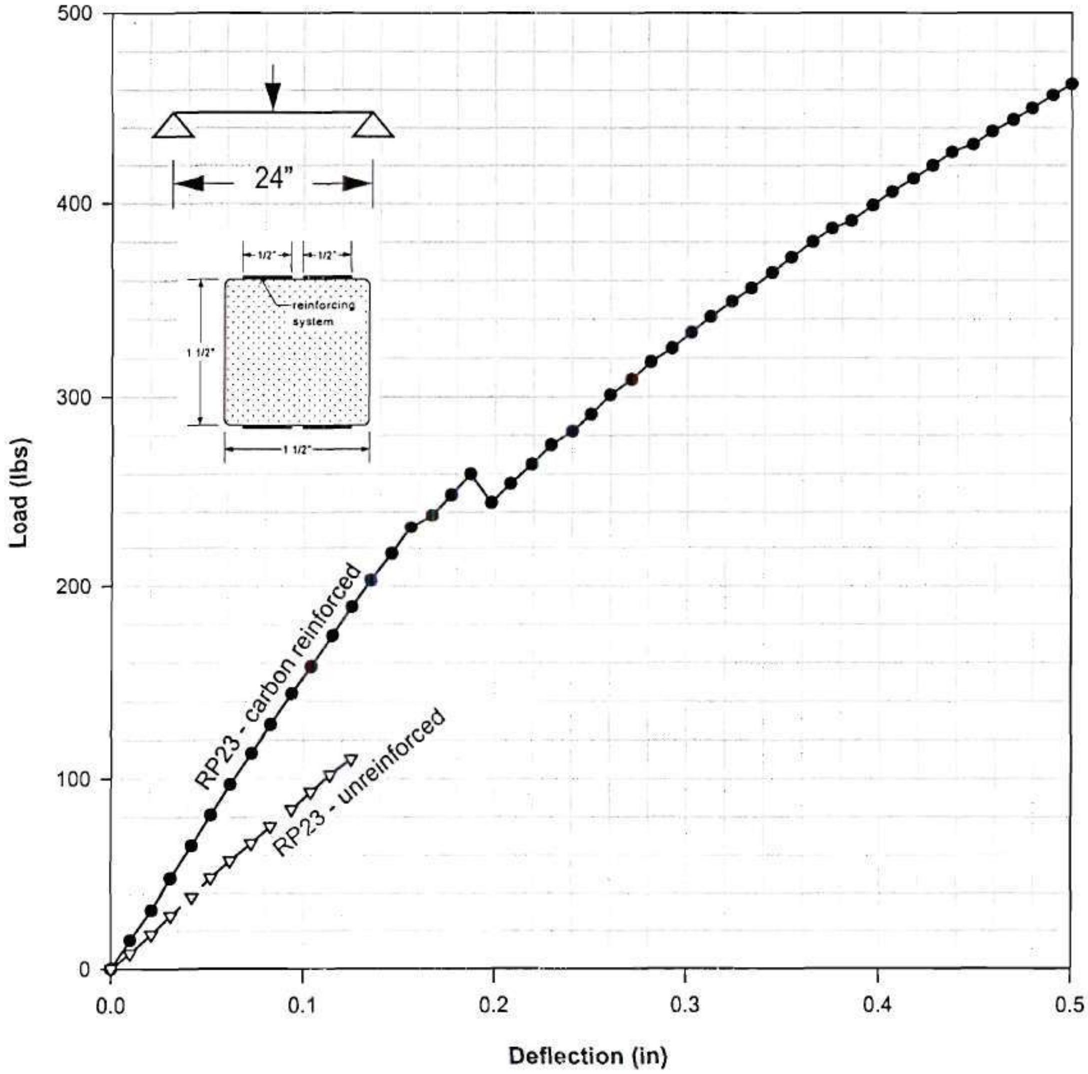

Figure 3.11: Load - deflection curves for RP23

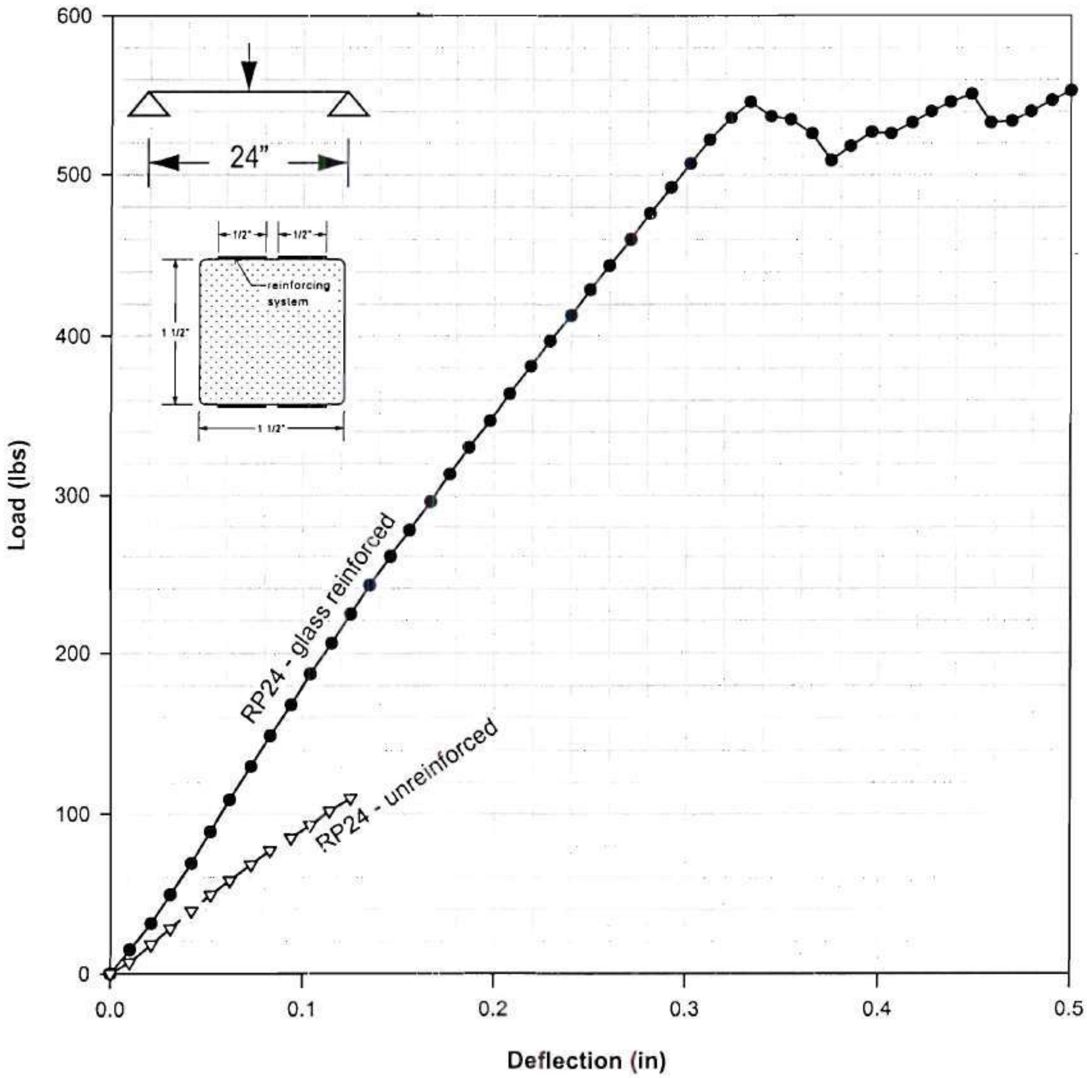

Figure 3.12: Load - deflection curves for RP24

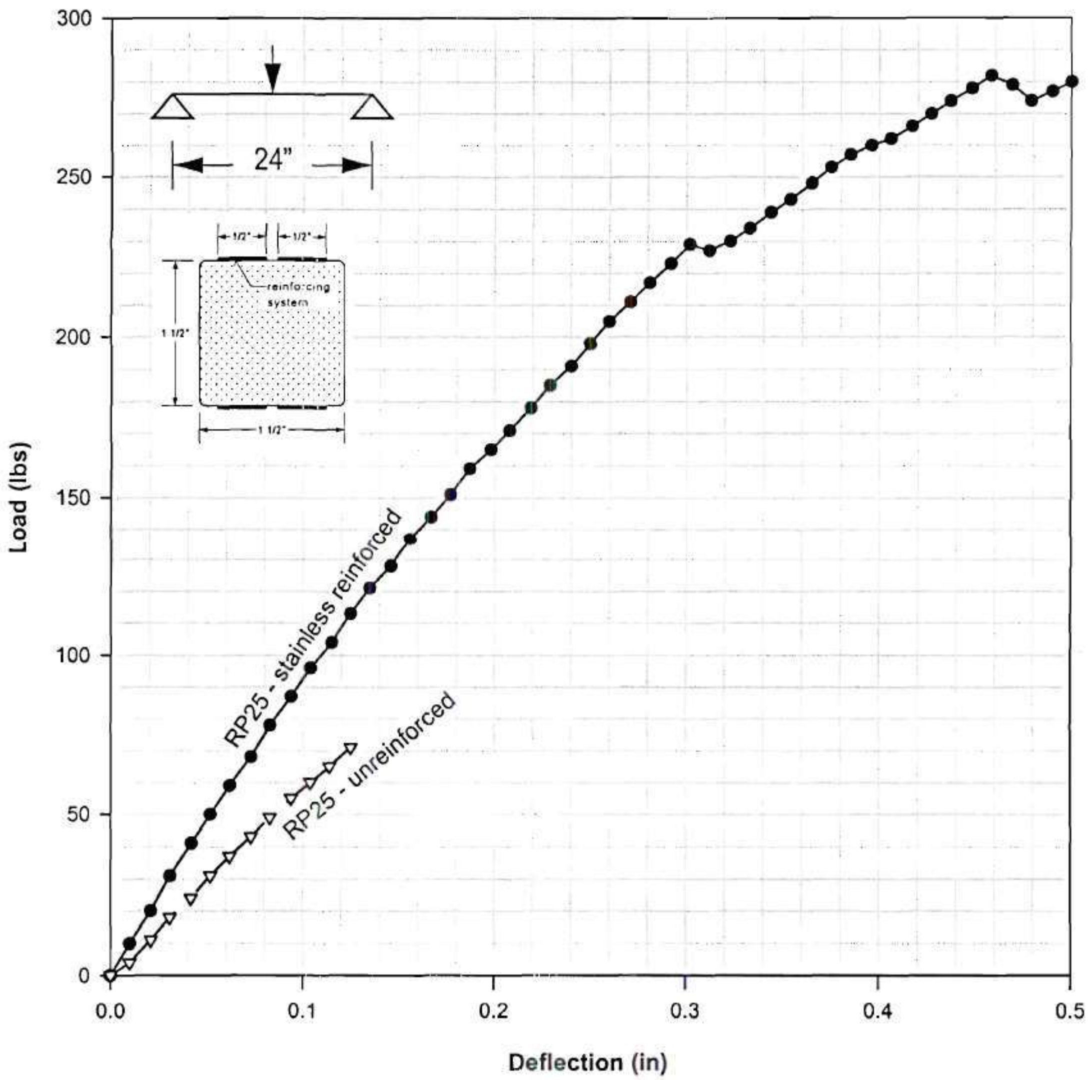

Figure 3.13: Load - deflection curves for RP25

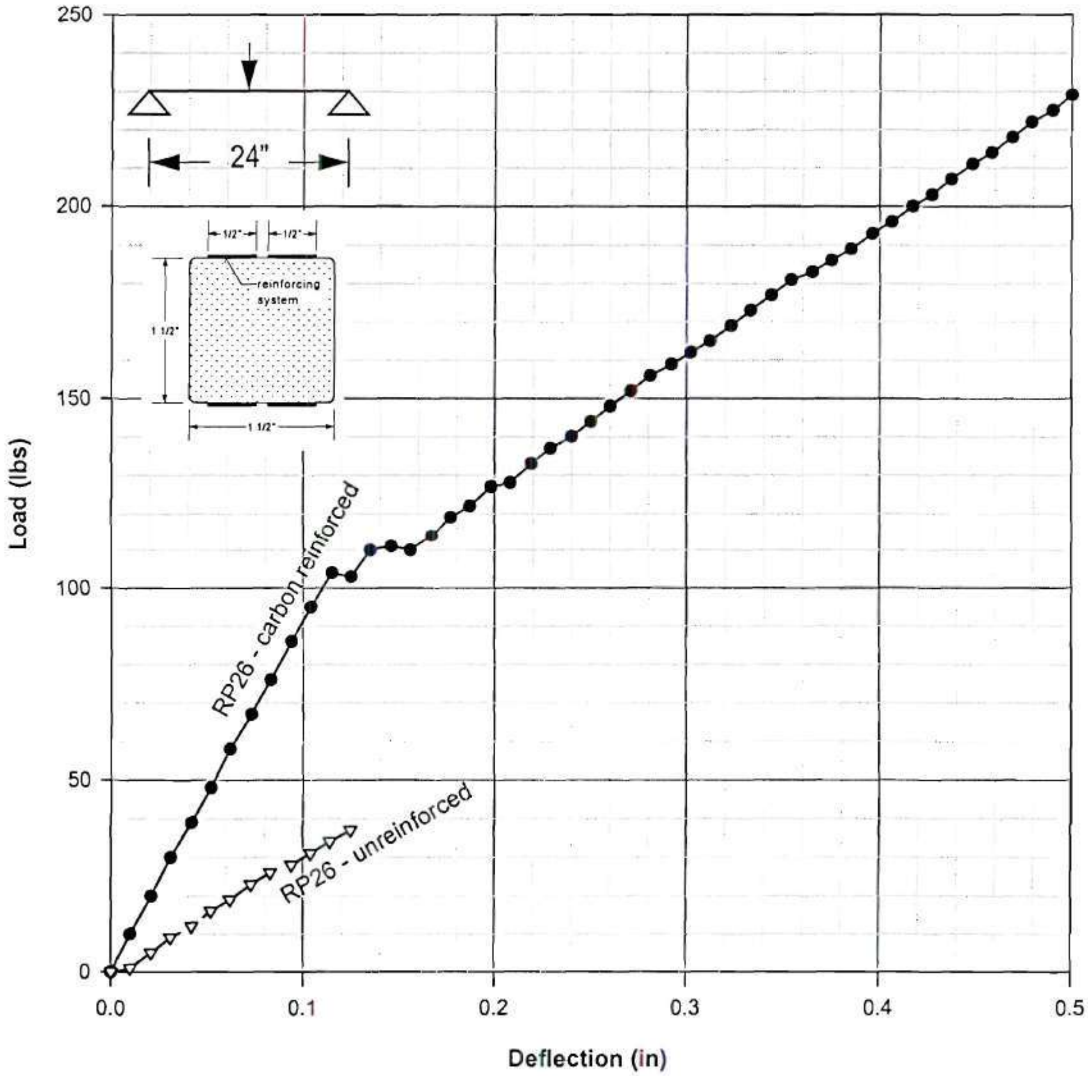

Figure 3.14: Load - deflection curves for RP26

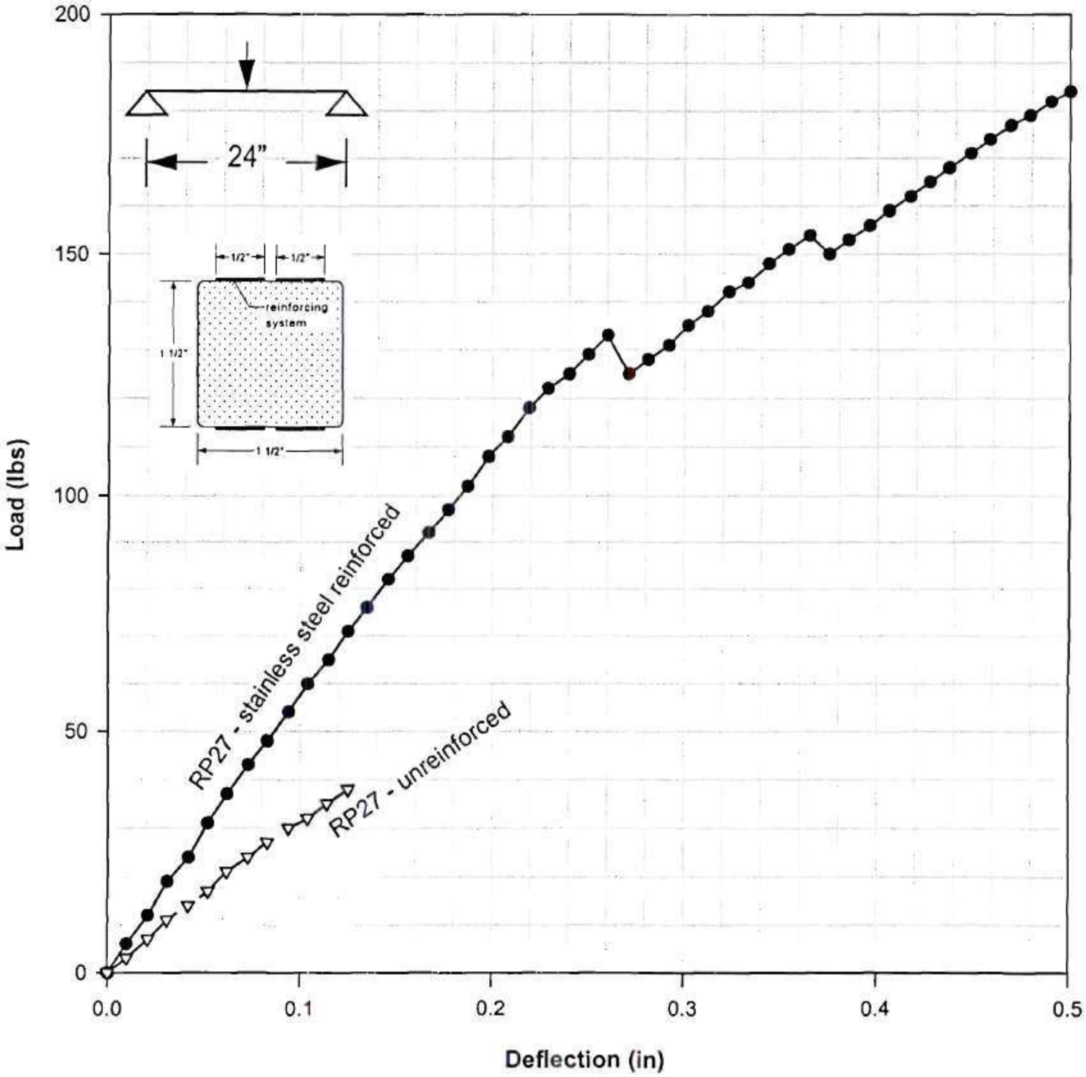

Figure 3.15: Load - deflection curves for RP27

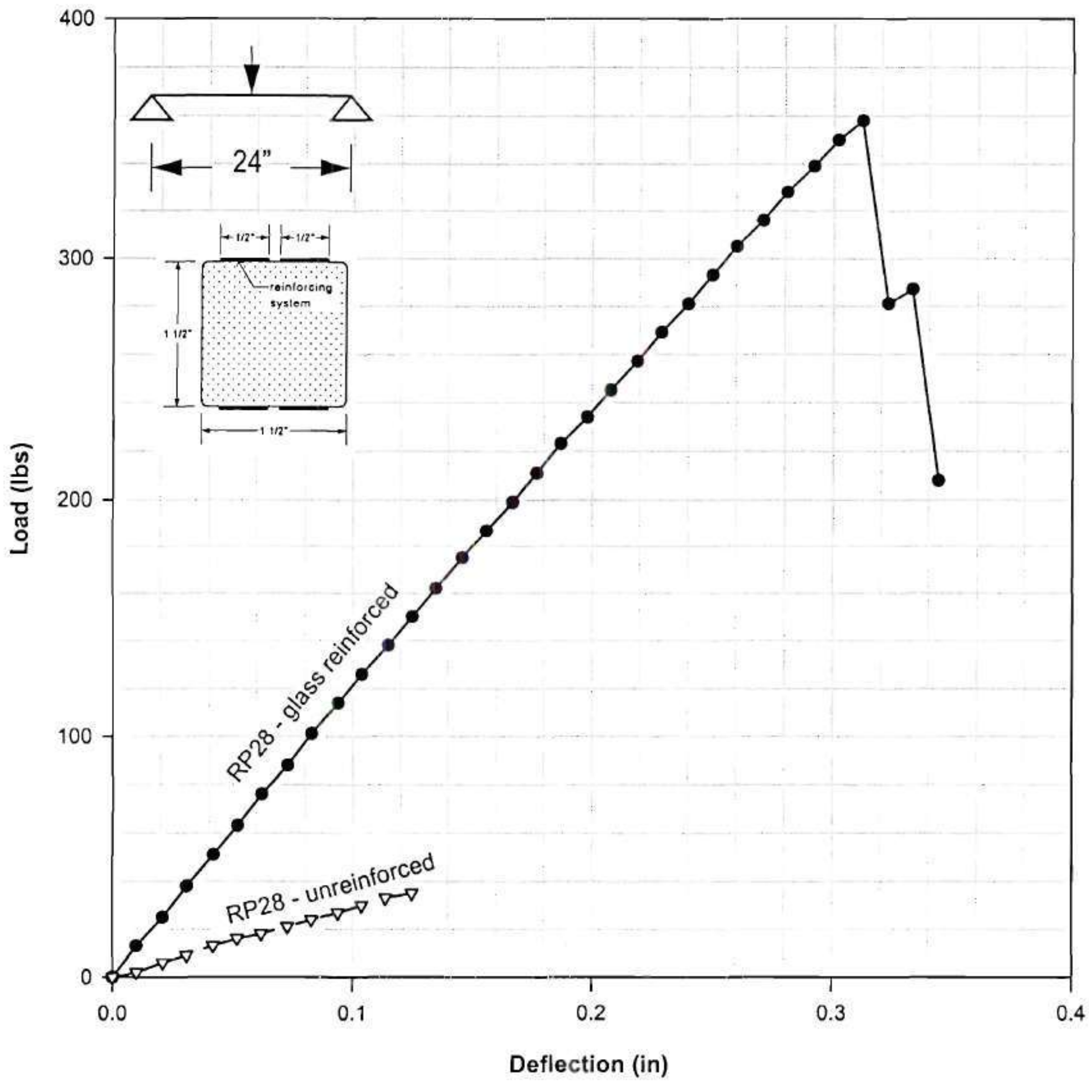

Figure 3.16: Load - deflection curves for RP28

Table 3.7: D_z and E_a of unreinforced and reinforced RP specimen

Specimen No.	reinforcement material	D_z^u (lbs in^2)	E_a^u (lbs/in^2)	D_z^r (lbs in^2)	E_a^r (lbs/in^2)
RP23	carbon	256,985	609,150	438,624	1,039,701
RP24	glass	260,490	617,458	531,648	1,260,203
RP25	stainless	167,875	397,926	259,747	615,697
RP26	carbon	91,253	216,303	259,834	615,902
RP27	stainless	86,892	205,967	163,181	386,799
RP28	glass	83,782	198,595	348,192	825,344

Specimens RP23, RP24 and RP25 were manufactured from the same mix as shown in Table 3.2. Therefore, there is no known reason why the unreinforced modulus of specimen RP25 did not correlate with the modulus of RP23 and RP24 except for an inconsistency in the manufacturing process. The failure of the reinforced beams were from the top reinforcement becoming delaminated from the specimen to the right or left of the load point. The specimens reinforced with the E-glass reinforcing systems showed the greatest improvement in stiffness.

Description of Internally reinforced RP beams

E-glass reinforcement was manufactured within a 100% HDPE cross section to determine the benefit of internally reinforcing the small-scale recycled plastic beams. There was no filler or fiber within the cross section except for the reinforcing tape within specimen RP19 and RP20 as shown in Figure 3.17. The glass reinforcement had an average cross section of 0.6 inches x 0.0115 inches and its depth varied along its length. The nominal dimensions of the cross section was 1.5 inches x 1.5 inches as shown in Figure 3.17. Specimen RP21 and RP22 are identical to that of specimen RP19 and RP20, but without the E-glass tape reinforcement as shown in Figure 3.18.

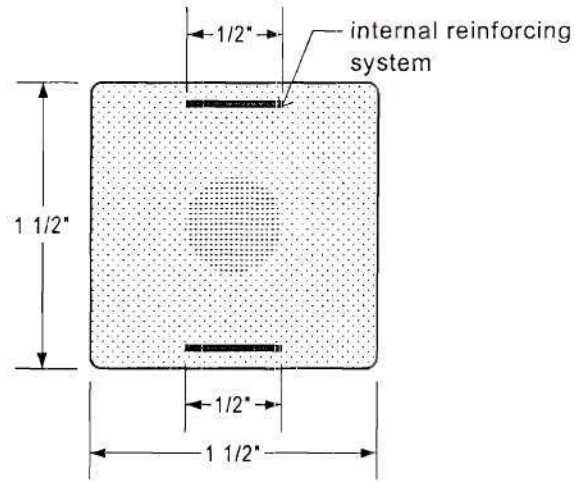

Figure 3.17: HDPE specimen with E-glass internal reinforcing system

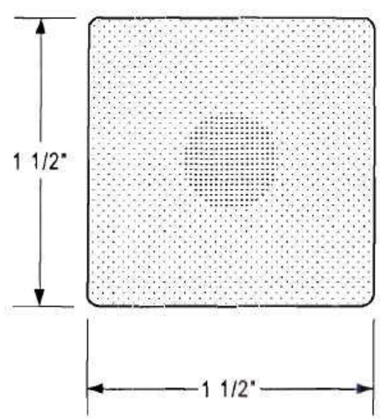

Figure 3.18: HDPE specimen without reinforcing system

Results of Internally reinforced RP beams

The load - deflection curves for RP19, RP20, RP21 and RP22 are shown in Figure 3.19, Figure 3.20, Figure 3.21 and Figure 3.22, respectively. The stiffness and Modulus values of RP beam specimens RP19 through RP22 are shown in Table 3.8.

The average stiffness of the reinforced specimens RP 19 and RP 20 (27.8 kips-in^2) increased 10% over their unreinforced counterparts RP 21 and RP 22 (25.2) as shown in Table 3.8.

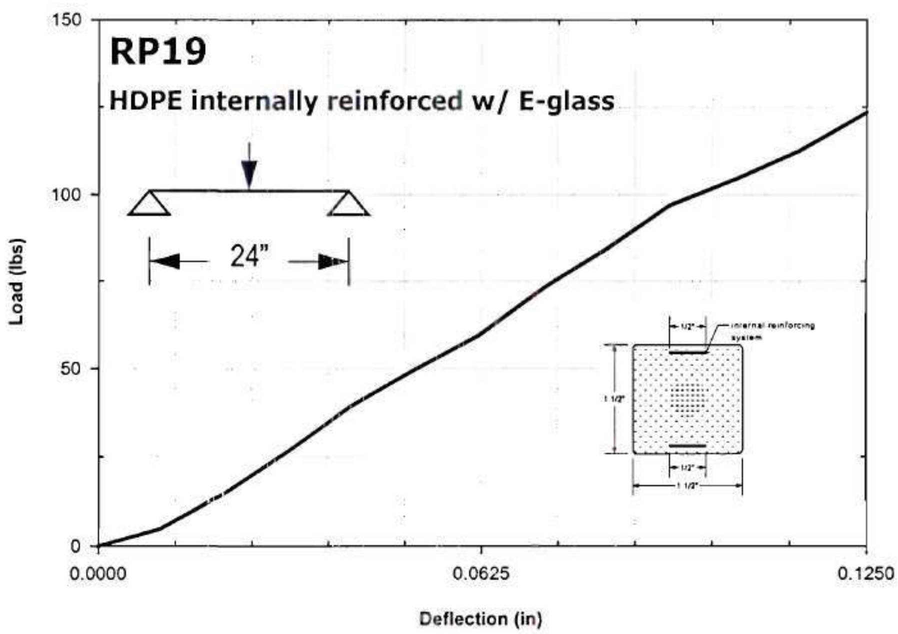

Figure 3.19: Load - deflection curves for RP19

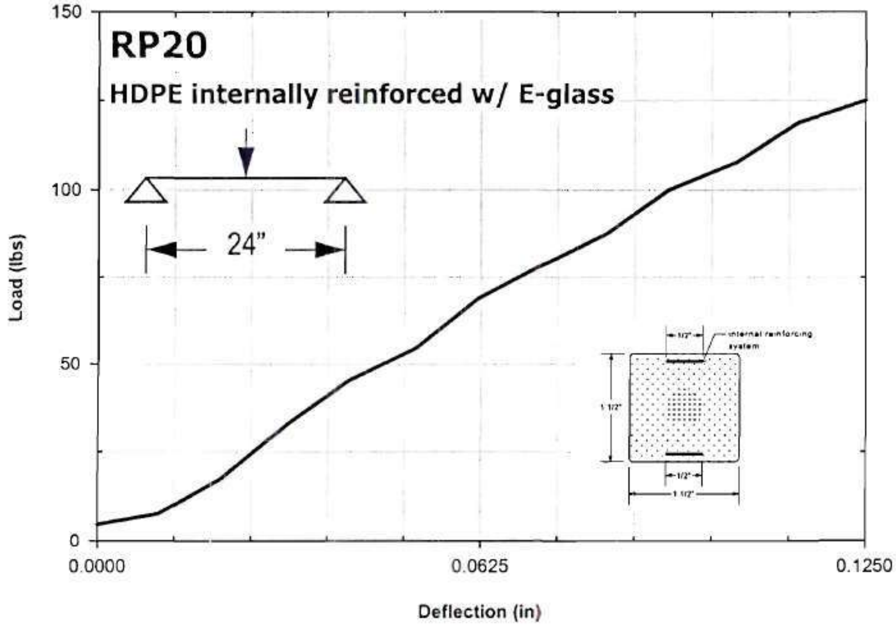

Figure 3.20: Load - deflection curves for RP20

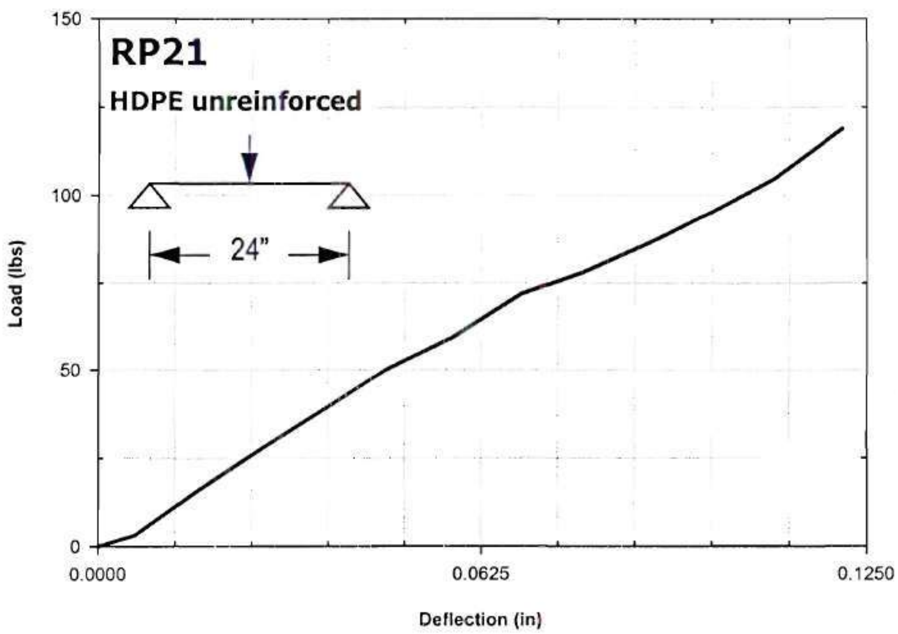

Figure 3.21: Load - deflection curves for RP21

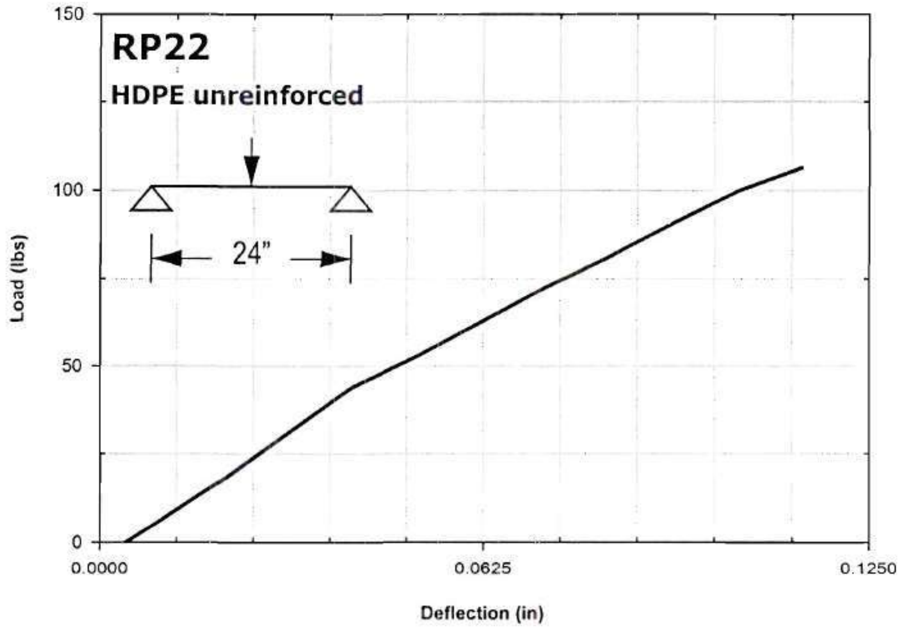

Figure 3.22: Load - deflection curves for RP22

Table 3.8: D_z and E_a of internally reinforced RP specimen

Specimen No.	Seaward ID No.	Material Description	Polymer %	Fiber %	Filler %	D_z (lbs in^2)	E_a (lbs/in^2)
RP19	4-13-00 003	HDPE w/ glass tape reinf.	100	0	0	28,264	
RP20	4-13-00 004	HDPE w/ glass tape reinf.	100	0	0	27,341	
RP21	4-21-00 002	HDPE	100	0	0	24,745	58,654
RP22	4-21-00 004	HDPE	100	0	0	25,734	60,998

CHAPTER IV

FULL-SCALE SPECIMENS

Introduction

The flexural performance of beams, having cross sectional dimensions comparable to those used as railroad ties, with and without reinforcement, is presented in this chapter. Wood, Duratie® ties and Seatimber® ties were tested under three point bending. In addition, three different reinforcements were tested: 1.25-inch diameter internal E-glass reinforcement bars, 0.5-inch diameter internal E-glass reinforcement bars and externally applied carbon fabric wrap.

Test Specimens

The three types of full-scale crossties and the number of beam specimens tested is listed:

- Wood - Specimen 1
- Duratie® - Specimens 2, 3 and 4
- Seatimber® - Specimens 5, 6, 7, 8, 9, 10, 11 and 12

Wood

Specimen 1: This specimen was a 9-inch x 7-inch red oak wood rail road tie having dressed dimensions of 8.5 inches x 6.75 inches. The cross section is shown in Figure 4.1.

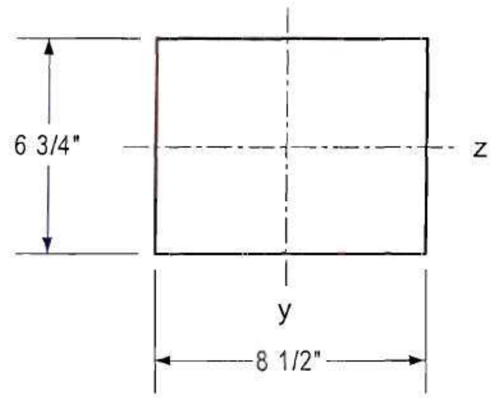

Figure 4.1: Cross section of specimen 1

Duratie®

Specimens 2 and 3: These specimens were made of a rubber like material with no reinforcement. Specimen 3 had a checkered surface. The dimensions of the cross section are 9.19 inches x 7.31 inches as shown in Figure 4.2.

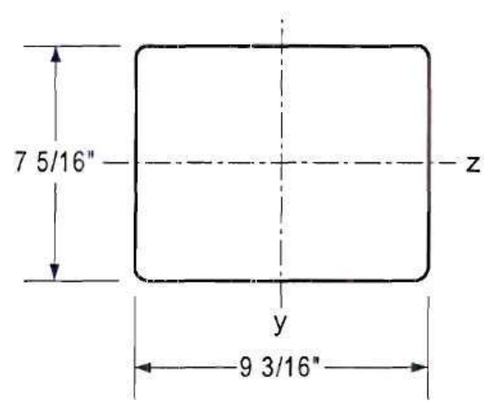

Figure 4.2: Cross section of specimen 2 and specimen 3

Specimen 4R1: This specimen was a Duratie® reinforced externally with one layer of longitudinal reinforcement with 9oz/sq. yd. of carbon fibers. The dimensions of the cross section were 9.19 inches x 7.31 inches. The cross section is shown in Figure 4.3.

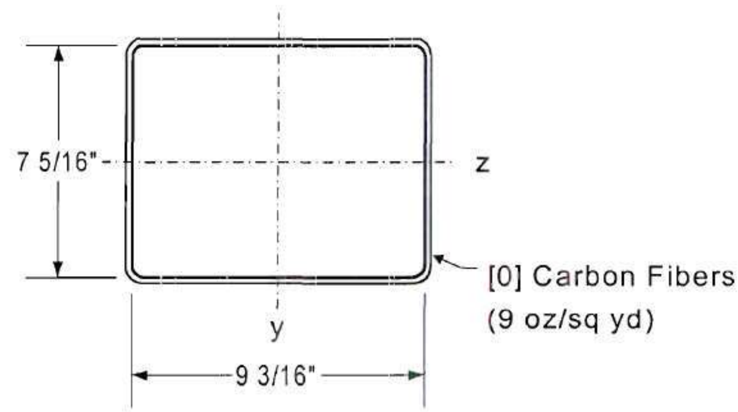

Figure 4.3: Cross section of specimen 4R1

Specimen 4R2: This specimen was specimen 4R1 with an added second layer of longitudinal carbon fibers; this resulted in a total of 18 oz./sq. yd. of carbon fibers. The cross section is shown in Figure 4.4.

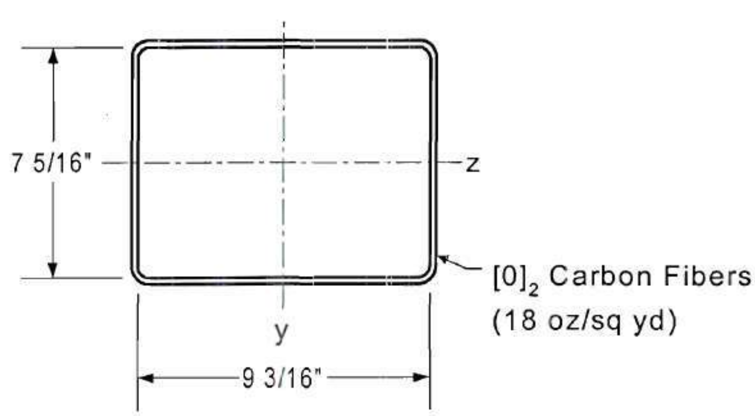

Figure 4.4: Cross section of specimen 4R2

Seatimber®

Specimens 5 and 6: These specimens were manufactured from recycled plastics with no bar reinforcement. The matrix recycled plastic composition consists of a cold core, blown air and no fiberglass. The dimensions of the cross section are 12 inches x 8 inches and is shown in Figure 4.5.

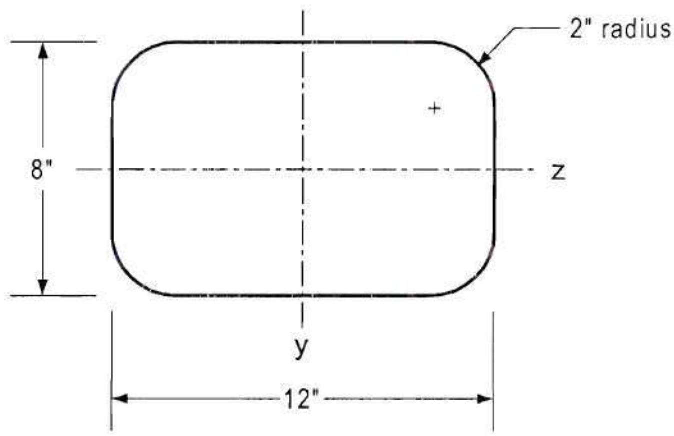

Figure 4.5: Cross section of specimen 5 and specimen 6

Specimen 7 and 8: These specimens were manufactured from recycled plastics with 4 - 1.25-inch diameter E-glass reinforcement bars and was tested as received. The recycled plastic matrix composition consists of a cold core and blown air. Specimen 7 had no fiberglass, while specimen 8 had fiberglass. The dimensions of the cross section are 12 inches x 8 inches as shown in Figure 4.6.

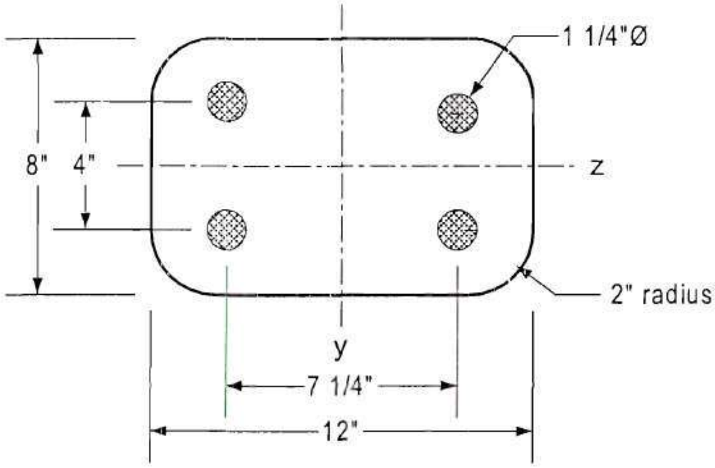

Figure 4.6: Cross section of specimen 7 and specimen 8

Specimen 9: This specimen was manufactured from recycled plastics with 12 - 0.5-inch diameter E-glass reinforcement bars and was tested as received. The dimensions of the cross section are 12 inches x 8 inches. The cross section and the location of reinforcement are shown in Figure 4.7.

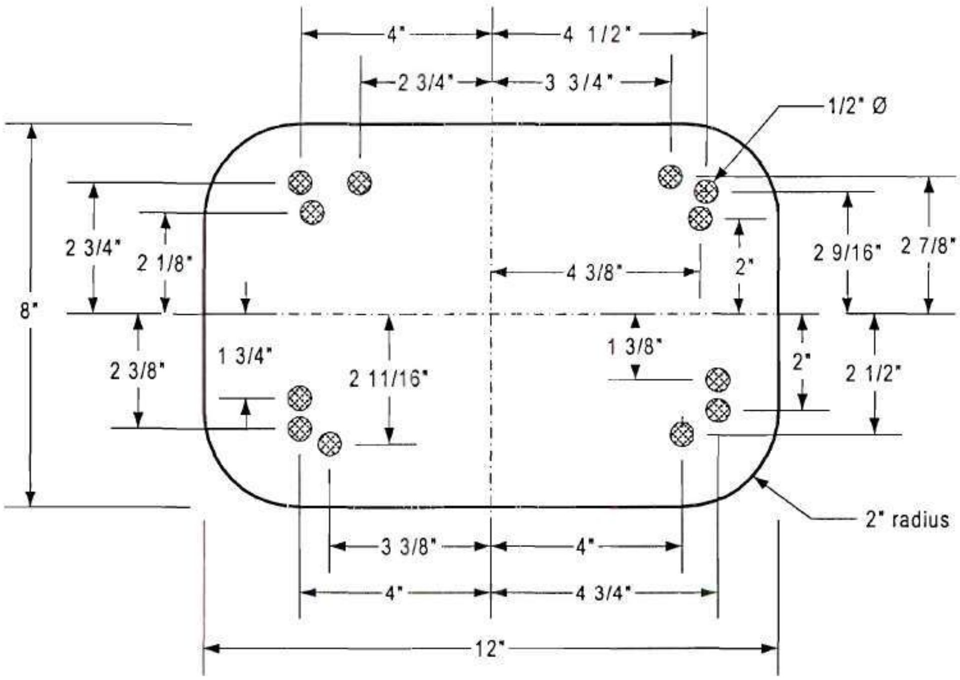

Figure 4.7: Cross section of specimen 9

Specimen 10: This specimen manufactured from recycled plastics with 12 - 0.50-inch diameter E-glass reinforcement bars and was tested as received. The dimensions of the cross section are 12 inches x 8 inches. The cross section and the location of reinforcement are shown in Figure 4.8.

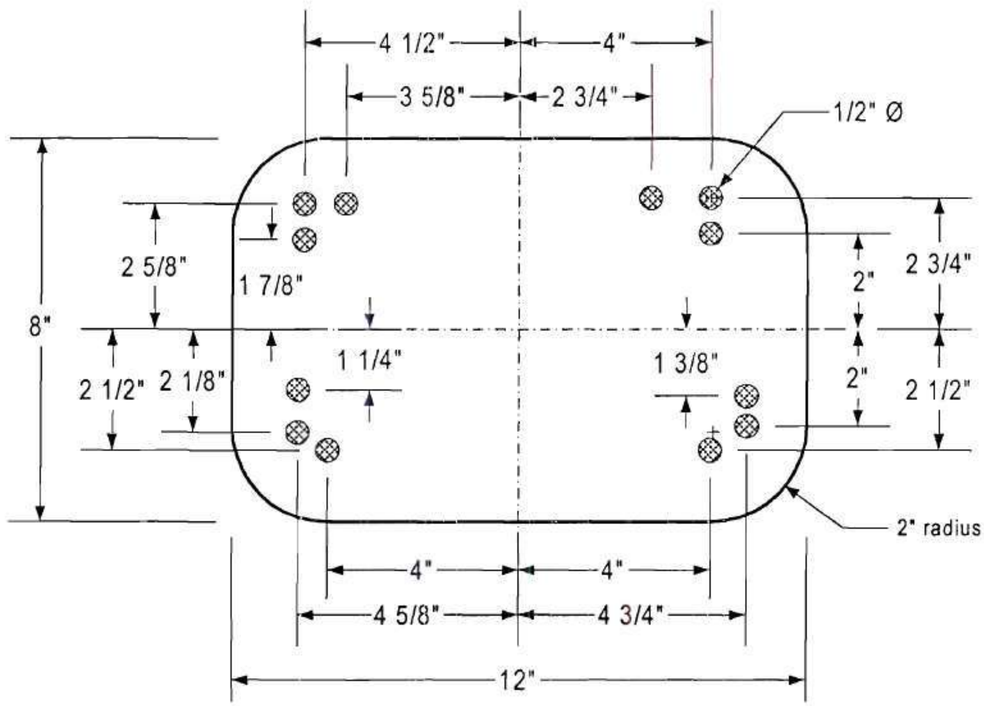

Figure 4.8: Cross section of specimen 10

Specimen 11: This specimen was manufactured from recycled plastics with 4 - 0.50-inch diameter E-glass reinforcement bars and was tested as received. The dimensions of the cross section are 12 inches x 8 inches. The cross section and the location of reinforcement are shown in Figure 4.9.

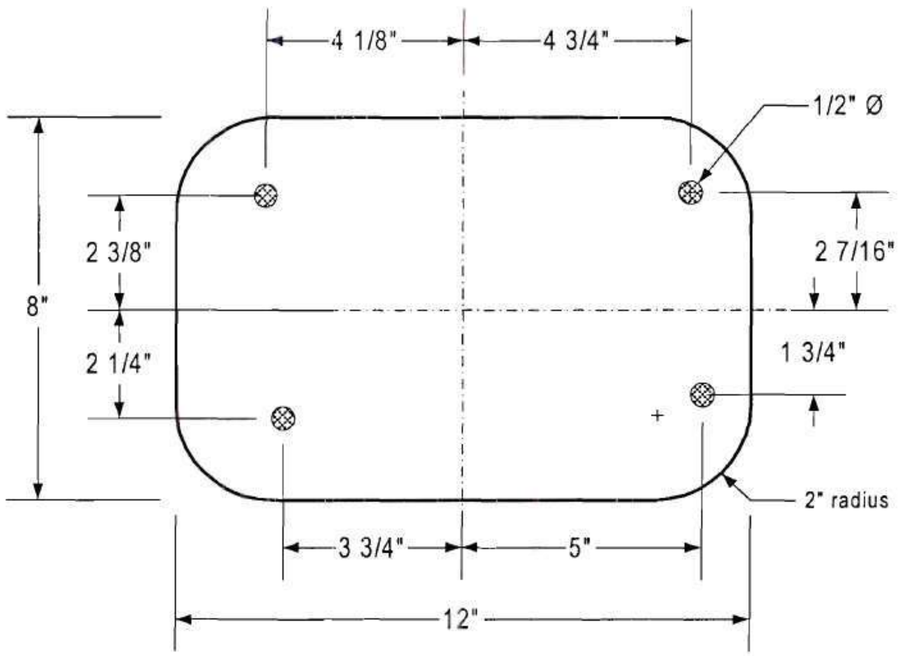

Figure 4.9: Cross section of specimen 11

Specimen 12R1: This specimen was an 8 inches x 12 inches Seatimber® reinforced externally with one layer of longitudinal reinforcement with 9oz/sq. yd. of carbon fibers. The cross section is shown in Figure 4.10.

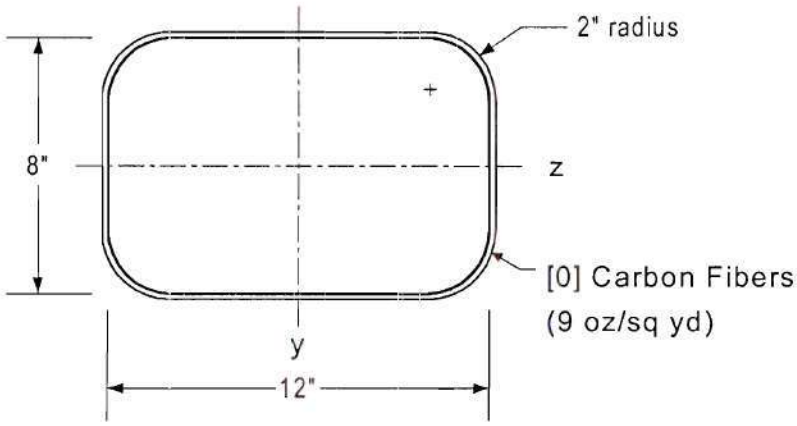

Figure 4.10: Cross section of specimen 12R1

Specimen 12R2: This specimen was specimen 12R1 with an added second layer of longitudinal carbon fibers; this resulted in a total of 18 oz./sq. yd. of carbon fibers. The cross section is shown in Figure 4.11.

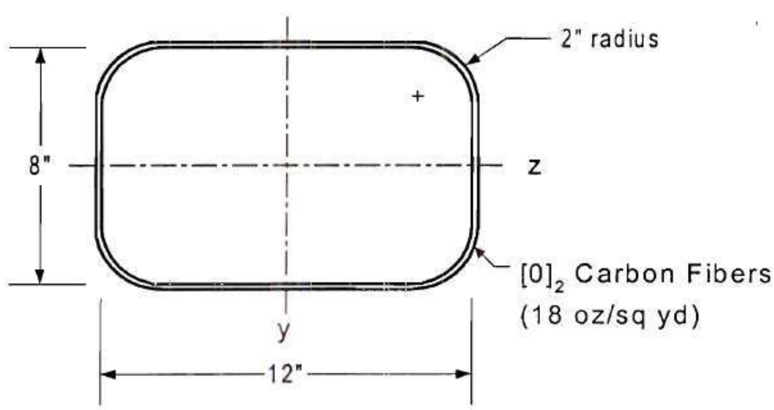

Figure 4.11: Cross section of specimen 12R2

Test Set-up and Procedure

All full-scale beam tests were three point bending with a span of 8 feet and an approximate span to depth ratio of 12:1. The boundary conditions consisted of knife-edge supports centered on a six-inch bearing length as shown in Figure 4.12. The load was applied with a mechanical screw driven Reihle testing machine. Attached to the head of the press was an Interface 100 kip load cell and a 12-inch long steel pipe with a six-inch diameter pipe which was used to transfer the load to the beam (Figure 4.12). A wire potentiometer was used to measure the mid-span displacement (δ). Data were recorded with a Megadac data acquisition system at the rate of two readings per second. The beams were not loaded to failure, but to a maximum deflection between 0.25 and 0.5 inches.

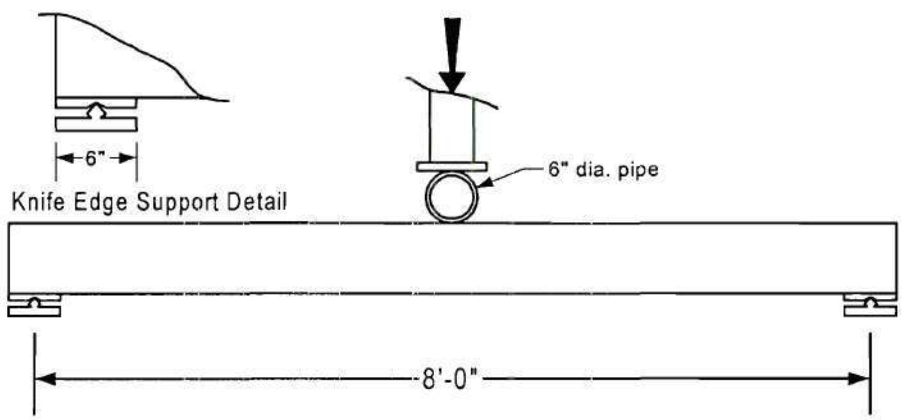

Figure 4.12: Elevation view of full-scale test set-up

Full-Scale Results

For all full-scale specimen, the apparent flexural stiffness (D_z) was determined from the linear regression line of the load (P) - deflection (δ) curve. The regression was performed on data between the limits 0.0 inches < δ < 0.25 inches using equation (7):

$$D_z = \frac{P}{\delta}\frac{L^3}{48} \tag{7}$$

where the length (L) is 96 inches and δ is the mid-span deflection. The apparent flexural modulus (E_a) was determined by the following equation:

$$E_a = \frac{D_z}{I_z} \tag{8}$$

Results

Figure 4.13, Figure 4.14 and Figure 4.15 show the load - deflection curves at a 8 foot span of the full-scale specimens about their weak axis (z-axis). The load - strain curves of the 1-layer carbon composite wrapped beams are shown in Figure 4.16. The D_z of beam specimens, as well as the modulus of elasticity (E_z) of the unreinforced specimens is shown in Table 4.1.

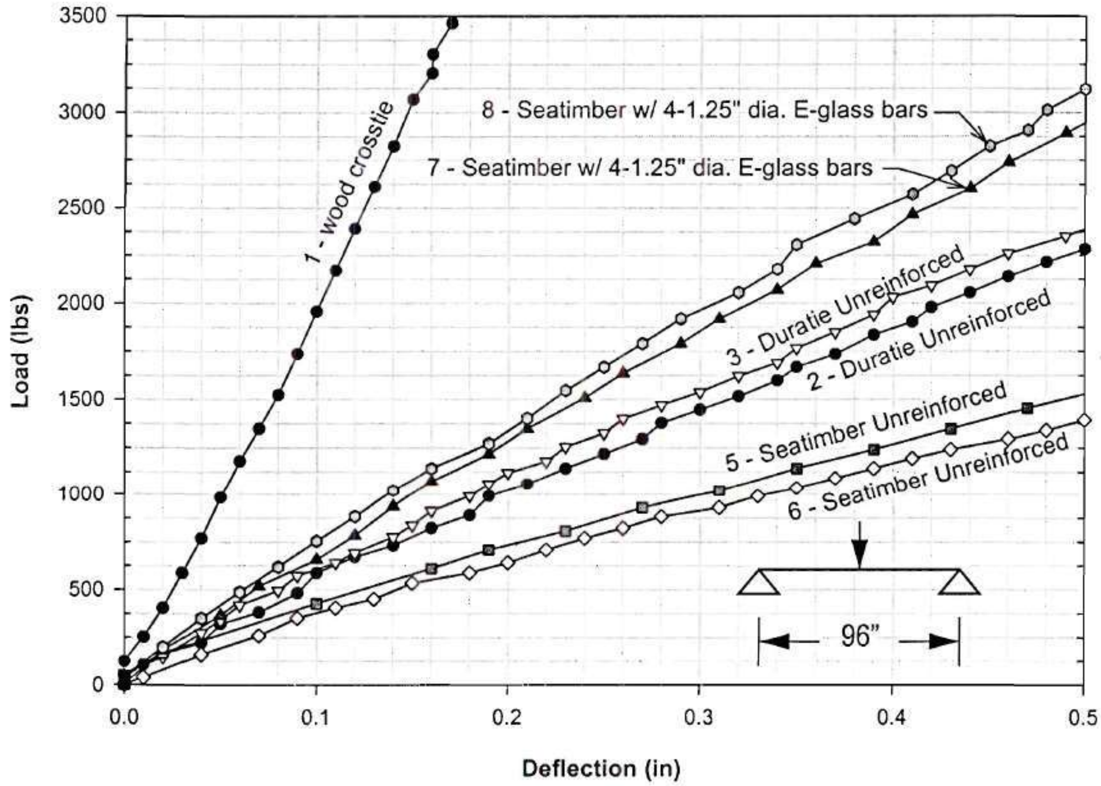

Figure 4.13: Load - deflection curves of specimens 1, 2, 3, 5, 6, 7, and 8

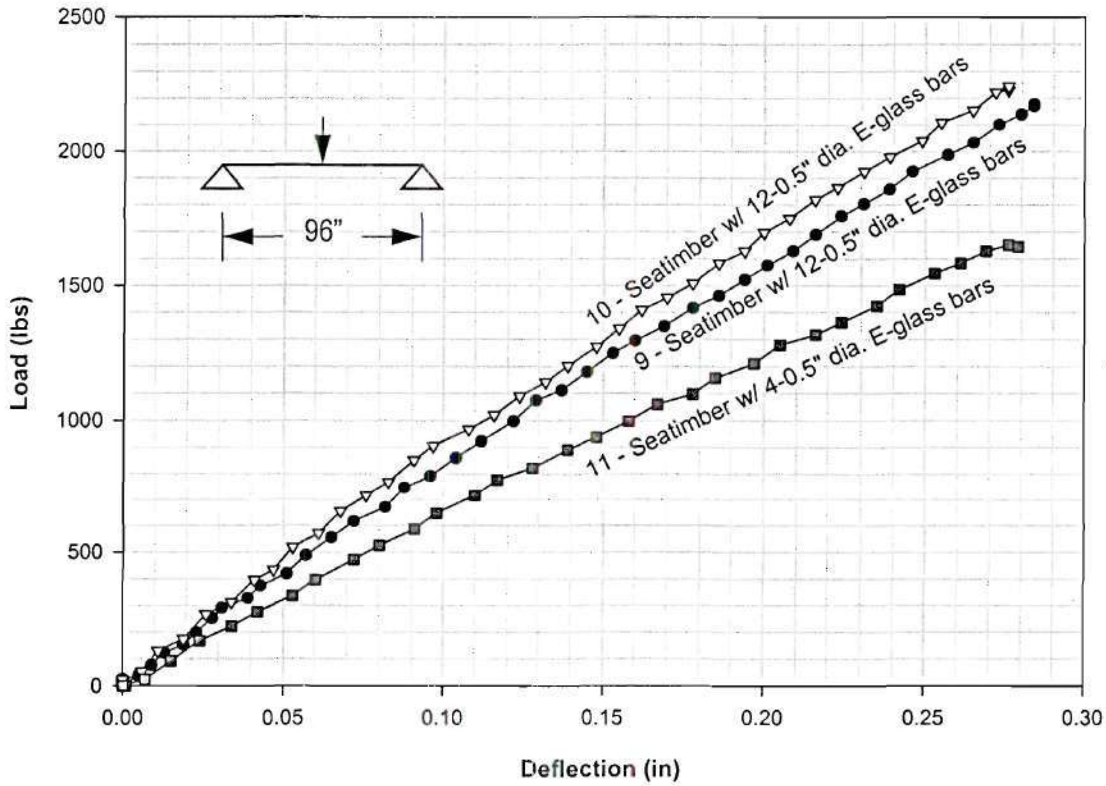

Figure 4.14: Load - deflection curves of full-scale specimens with 0.5-inch bars

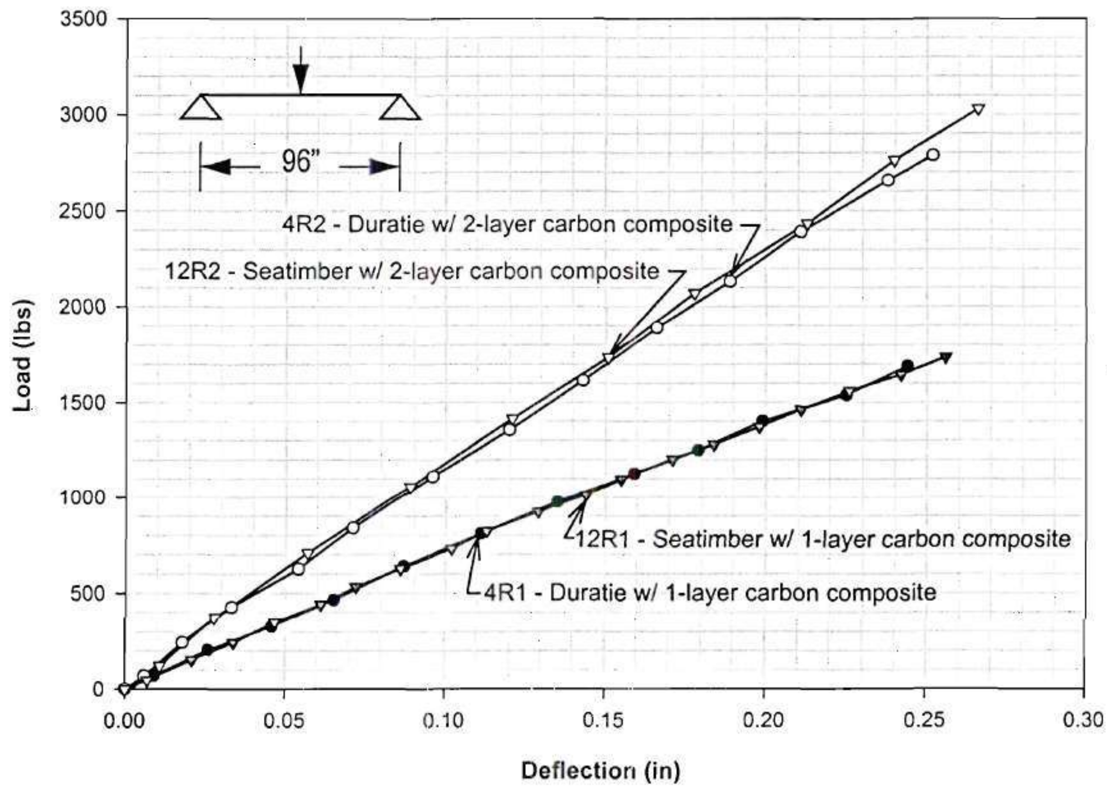

Figure 4.15: Load - deflection curves of full-scale specimens with carbon wrap

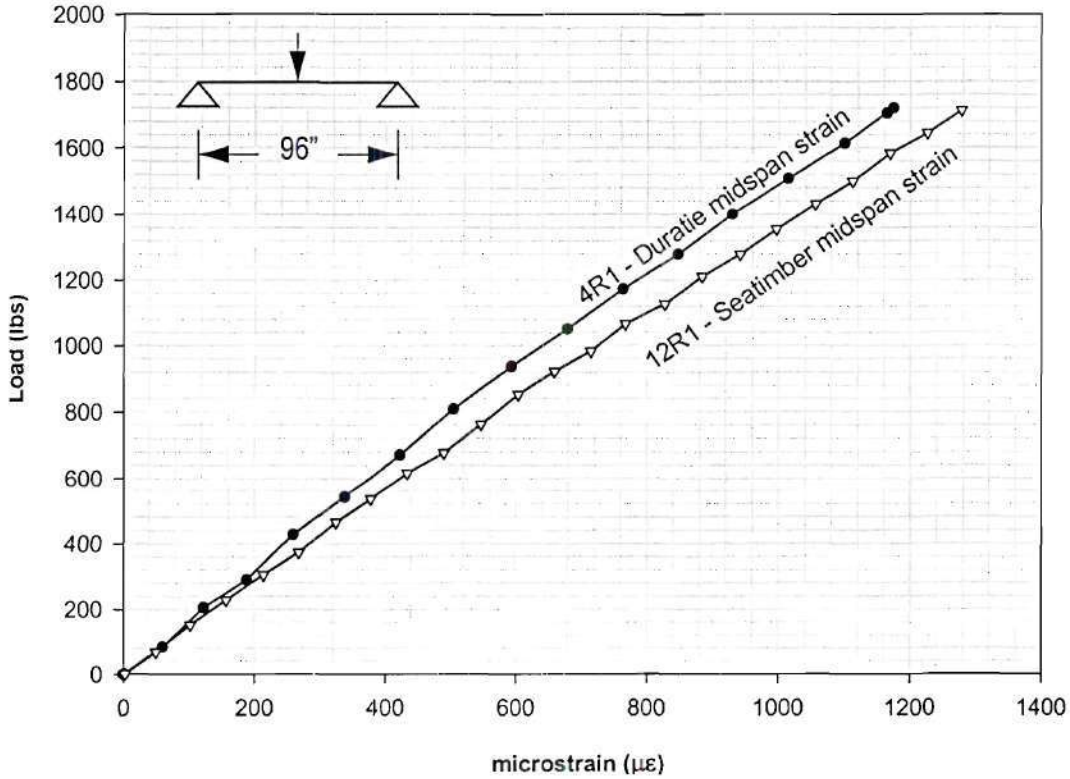

Figure 4.16: Strain comparison of the 1-layer carbon wrapped specimens

Table 4.1: Average apparent stiffness full-scale specimens 1 through 12

Specimen Number	Specimen Description	D_z (kip-in^2)	I_z (in^4)	E_a (ksi)
1	Wood Crosstie	345,066	217.85	1,584.0
2	Duratie® Unreinforced	76,253	299.37	254.7
3	Duratie® Unreinforced	80,328	299.37	268.3
4R1	Duratie® 1-layer carbon wrap	126,655		
4R2	Duratie® 2-layer carbon wrap	204,761		
5	Seatimber® Unreinforced	54,225	468.11	115.8
6	Seatimber® Unreinforced	49,064	468.11	104.8
7	Seatimber® 4 -1.25" dia. E-glass bars	105,285		
8	Seatimber® 4 -1.25" dia. E-glass bars	111,842		
9	Seatimber® 12 - 0.5" dia. glass bars	143,991		
10	Seatimber® 12 - 0.5" dia. glass bars	153,852		
11	Seatimber® 4 - 0.5" dia. glass bars	114,389		
12R1	Seatimber® 1-layer carbon wrap	126,086		
12R2	Seatimber® 2-layer carbon wrap	212,410		

Discussion of full-scale Results

The modulus of the 1.25-inch diameter and 0.5-inch diameter E-glass reinforcing rods were both assumed to be equal to 5,000 ksi. If this assumption was correct, the stiffness of specimens with more reinforcement area should be greater than stiffness of the specimens with a smaller cross sectional area.

The stiffness of the Seatimber® specimen with the internal E-glass bar reinforcement at least doubled. The ratio of the average stiffness of specimen 7 and specimen 8 (109,000 kip-in^2) to the average stiffness of the specimen 5 and specimen 6 (51,600 kip-in^2) is 2.10.

The two layer carbon reinforced specimens had the highest stiffness. The wood crosstie was the stiffest of the full-scale beams tested.

CHAPTER V

ANALYSIS OF REINFORCED SPECIMENS

The analysis of the previously tested reinforced specimens from the previous chapters is presented in this chapter. This analysis is based on the assumption that the materials behave linear and elastically. This is reasonably true for the initial stages of loading, but the recycled plastic materials are known to creep under sustained load and the stiffness is affected by the loading rate. All properties used in the analysis were limited to the initial loading stage for which the ratio of the deflection over the span length (δ/L) was less than 1/384 for the full-scale beam specimens and less than 1/192 for the small-scale beam specimens

The reinforced specimens are divided into three groups:

• Full-scale specimens with internal E-glass reinforcing bars.

• Full-scale specimens reinforced with carbon fabric system.

• Small-scale specimens with four - 1/2-inch wide reinforcing strips

Full-scale Specimens with Internal E-glass Reinforcing Bars

In this section, five Seatimber® specimens (7, 8, 9, 10, and 11) reinforced with E-glass reinforcing bars are analyzed. All of the specimens were the 8-inch x 12-inch Seatimber® cross section, but the number and diameter of the reinforcing bars varied among the specimens. The modulus of elasticity of the E-glass reinforcing bars (E_r) was assumed to be 5,000 ksi, which corresponds to a glass fiber volume of approximately 50%. The modulus of elasticity of the matrix material (E_m) was assumed to be equal to the average initial apparent modulus of elasticity (E_a) of the unreinforced Seatimbers®, specimens 5 and 6, as presented in Table 5.1.

Table 5.1: Average apparent modulus (E_m) of unreinforced Seatimbers®

Specimen Number	Specimen Description	Average Apparent Modulus E_a (ksi)
5	unreinforced Seatimber®	115.8[a]
6	unreinforced Seatimber®	104.8[a]
Average Modulus of Matrix Material E_m		110.3

a. Values from Table 4.1

Figure 5.1, Figure 5.2 and Figure 5.3 present the assumed strain and corresponding force diagrams for specimens reinforced with internal E-glass reinforcing bars. In these figures the strain at the top of the cross section (ε_{top}) was taken as the reference value for subsequent calculations. The neutral axis is assumed to be located at the mid height of the cross section.

The resultant forces of the matrix material (F_{top}, F_{bot}) are calculated by averaging the stress wedge multiplied by the respective cross sectional area:

$$F_{top} = -F_{bot} = \frac{\varepsilon_{top} E_m}{2} \frac{A_m}{2} \tag{9}$$

where A_m is the gross cross sectional area of the matrix material (92.56 in^2). The resultant force of the matrix material is then located at the centroid of the stress wedge.

The resultant forces of the reinforcing material (F_1, F_2, F_3,... F_n) are calculated by multiplying the stress at the centroid of the reinforcement area and the reinforcement area (A_r).

$$F_i = \left(\frac{d_i \varepsilon_{top}}{c} - \varepsilon_{top}\right) E_m (n-1) A_r \tag{10}$$

where d_i is the distance from the base line to the centroid of the respective reinforcement, as seen in Figure 5.1, Figure 5.2 and Figure 5.3. Half the depth of the cross section is (c). Since the reinforcement material is within the matrix material, the expression $E_m(n-1)$ is used instead of E_r. This expression allows the previous calculation of the matrix resultant force to be constant, without removing the areas occupied by the reinforcement. The modulus ratio (n) is defined by equation (11):

$$n = \frac{E_r}{E_m} \tag{11}$$

where E_r and E_m are the modulus of elasticity values of the E-glass reinforcing bars and the matrix respectively.

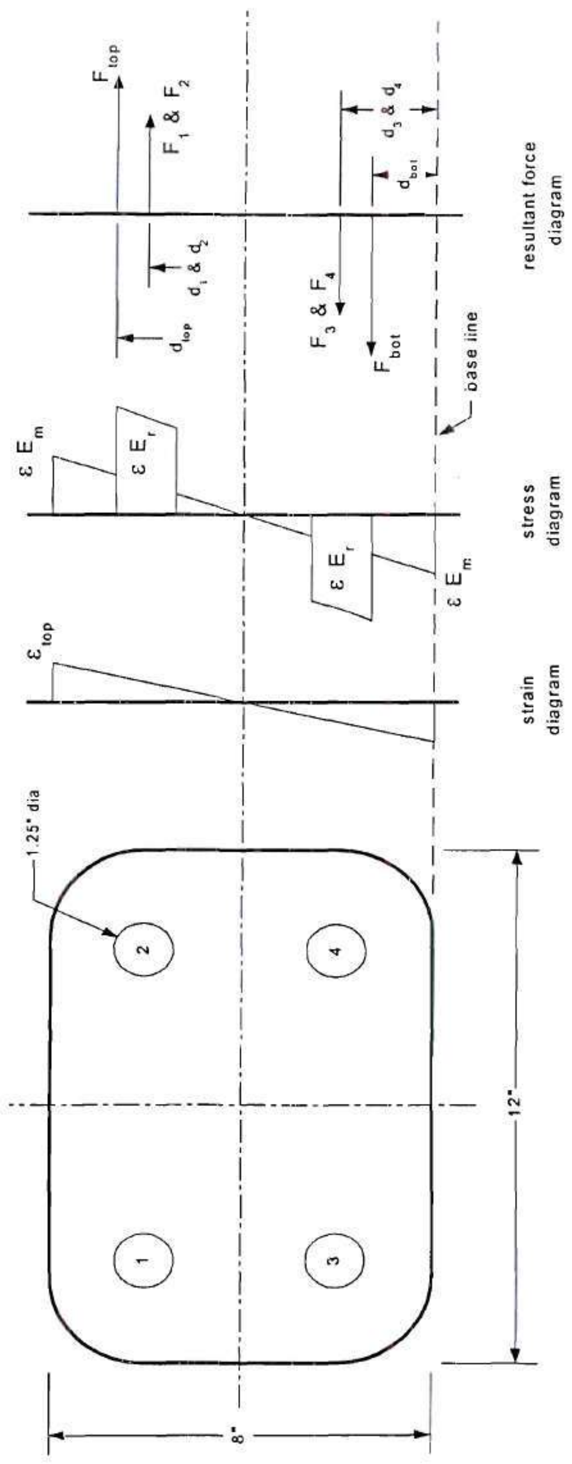

Figure 5.1: Cross section of Seatimber® with four 1.25-inch diameter E-glass reinforcement bars (a) strain diagram (b) stress diagram (c) resultant force diagram

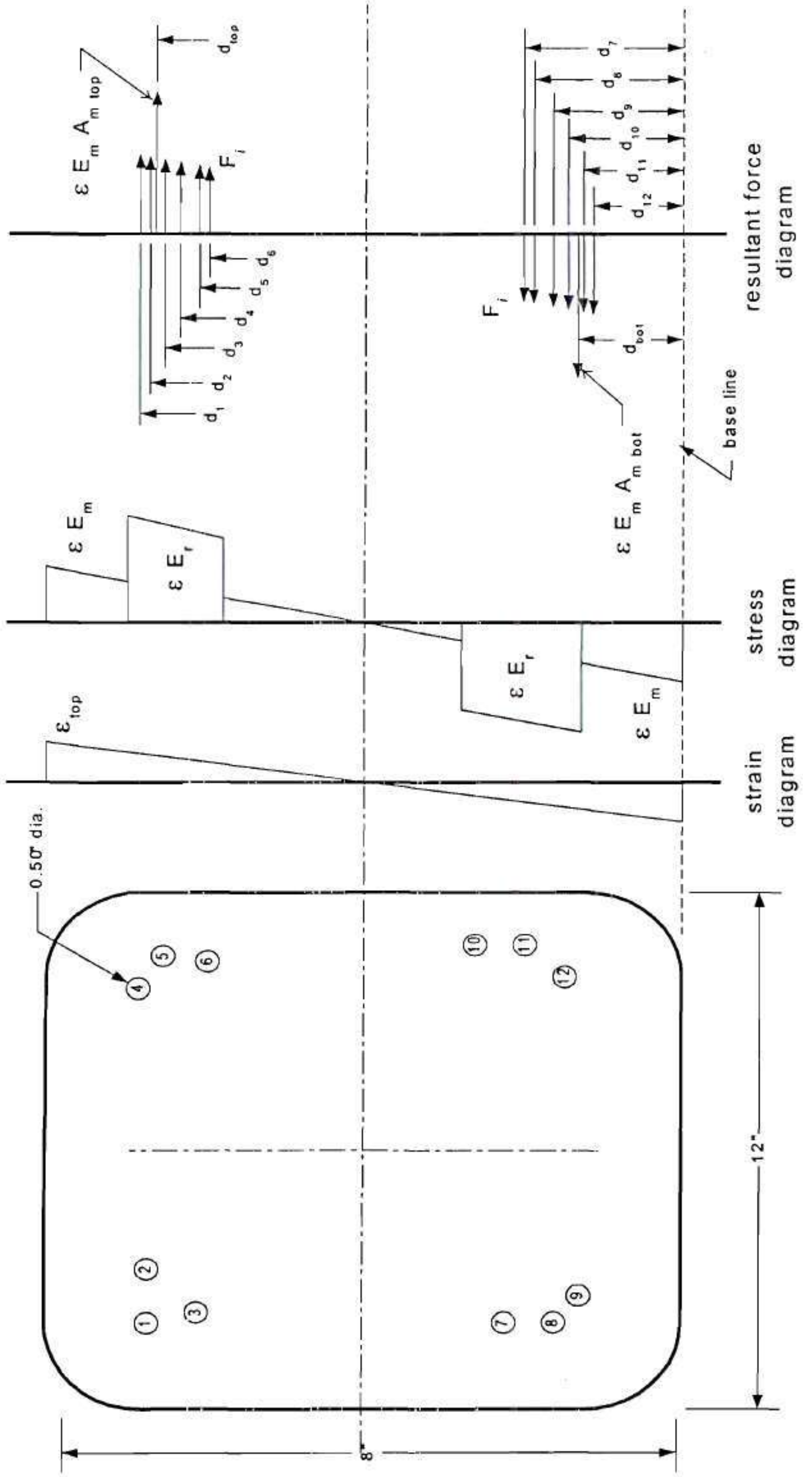

Figure 5.2: Seatimber® cross section with 12 - 0.5-inch diameter E-glass reinforcement bars (a) strain diagram (b) stress diagram (c) resultant force diagram

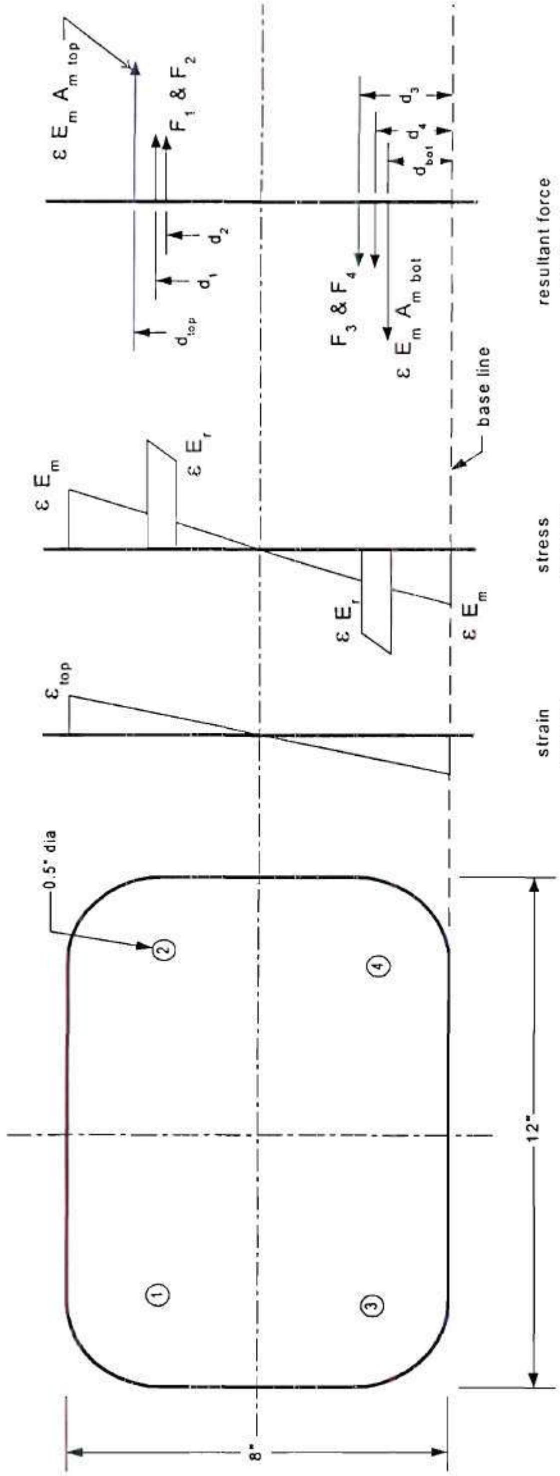

Figure 5.3: Cross section of Seatimber® with four 0.5-inch diameter E-glass reinforcement bars (a) strain diagram (b) stress diagram (c) resultant force diagram

The moment, M, of was computed from the following equation:

$$M = F_{top}\, d_{top} + F_{bot}\, d_{bot} + \sum_{i=1}^{n} F_i\, d_i \tag{12}$$

The apparent stiffness of the composite cross section, D_z^{cal}, can be then calculated using the following equation:

$$D_z^{cal} = \frac{M c}{\varepsilon_{top}} \tag{13}$$

The results of the equations and the ratio of the experimental initial apparent stiffness, D_z, to the calculated apparent stiffness, D_z^{cal}, are given in Table 5.2.

Table 5.2: Experimental and analytical results of full-scale specimens reinforced with E-glass bars

Specimen	reinforcing system	E_m (ksi)[(a)]	$E_{reinf.}$ (ksi)[(b)]	D_z (kip-in^2)	D_z^{cal} (kip-in^2)	$\frac{D_z}{D_z^{cal}}$
7	4 - 1.25" dia. glass reinf.	110.3	5,000	105,285	150,300	0.700
8	4 - 1.25" dia. glass reinf.	110.3	5,000	111,842	150,300	0.744
9	12 - 0.5" dia. glass reinf.	110.3	5,000	143,991	133,100	1.082
10	12 - 0.5" dia. glass reinf.	110.3	5,000	153,852	129,700	1.186
11	4 - 0.5" dia. glass reinf.	110.3	5,000	114,389	76,340	1.498

a. Value from average apparent modulus of specimen 5 and 6 see Table 5.1
b. Assumed value

<u>Specimens Reinforced with Carbon Fabric</u>

This set of specimens were unreinforced when received. Specimen 12 was an 8-inch x 12-inch Seatimber® beam that was first reinforced with one (12R1), and then with two layers (12R2) of unidirectional carbon fiber composite sheet. Specimen 4 was a full-scale Duratie® beam that was also reinforced with one (4R1) and then two layers (4R2) of carbon fiber composite sheet. A single layer of unidirectional carbon fabric weighed 9 oz./yd^2. The thickness of the carbon composite wrap was found using equation (14) and (15). First, the ratio of fiber content by weight was found using equation (14):

$$\frac{\omega_m}{\omega_f} = \frac{\rho_m}{\rho_f}\frac{V_m}{V_f} \tag{14}$$

where $(\rho_m/\rho_f)$is the density ratio of the matrix material over the fiber material. Then (V_m/V_f) is the volume ratio of the epoxy matrix content over the fiber content. The density of the carbon fibers, ρ_f, is 110 pcf and the density of the matrix material, ρ_m, is 72pcf. The volume ratios were assumed to be 30 percent, 62 percent, and 8 percent for the fibers, matrix, and voids respectively. The ratio of fiber content by weight (ω_m/ω_f) was then used to calculate the thickness, t, of the carbon FRP fabric from equation (15):

$$t = w_a\left[\frac{1}{\rho_f} + \frac{\omega_m}{\omega_f}\frac{1}{\rho_m}\right] \tag{15}$$

The nominal fiber areal weight of the carbon fibers (w_a) was 9 oz/yd.^{2}. The thickness, t, was calculated as 0.021 inches per layer.

The Duratie® and Seatimber® cross sections are shown in Figure 5.4. The average flexural modulus values of the matrix material (E_m) for the Seatimber® and for Duratie®

are 110.3 ksi and 261.5 ksi respectively. The E_m for the Duratie® was found by averaging the E_a values from flexural test of specimen 2 and 3 as reported in Table 5.3.

Table 5.3: Average apparent modulus (E_a) of unreinforced Duraties®

Specimen Number	Specimen Description	Apparent Flexural Modulus E_a (ksi)
2	unreinforced Duratie®	254.7[a]
3	unreinforced Duratie®	268.3[a]
Average Modulus of Matrix Material E_m		261.5

a. Values from Table 4.1

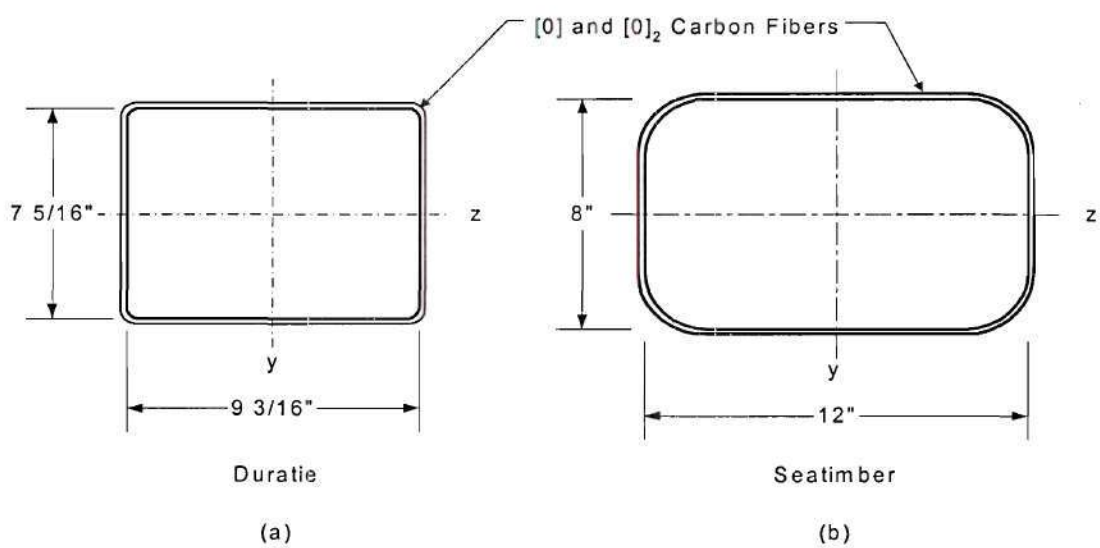

Figure 5.4: Carbon wrapped cross sections of (a) Duratie® and (b) Seatimber®

Specimens reinforced with carbon fiber composites

Figure 5.5 and Figure 5.6 present the assumed strain and corresponding force diagrams for specimens reinforced with an external carbon fiber composite. In these figures, the strain at the top of the cross section (ε_{top}) was taken as the reference value for subsequent calculations.

The resultant forces of the matrix material (F_{top}, F_{bot}) are calculated by averaging the stress wedge multiplied by the respective cross sectional area.

$$F_{top} = -F_{bot} = \left(\frac{d_i \varepsilon_{top}}{c} - \varepsilon_{top}\right) E_m \frac{A_m}{2} \qquad (16)$$

where c is one-half the depth of each specimen. The cross sectional area of the matrix material (A_m) is 92.56 in^2 for the Seatimber® specimen and 67.18in^2 for the Duratie® specimen. The resultant force of the matrix material is then located at the centroid of the stress wedge. This can be seen in Figure 5.5 and Figure 5.6.

The resultant forces of the reinforcing material (F_1, F_2,... F_n) are calculated by multiplying the average stress of the reinforcement section and the reinforcement area A_r:

$$F_i = \left(\frac{d_i \varepsilon_{top}}{c} - \varepsilon_{top}\right) E_r \; A_{ri} \qquad (17)$$

where d_i is the distance from the base line to the centroid of the respective reinforcement, as shown in Figure 5.5. For the Seatimber® specimens: A_1, A_3, A_8 and A_{10} are the corner radius sections of reinforcement; A_4, A_5, A_6 and A_7 represent the side sections of reinforcement, with each side split in two sections by the centroid of the cross section; A_2 and A_9 are the top and bottom sections of reinforcement respectively. For the Duratie® the specimens, the radii were not considered. A_1, A_2, are the top and bottom sections of reinforcement and A_3, A_4, A_5 and A_6 represent the side sections of reinforcement, with each side split in two sections by the centroid of the cross section. The modulus of elasticity of the reinforcing systems (E_r) was assumed to be 8,000 ksi. The location of the resultant force of the top, bottom and the curved sections of reinforcement, is located at the centroid of the reinforcement area. The resultant forces of the four sections of reinforcement laying vertical on the sides of the beam, are located at the centroid of the stress wedge and can be seen in Figure 5.5 and Figure 5.6.

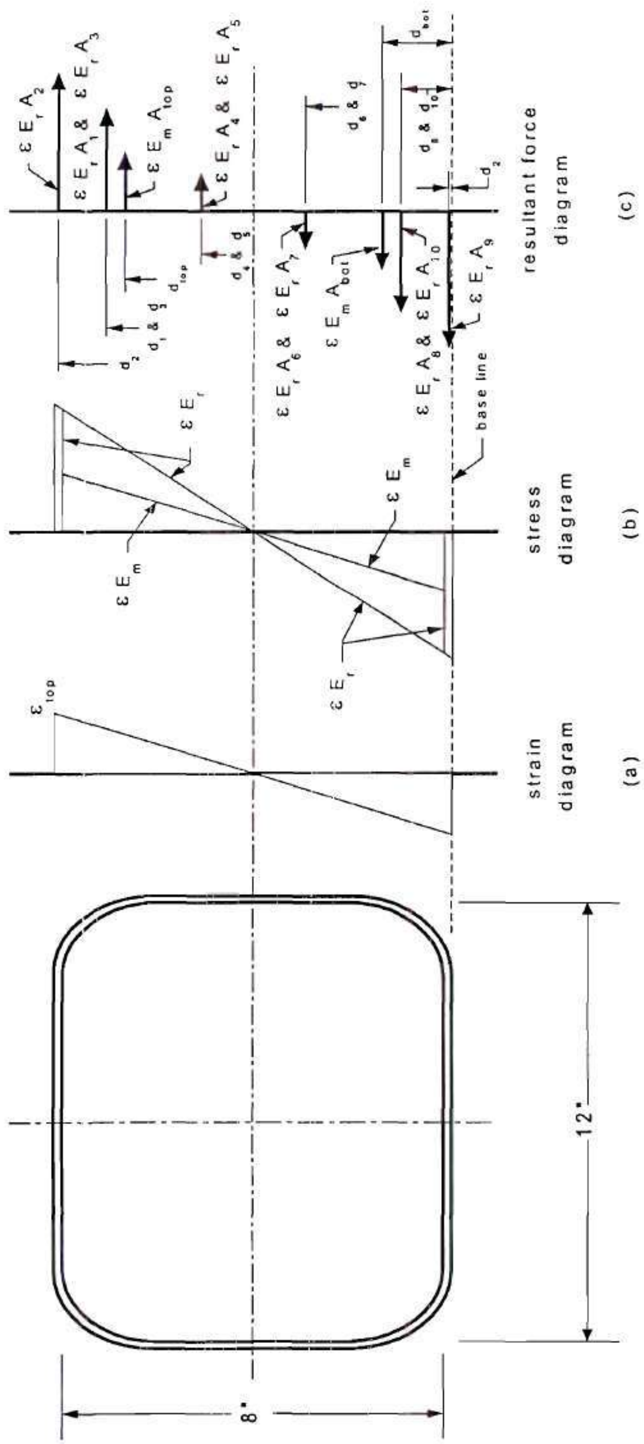

Figure 5.5: Cross section of a Seatimber® reinforced with carbon fabric
(a) strain diagram (b) stress diagram (c) resultant force diagram

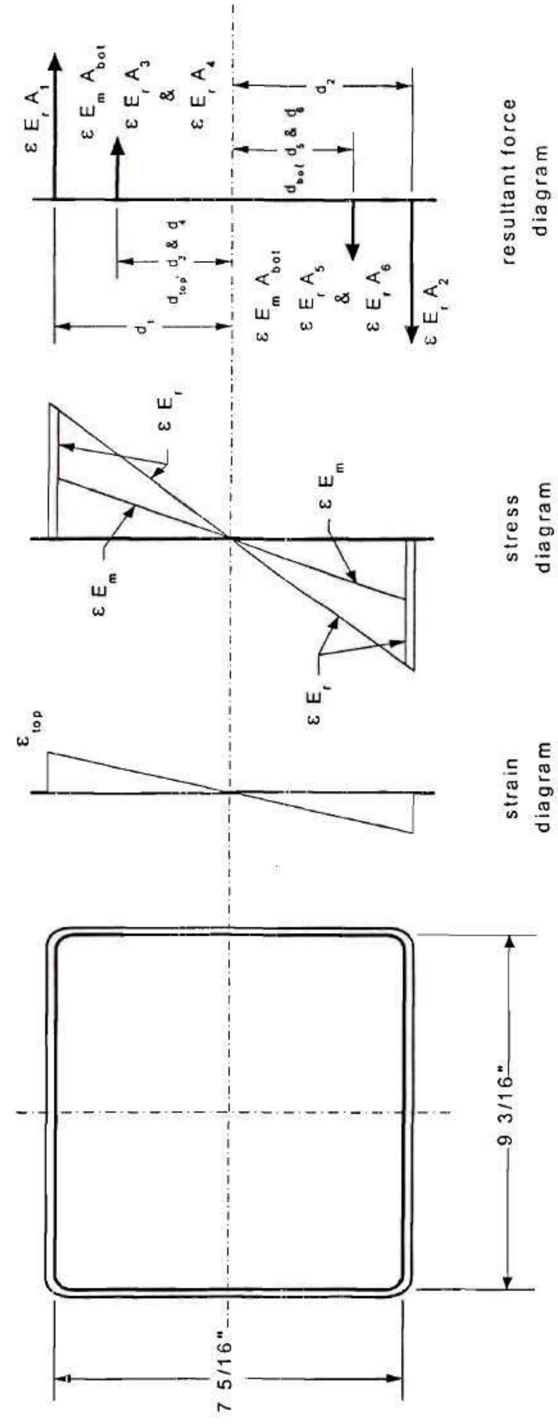

Figure 5.6: Cross section of a Duratie® reinforced with carbon fabric (a) strain diagram (b) stress diagram (c) resultant force diagram

The moment, M, was computed from equation (12). The calculated apparent stiffness (D_z^{cal}) was calculated from equation (13). Results of the calculations and the ratio of the experimental initial apparent stiffness, D_z, to calculated apparent stiffness, D_z^{cal}, are given in Table 5.4.

Table 5.4: Experimental and analytical results of full-scale specimens reinforced with carbon fabric

Specimen No.	specimen description	E_a^u (ksi)	$E_{reinf.}$ (ksi)	D_z (kip-in^2)	D_z^{cal} (kip-in^2)	$\frac{D_z}{D_z^{cal}}$
4R1	Duratie® w/1-layer carbon fabric	261.5	8,000	126,655	127,955	0.990
4R2	Duratie® w/2-layer carbon fabric	261.5	8,000	204,761	178,006	1.150
12R1	Seatimber® w/1-layer carbon fabric	110.3	8,000	126,086	122,008	1.033
12R2	Seatimber® w/2-layer carbon fabric	110.3	8,000	212,410	190,299	1.116

Small-scale Specimen with 4 - 1/2-inch Wide Reinforcing Strips

The last set of cross sections (RP23, RP24, RP 26 and RP28) analyzed was the small-scale specimens with a 1.5 inches x 1.5 inches square cross section with two reinforcement strips applied to the top and bottom of the unreinforced specimen as shown in Figure 5.7. Two different types of reinforcing material were analyzed, E-glass and carbon. Specimens RP24 and RP28 were reinforced with 1/2-inch wide E-glass strips, and specimens RP23 and RP26 were reinforced with 1/2-inch wide carbon strips. The stainless steel reinforcement system was not analyzed. The thickness of the E-glass and carbon are 0.04355 inches and 0.01282 inches, respectively. The modulus of elasticity of the matrix material (E_m) for each RP specimen was found by testing the unreinforced specimen in order to derive the initial modulus of the unreinforced specimen (E_a^u) before the reinforcement strips were applied. The E_r of the reinforcing system was found from tensile tests discussed in Chapter 3. The E_m and E_r for the four specimens is shown in Table 5.5.

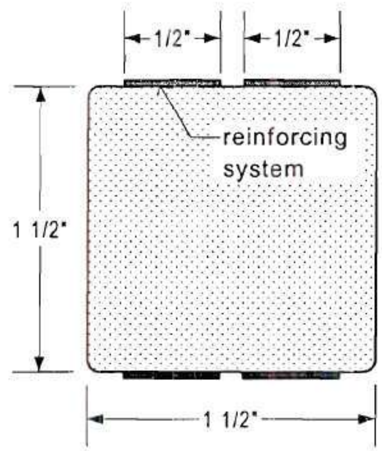

Figure 5.7: Typical cross section of small-scale specimen with four reinforcing strips

Table 5.5: Analytical values for reinforced small-scale specimens

Specimen	reinforcing system	Average Thickness (in)	c (in)	Average Area (A_r) (in^2)	E_m (ksi)	E_r (ksi)
RP 24	4 - E-glass strips	0.04355	.79355	2.12x10^{-2} in^2	617.5	4,875
RP 28	4 - E-glass strips	0.04355	.79355	2.12x10^{-2} in^2	198.6	4,875
RP 23	4 - carbon strips	0.01282	.76282	6.32x10^{-3} in^2	609.2	11,002
RP 26	4 - carbon strips	0.01282	.76282	6.32x10^{-3} in^2	216.3	11,002

Calculations related to the specimens reinforced with 1/2-inch strips

Figure 5.8 presents the assumed strain and corresponding force diagrams for specimens reinforced with externally with 1/2-inch reinforcing strips. In this figure, the strain at the top of the cross section (ε_{top}) was taken as the reference value for subsequent calculations. The neutral axis is assumed to be located at the mid height of the cross section.

The resultant forces of the matrix material (F_{top}, F_{bot}) are calculated similar to the full-scale specimen using equation (16), where the cross sectional area of the matrix material (A_m) is 2.25in^2. The resultant force of the matrix material is then located at the centroid of the stress wedge and can be seen in Figure 5.8.

The resultant forces of the reinforcing material (F_1, F_2, F_3 & F_4) are calculated by multiplying the stress at the centroid of the reinforcement area and the reinforcement area (A_r),

$$F_i = \left(\frac{d_i \varepsilon_{top}}{c} - \varepsilon_{top}\right) E_r\ A_r \tag{18}$$

where d_i is the distance from the base line to the centroid of the respective reinforcement, as shown in Figure 5.8. The modulus of elasticity of the reinforcing systems (E_r) can be found in Table 5.5. The location of the resultant force of the reinforcement is at the centroid of the reinforcement area and can be seen in Figure 5.8.

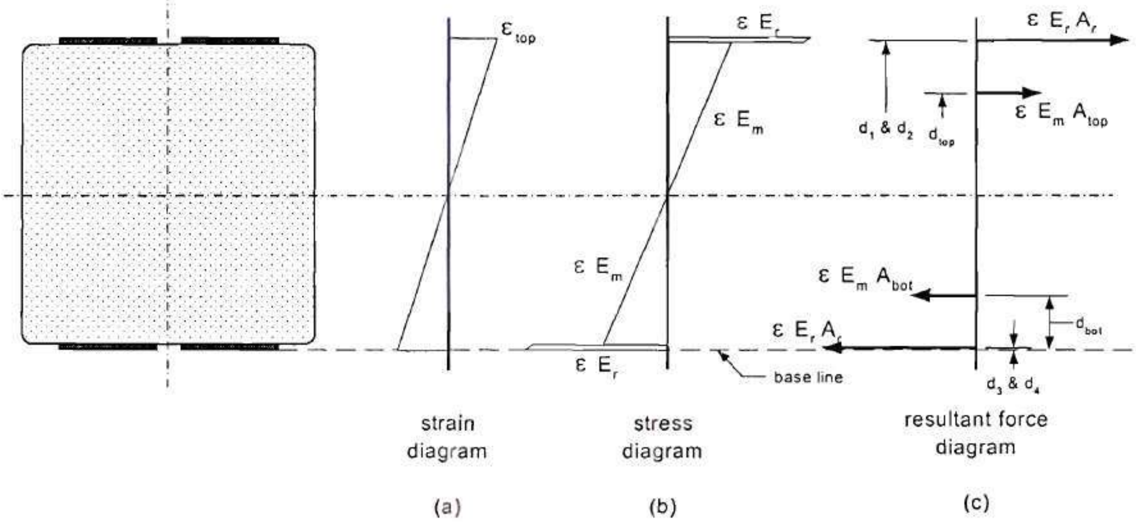

Figure 5.8: Cross section of the RP specimen with 4 - 1/2-inch wide reinforcing straps (a) strain diagram (b) Stress diagram (c) resultant force diagram

The moment (M) was calculated from following equation:

$$M = F_{top} d_{top} + F_{bot} d_{bot} + \sum_{i=1}^{4} F_i d_i \qquad (19)$$

The calculated apparent stiffness (D_z^{cal}) was calculated from equation (13). Results of the calculations and the ratio of the experimental initial apparent stiffness, D_z, to calculated apparent stiffness, D_z^{cal}, are given in Table 5.6.

Table 5.6: Experimental and analytical results of reinforced small-scale specimens

Specimen	reinforcing system	E_a^u (ksi)	$E_{reinf.}$ (ksi)	D_z (kip-in^2)	D_z^{cal} (kip-in^2)	$\frac{D_z}{D_z^{pre}}$
RP 24	4 - E-glass strips	617.5	4,875	531.6	506.3	1.050
RP 28	4 - E-glass strips	198.6	4,875	348.2	329.6	1.057
RP 23	4 - carbon strips	609.2	11,002	438.6	416.0	1.054
RP 26	4 - carbon strips	216.3	11,002	259.8	250.3	1.038

Sensitivity Analysis

A sensitivity analysis was performed where in the analysis from this chapter was altered by changing each variable by up to five percent, while holding the other variables constant. The ratio (D_z/D_z^{cal}) was plotted with respect to the percent the variable was altered. Each plot for each variable was combined on one graph for each specimen. The slope of the line is proportional to the effect the variable has on the analysis. The sensitivity analysis was conducted on one specimen from the internally reinforced full-scale specimen (specimen 8), a full-scale carbon wrapped specimen (specimen 12R1) and a small-scale specimen with the four 0.5-inch wide reinforcing strips (specimen 24).

The sensitivity analysis of Specimen 8 shows that the diameter of the reinforcement (R_{dia}) has the greatest effect on the D_z/D_z^{cal} of the composite beam, as shown in (Figure 5.9). The next steepest lines represent the reinforcement modulus and the matrix modulus. The area of the reinforcing material has the greatest impact on the analysis of the internally reinforced beams. The reinforcement properties such as the area and modulus, are proportional to the stiffness of the overall beam. By just increasing the diameter of the reinforcement (R_{dia}) by 5% (< 1/32 inch), the stiffness of the specimen increases by 15%.

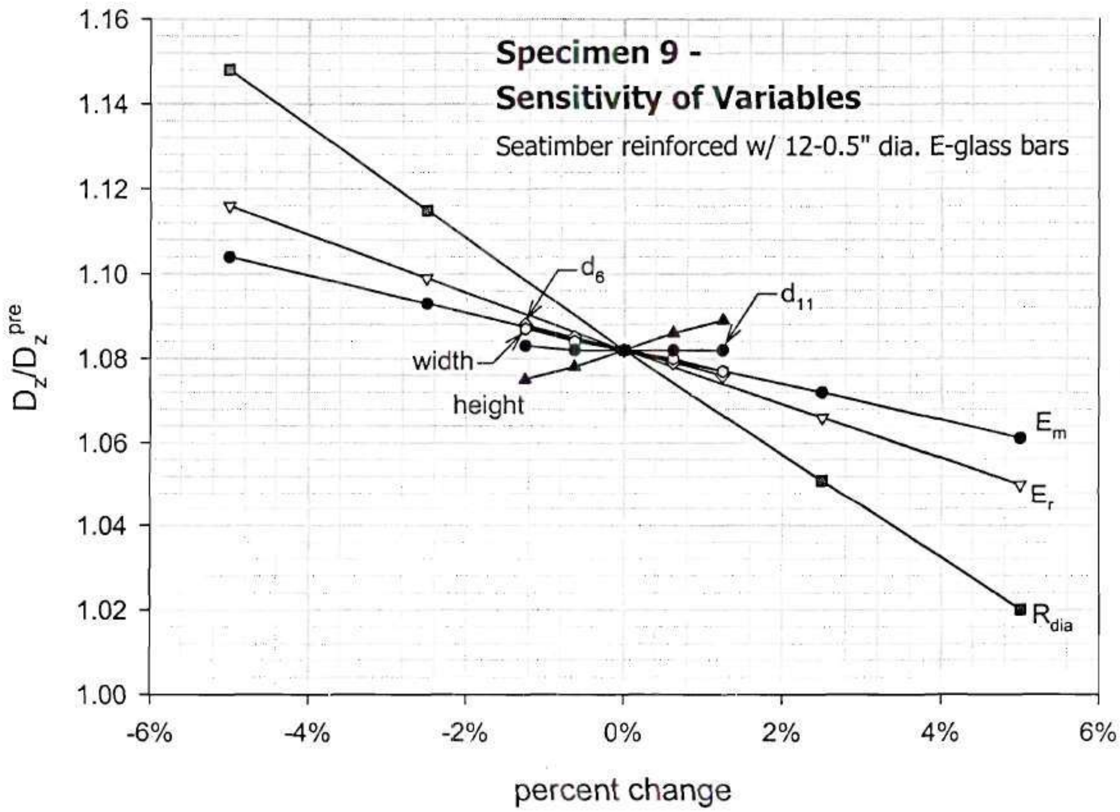

Figure 5.9: Sensitivity Analysis of specimen 9

The next sensitivity analysis is presented for Specimen 11, which is a Seatimber® section (Figure 5.5) with 1-layer externally applied carbon FRP wrap. For this sensitivity analysis the height of the cross section has the greatest effect on the variation of D_z/D_z^{cal}, as shown in Figure 5.10. The width of the cross section is the next steepest line. The height of the cross section controls where the location of the top and bottom sections of reinforcement, as well as the moment of inertia of the section ($I = bh^3/12$).

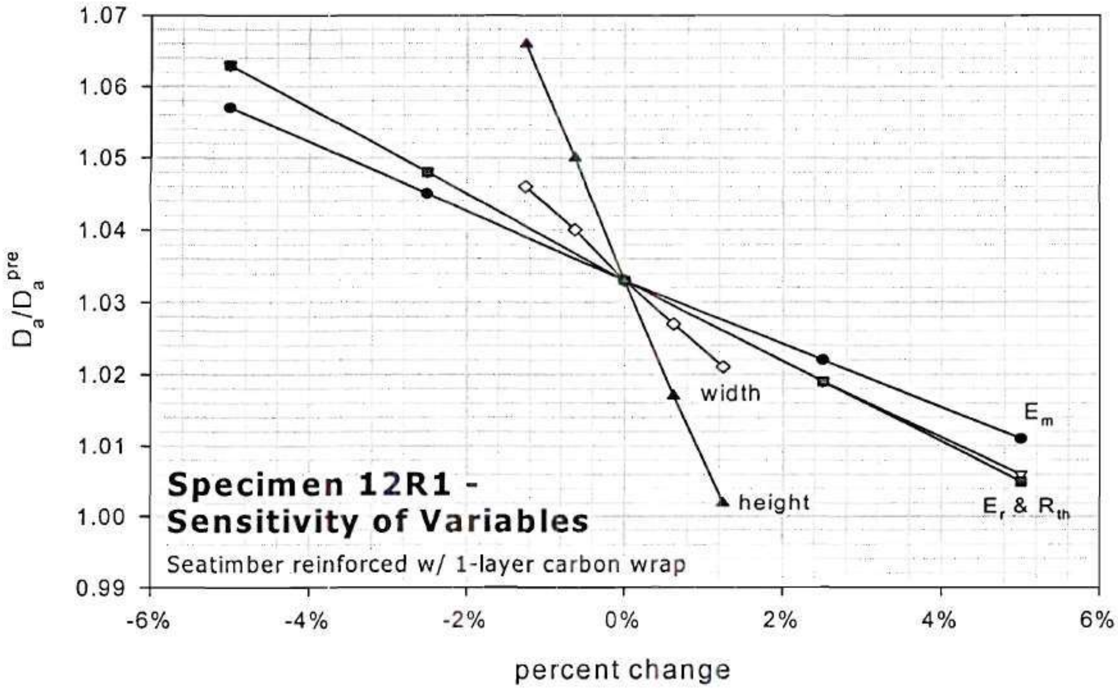

Figure 5.10: Sensitivity analysis of specimen 12R1

The third sensitivity analysis is presented for specimen 24 is a small-scale specimen reinforced with four 0.5-inch wide E-glass stripe (Figure 5.8). This is very similar to the sensitivity test of specimen 12R1. The height has a great impact on the analysis. All other variables' effect are equal as shown in by the equal slopes shown in Figure 5.11.

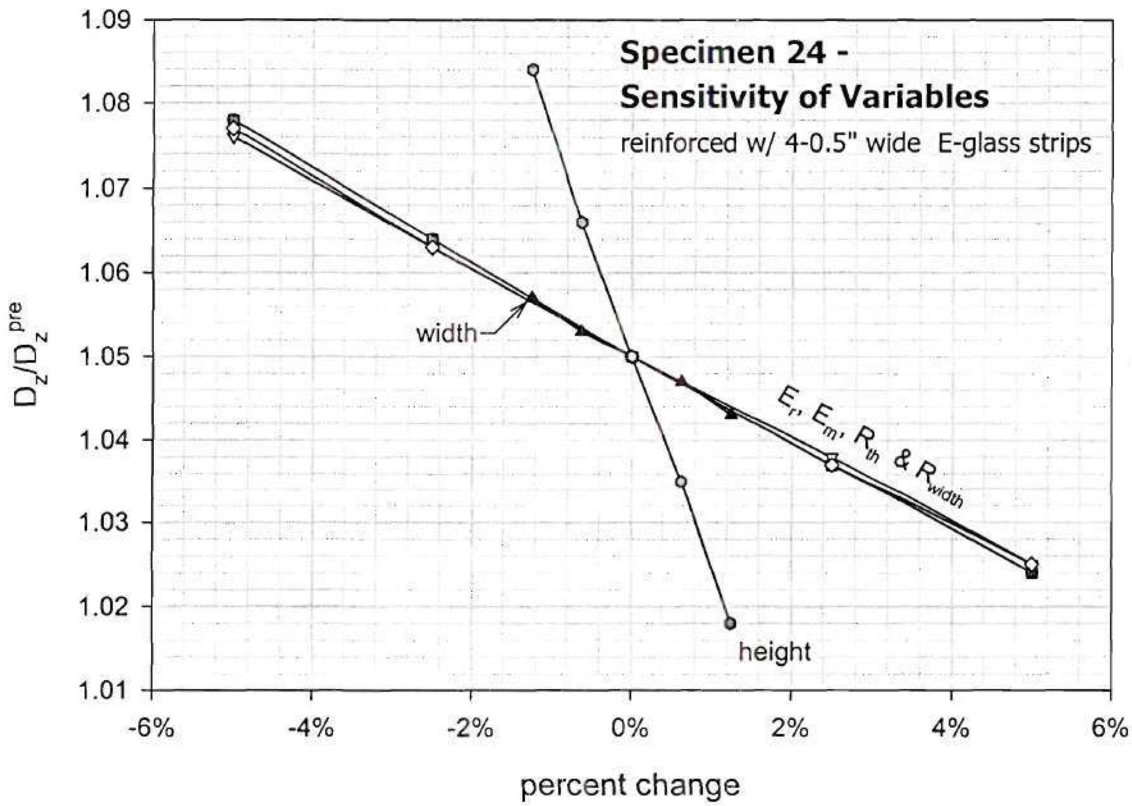

Figure 5.11: Sensitivity Analysis of specimen 24

CHAPTER VI

CONCLUSION

This research experimentally investigated the flexural response of recycled plastic beams reinforced with fiber reinforced composites using full-scale and small-scale flexural tests. The study also experimentally determined the flexural modulus of elasticity of recycled plastics using small scale flexural tests.

All test data were limited to the initial loading stage for which the ratio of the deflection over the span length (δ/L) was less than 1/384 for the full-scale beams and less than 1/192 for the small-scale beams. Specific conclusions concerning the study are presented below.

Unreinforced Recycled Plastic Specimens

Eastpoint (2001) reported average flexural modulus values of High Density Polyethylene (HDPE), Low Density Polyethylene (LDPE), and Low Linear Density Polyethylene (LLDPE) as 120 ksi, 22 ksi, and 70 ksi, respectively. Specimens RP1, RP2, RP4 and RP5 all contain some form of HDPE within the formulation of the beam specimen. The E_a of RP2 and RP4 was 133 ksi and 127 ksi, respectively, and these values averaged 8% greater than that given by Eastpoint. RP1 and RP5 had E_a values of 10.6 ksi and 8.65 ksi, respectively, and these values averaged 92% lower then that given by Eastpoint. The E_a of specimen RP15, which was made up of a LLDPE material, was 130 ksi, 86% greater then the value given by Eastpoint. The E_a of RP16, made of LDPE, was 68.6 ksi, and this value is 310% greater then that given by Eastpoint. A reason for the large differences is that the average flexural modulus values from Eastpoint represent pure plastic mixes and specimens RP1, RP5, RP15 and RP16 were not pure mixes. There were other constituents that made up the overall composition of these small-scale beam specimens. The exact formulation of each of the RP beam specimens were proprietary to Seaward International.

Recycled Plastic Materials Reinforced with Polymer Composites

Full-scale

Five of the Seatimber® specimens were reinforced internally with E-glass reinforcing bars. Two full-scale beams (Duratie® and Seatimber®) were reinforced with one and two layers of unidirectional carbon fiber/epoxy composites.

The analysis of the full-scale specimens internally reinforced with E-glass reinforcing bars (specimens 7, 8, 9, 10, and 11) show a difference between the theoretical stiffness and the predicted stiffness called the difference ratio (D_z/D_z^{cal}) ranging from 0.70 to 1.50 when the E_r was assumed to be 5,000 ksi. An experimental modulus (E_r^{exp}) was back-calculated from the D_z value of each beam using a simple strength of materials analysis, because the assumption of the value for E_r was believed to be the reason for the inconsistency. The E_r^{exp} values are shown in Table 6.1.

The average E_r^{exp} value for specimens 7 and 8 was 2,850 ksi and the average E_r^{exp} value for specimens 9, 10 and 11 was 6,800 ksi. The 1.25-inch diameter having a lower modulus value is expected since complete curing becomes more difficult as the diameter of the bars increase. The 0.5-inch diameter E-glass rod with higher modulus values is more efficient then the larger, incompletely cured E-glass rods.

Table 6.1: E_r^{exp} of Seatimbers® with internal E-glass reinforcement

Specimen	reinforcing system	D_z (kip-in^2)	E_r^{exp} (ksi)
7	4 - 1.25 - inch dia. glass reinf.	105,285	2,700
8	4 - 1.25 - inch dia. glass reinf.	111,842	3,000
9	12 - 0.5 - inch dia. glass reinf.	143,991	6,100
10	12 - 0.5 - inch dia. glass reinf.	153,852	7,100
11	4 - 0.5 - inch dia. glass reinf.	114,389	7,200

The ratios of D_z/D_z^{cal} for all specimens reinforced with one and two layers of unidirectional carbon fiber composite sheets ranged from 0.99 to 1.15.

Small-scale

Six of the small-scale specimens were reinforced with external strips of E-glass, carbon, and stainless steel/epoxy reinforcing systems, and two of the specimens were reinforced with internal E-glass polymer composite strips.

The average stiffness of the reinforced specimens RP 19 and RP 20 (27.8 kips-in^2) increased 10% over their unreinforced counterparts RP 21 and RP 22 (25.2) as shown in Table 3.8.

For specimens RP 23, RP 24, RP 26 and RP 28, the ratios (D_z/D_z^{cal}) were less than 1.06. The reinforcing system properties were determined by prior testing. The location of the reinforcing strips was constant throughout the length of the each specimen, and the load rate was constant for all of the small-scale tests. Better predictions were obtained when the properties of each of the constituents was determined experimentally.

APPENDIX A

LOAD - DEFLECTION CURVES FOR RP1 THROUGH RP18

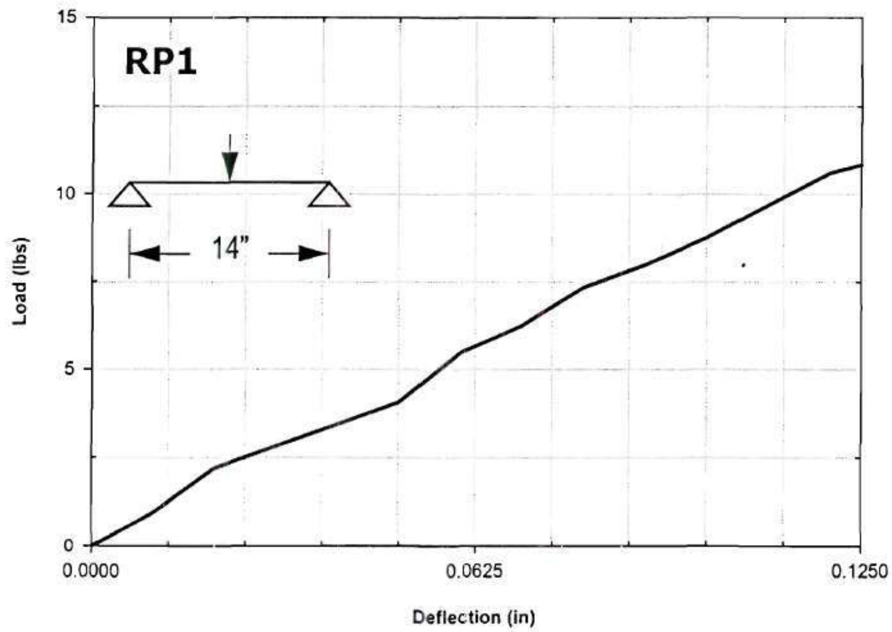

Figure A-1: Load - deflection curves for RP1

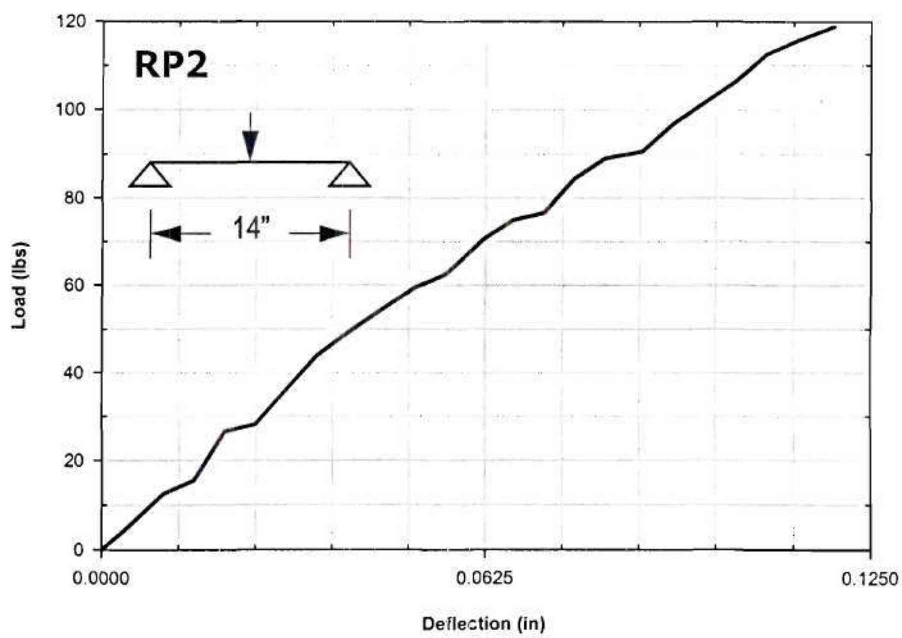

Figure A-2: Load - deflection curves for RP2

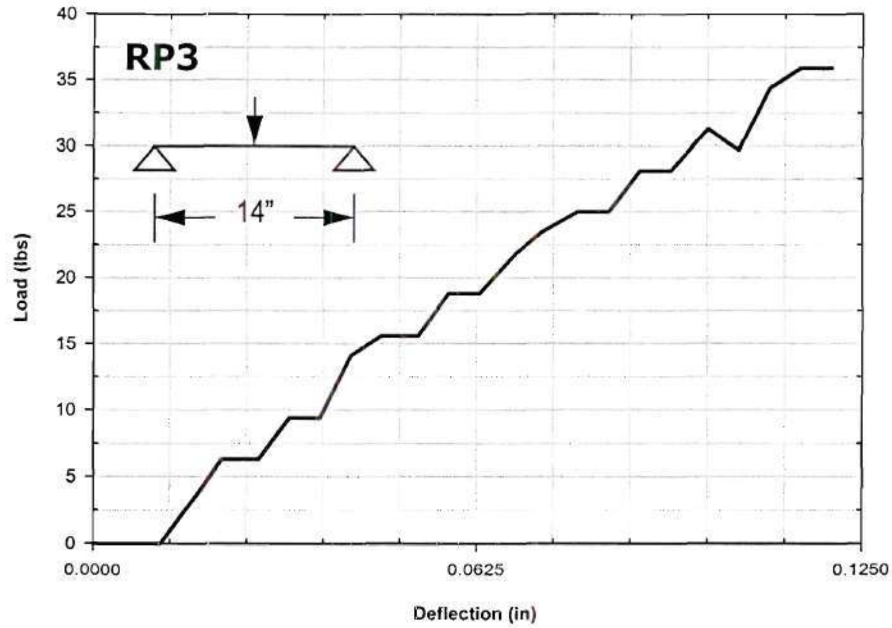

Figure A-3: Load - deflection curves for RP3

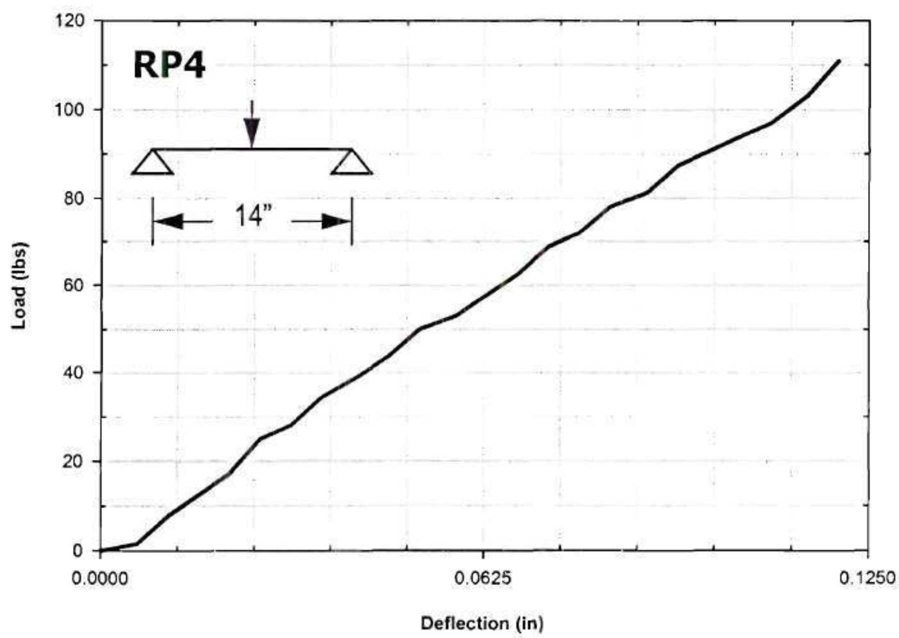

Figure A-4: Load - deflection curves for RP4

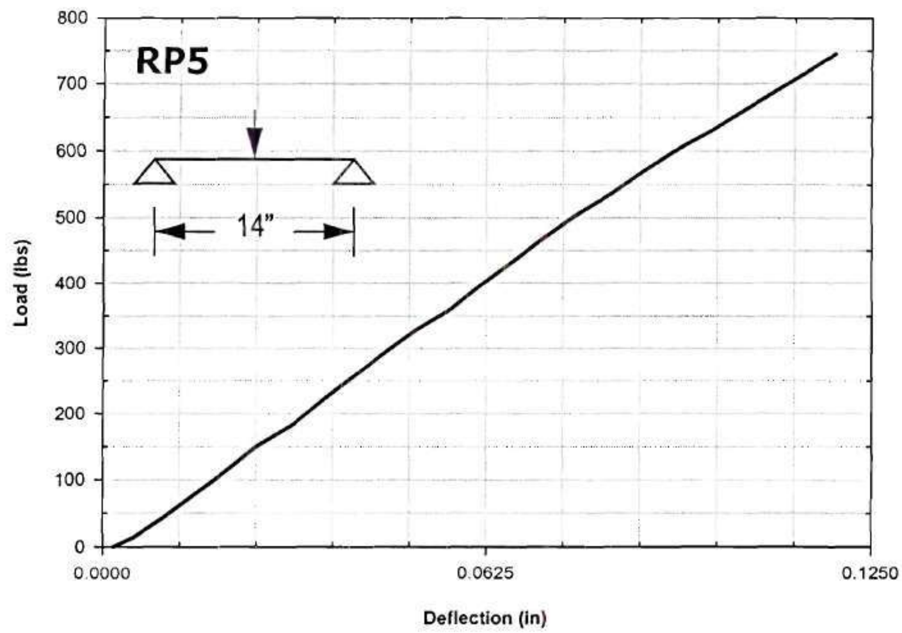

Figure A-5: Load - deflection curves for RP5

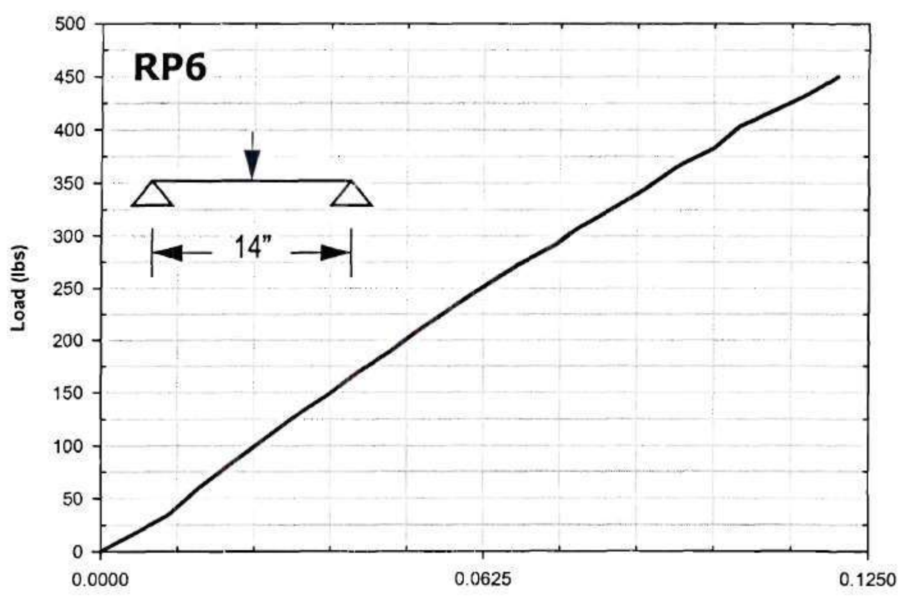

Figure A-6: Load - deflection curves for RP6

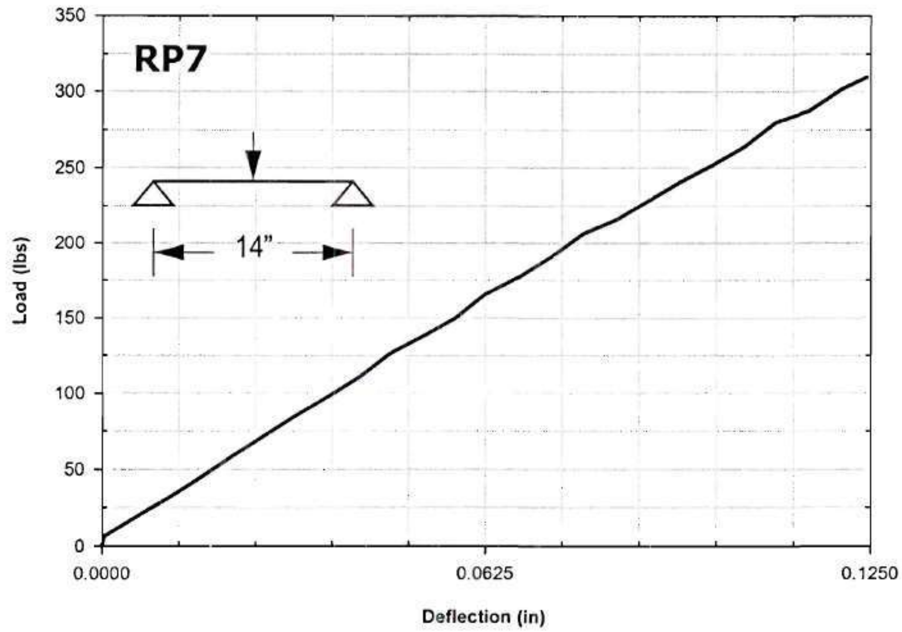

Figure A-7: Load - deflection curves for RP7

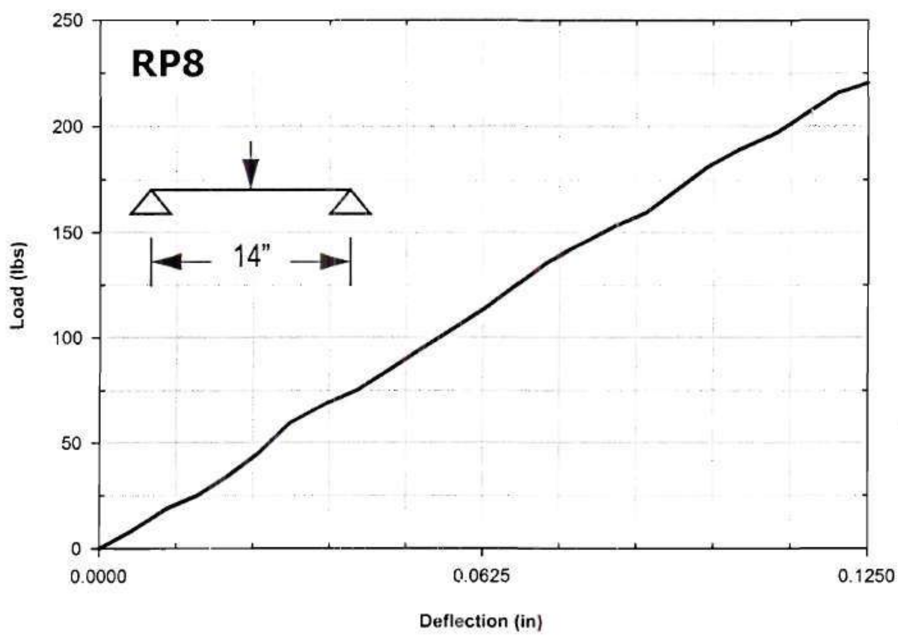

Figure A-8: Load - deflection curves for RP8

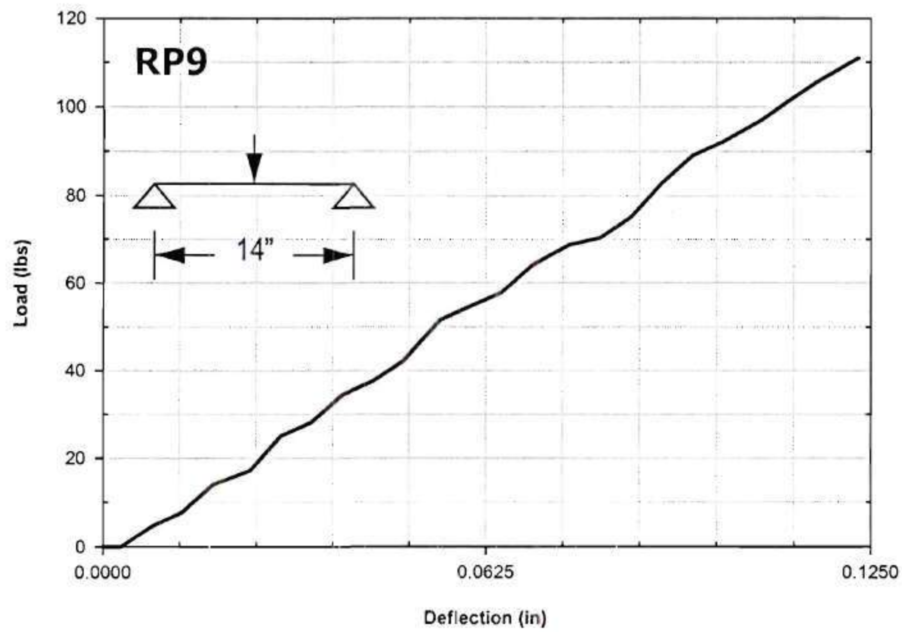

Figure A-9: Load - deflection curves for RP9

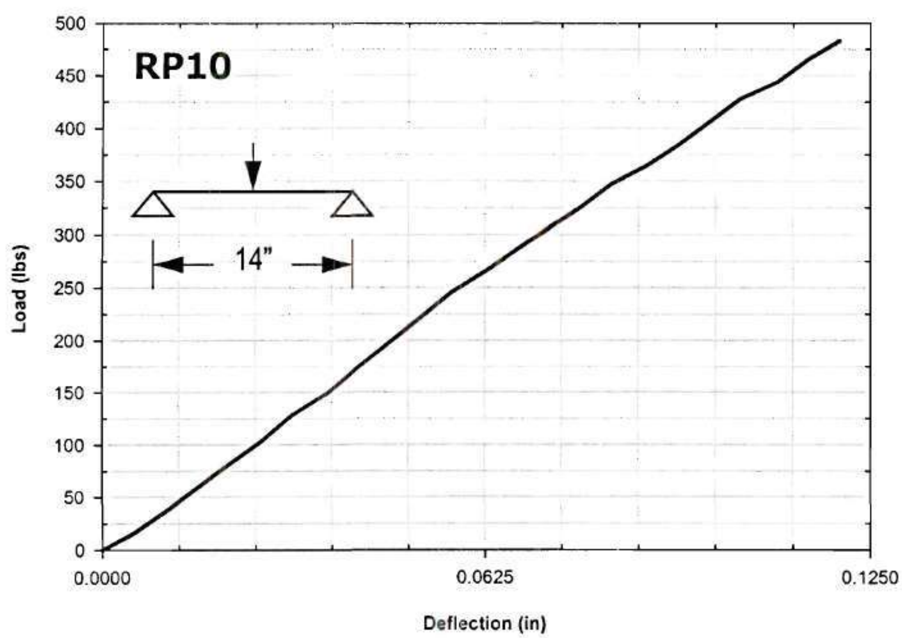

Figure A-10: Load - deflection curves for RP10

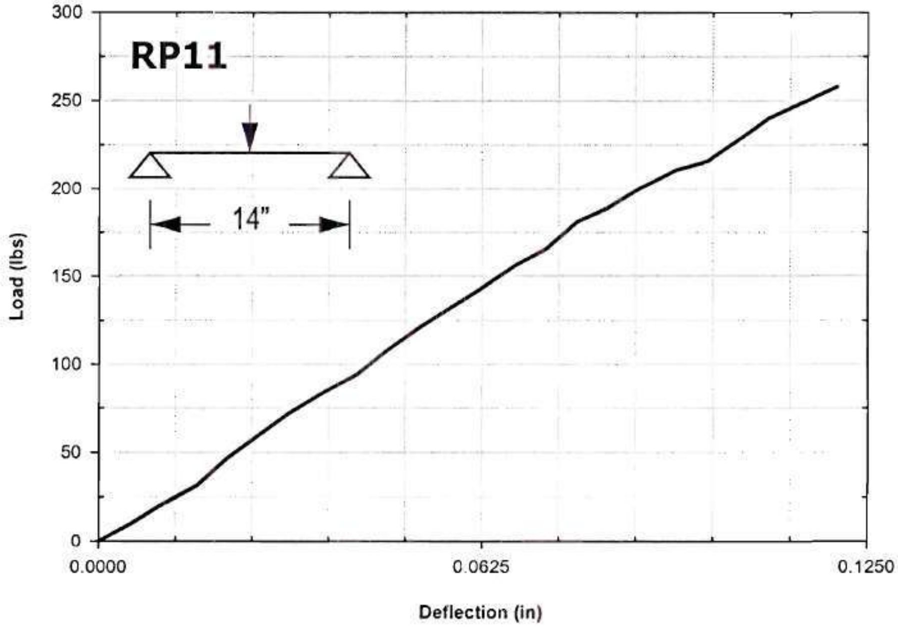

Figure A-11: Load - deflection curves for RP11

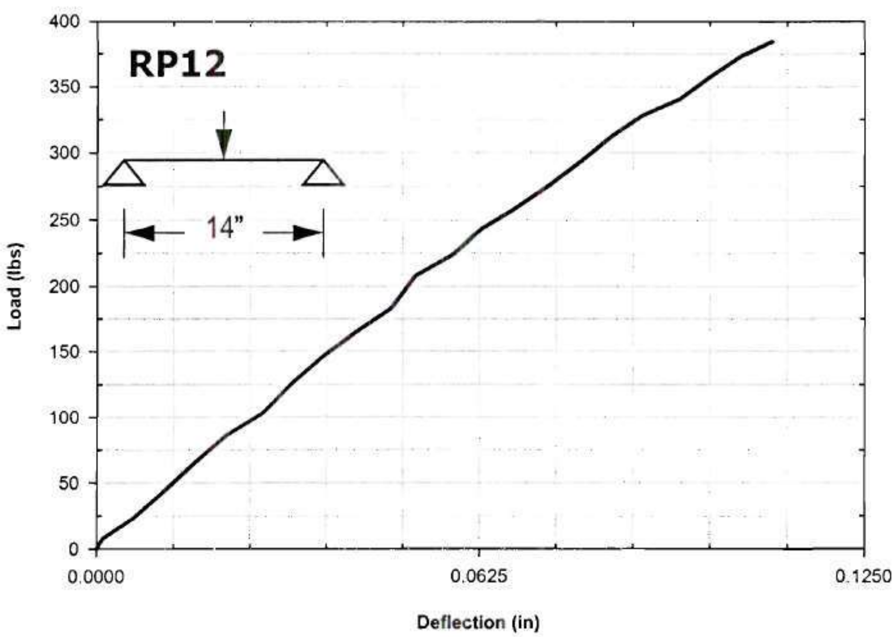

Figure A-12: Load - deflection curves for RP12

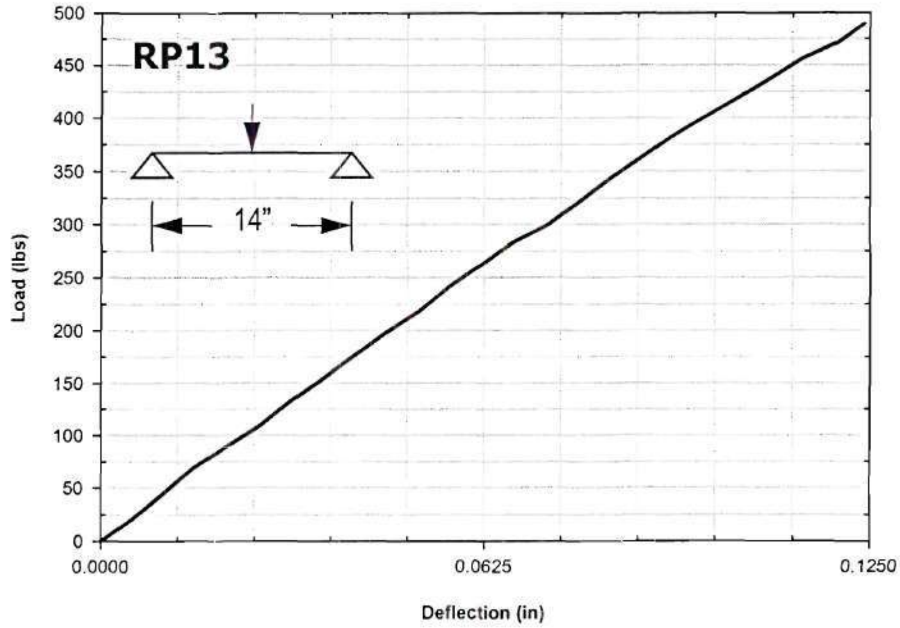

Figure A-13: Load - deflection curves for RP13

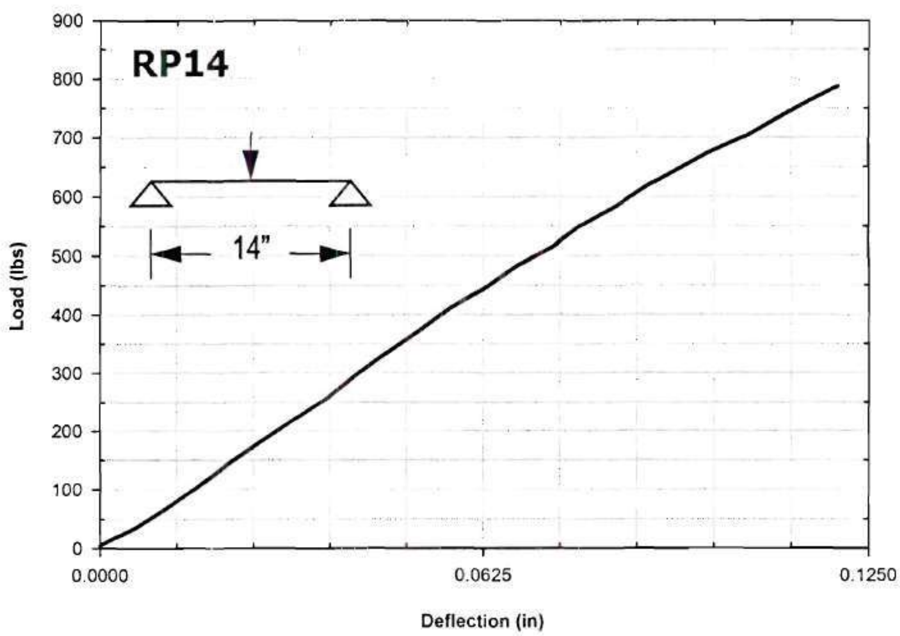

Figure A-14: Load - deflection curves for RP14

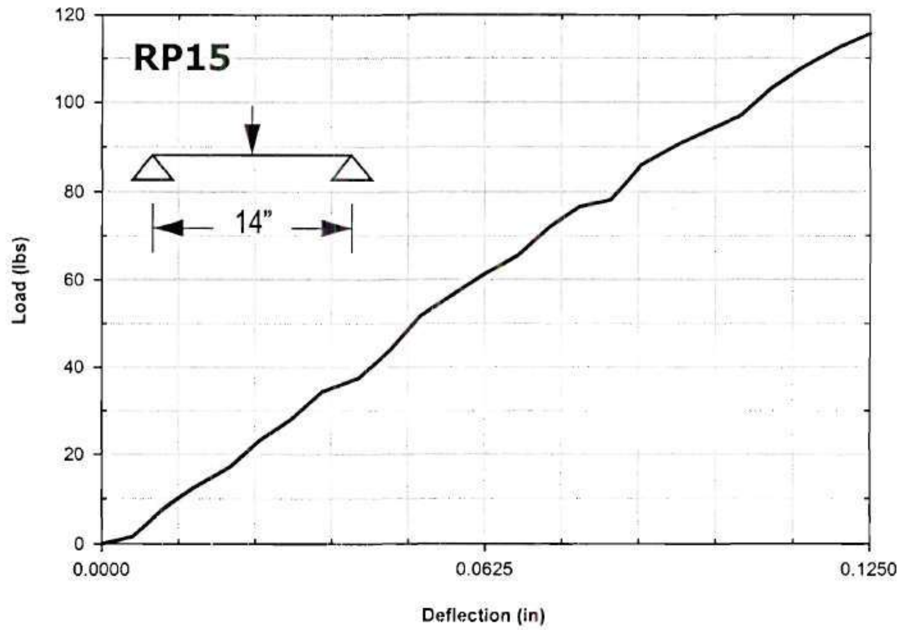

Figure A-15: Load - deflection curves for RP15

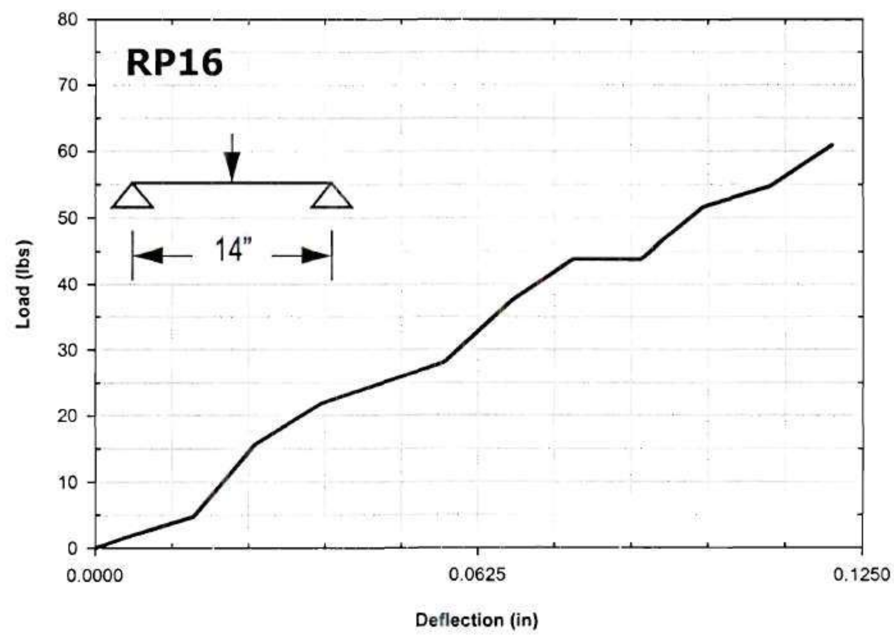

Figure A-16: Load - deflection curves for RP16

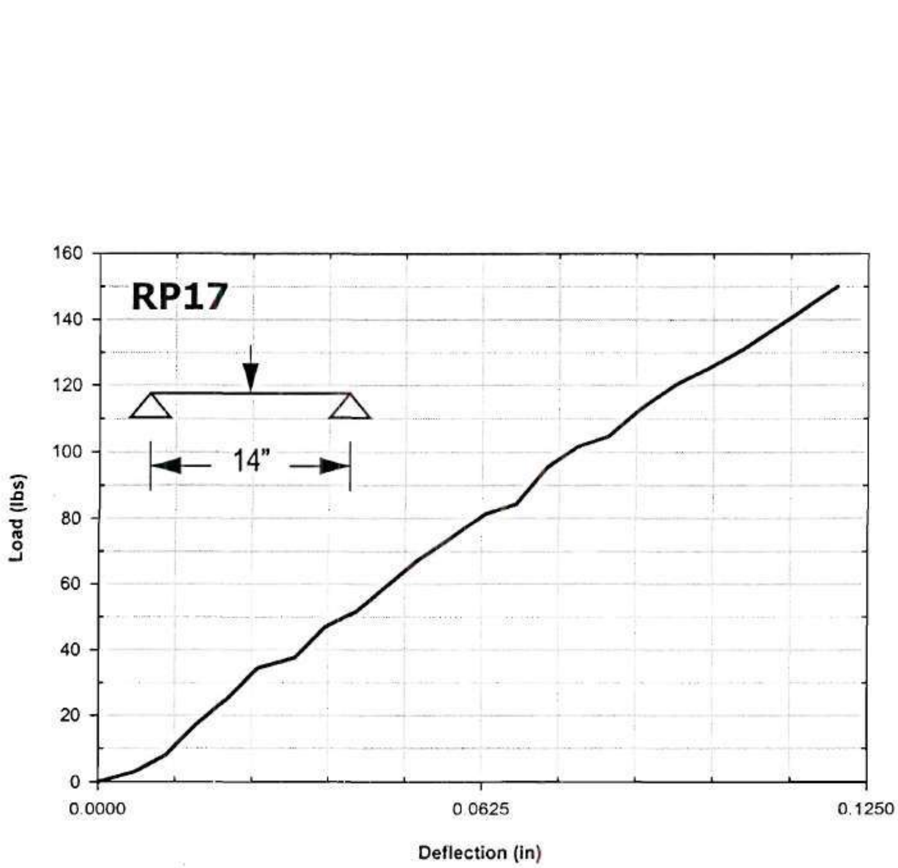

Figure A-17: Load - deflection curves for RP17

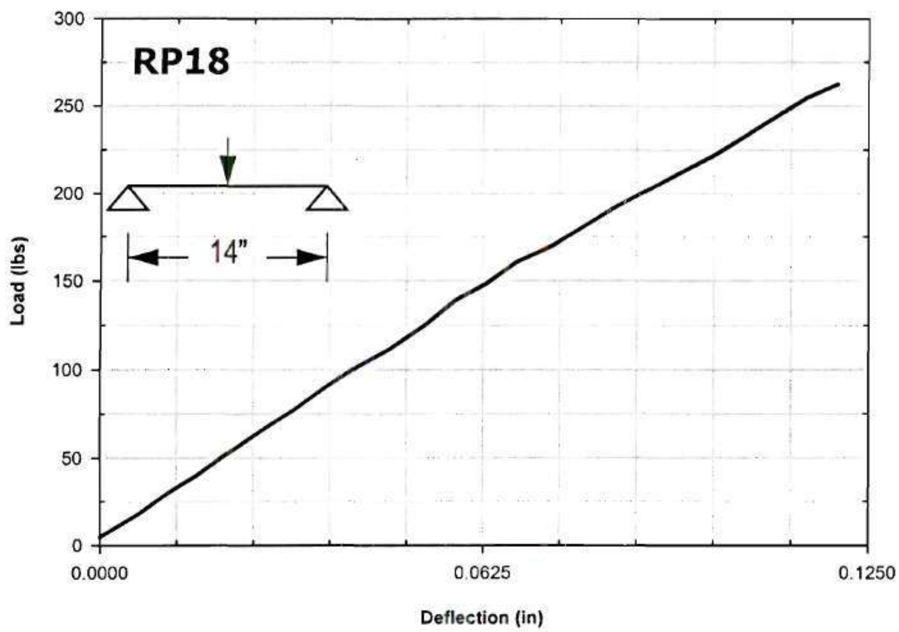

Figure A-18: Load - deflection curves for RP18

APPENDIX B

LOAD - DEFLECTION CURVES OF RP2-1 THROUGH RP2-74

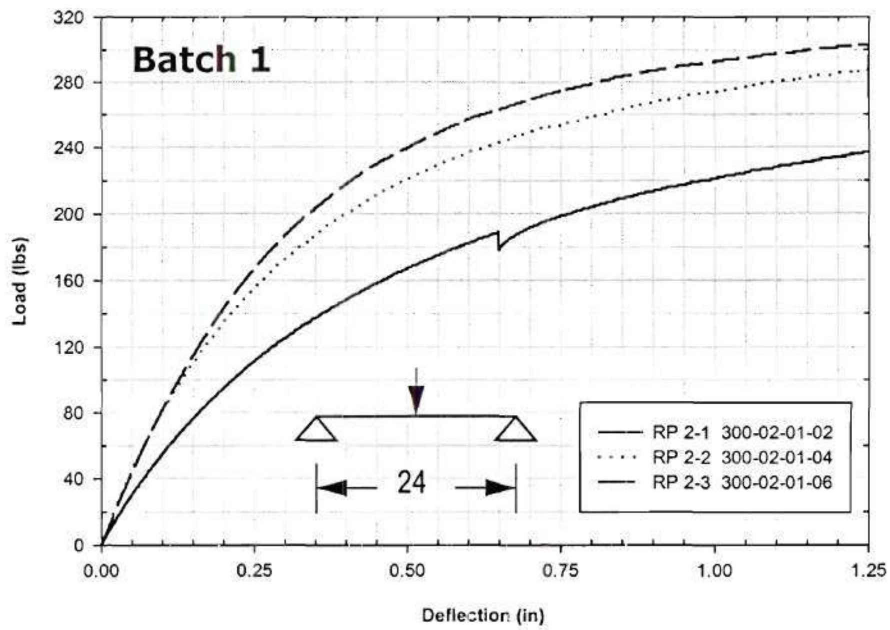

Figure B-1: Load - deflection curves for batch 1 specimens

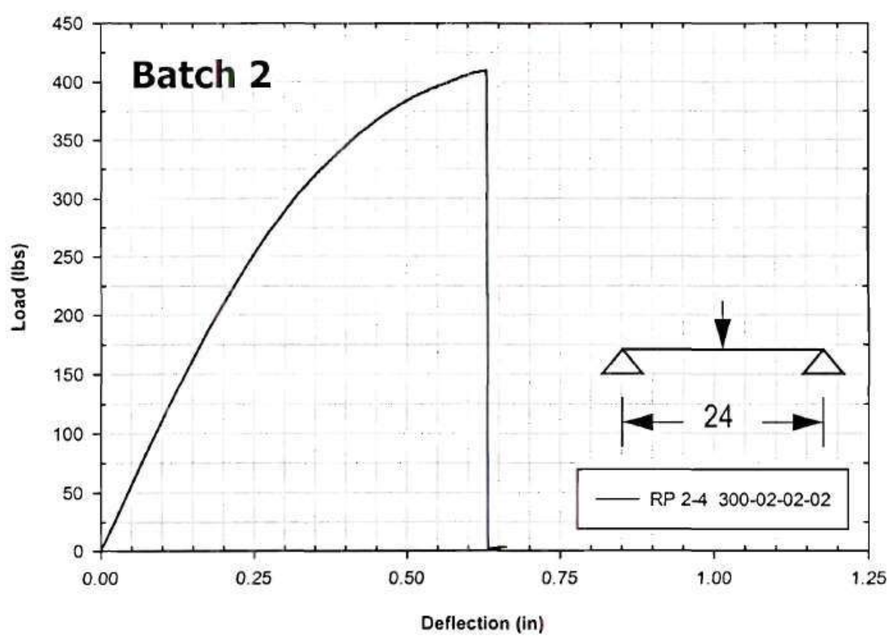

Figure B-2: Load - deflection curves for batch 2 specimen

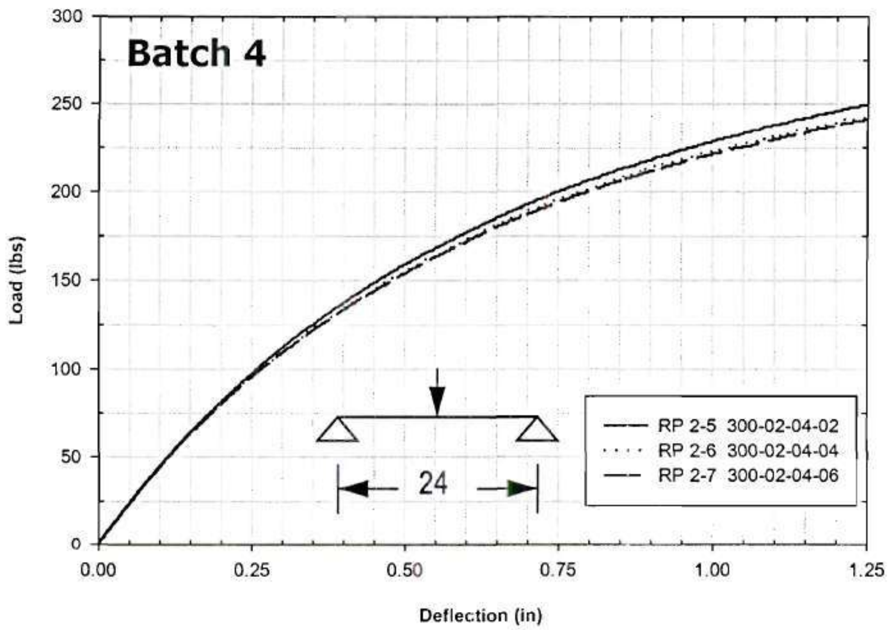

Figure B-3: Load - deflection curves for batch 4 specimens

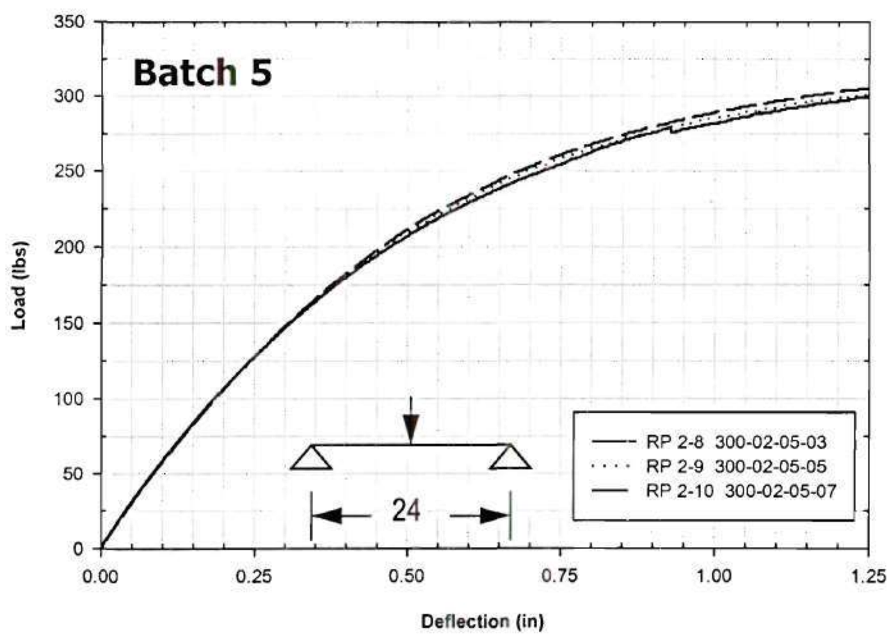

Figure B-4: Load - deflection curves for batch 5 specimens

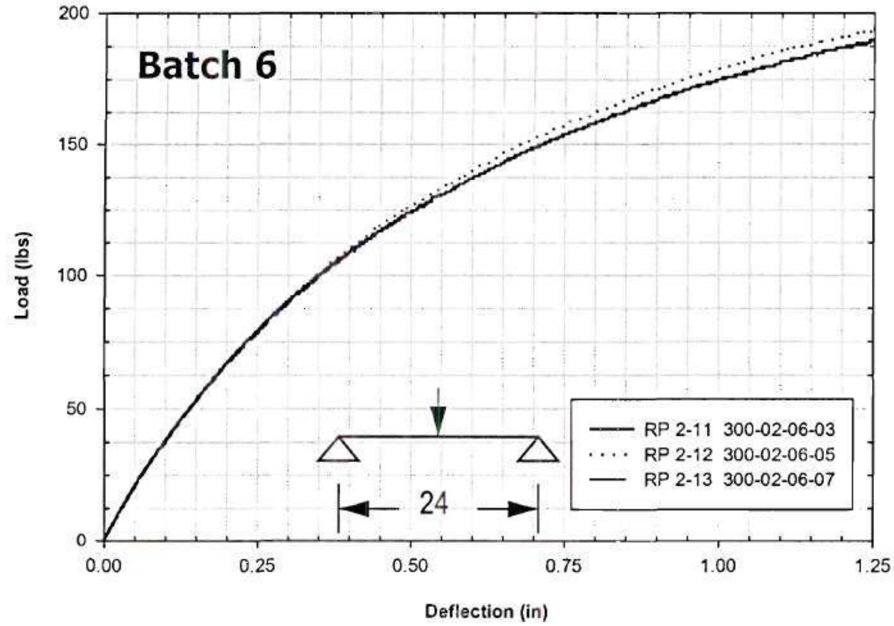

Figure B-5: Load - deflection curves for batch 6 specimens

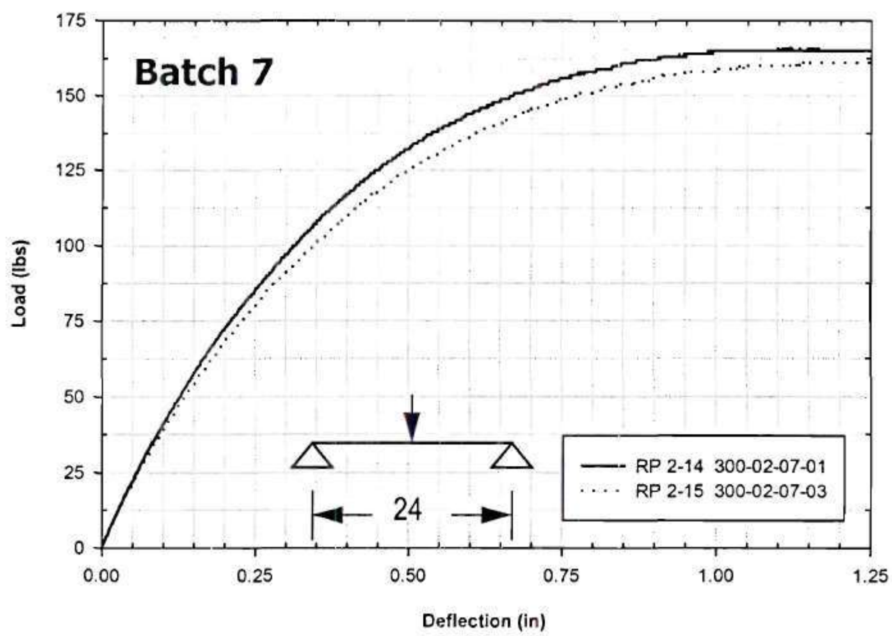

Figure B-6: Load - deflection curves for batch 7 specimens

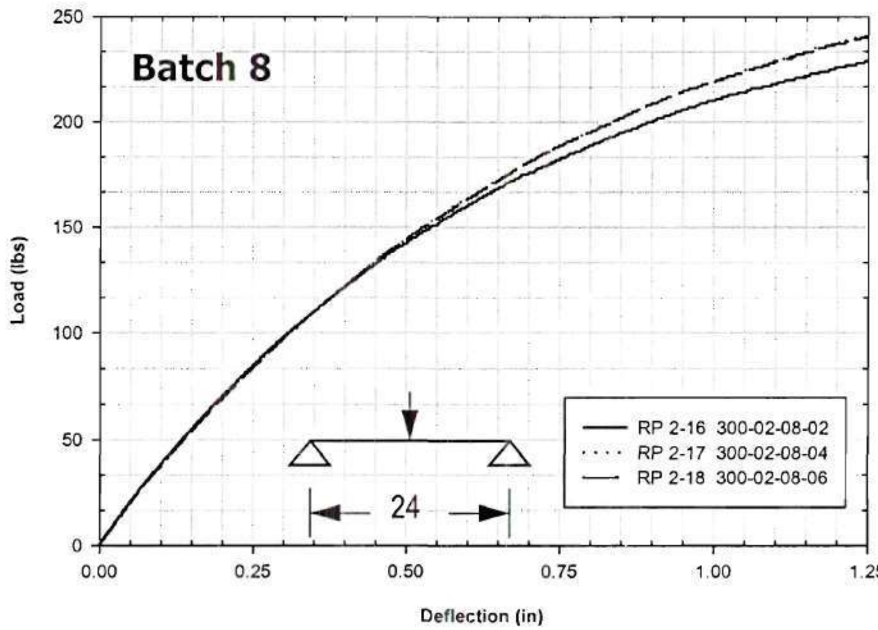

Figure B-7: Load - deflection curves for batch 8 specimens

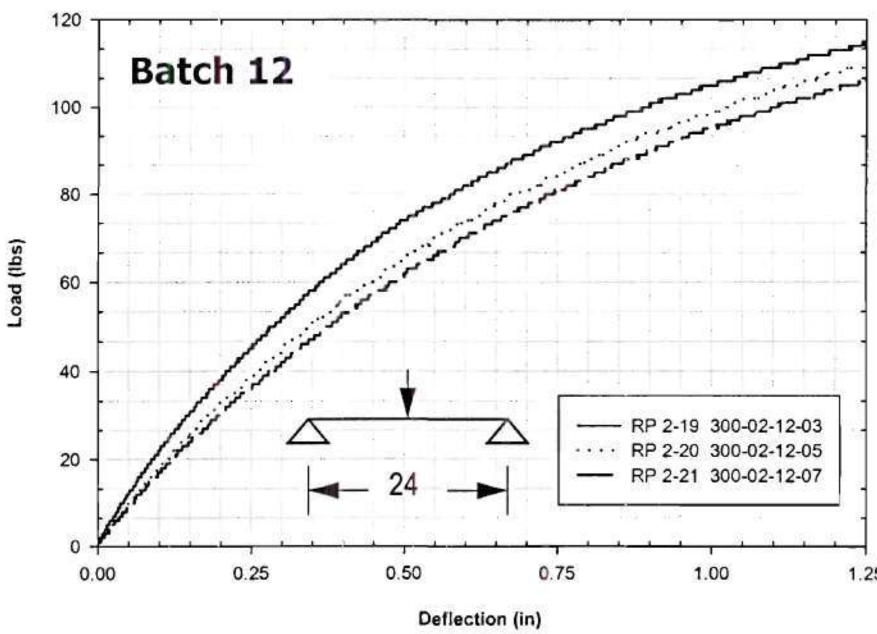

Figure B-8: Load - deflection curves for batch 12 specimens

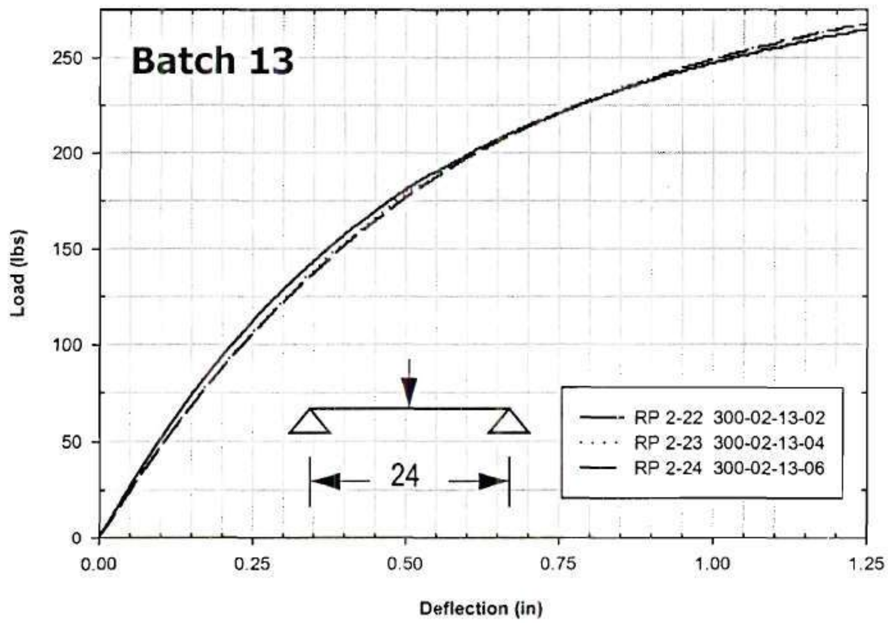

Figure B-9: Load - deflection curves for batch 13 specimens

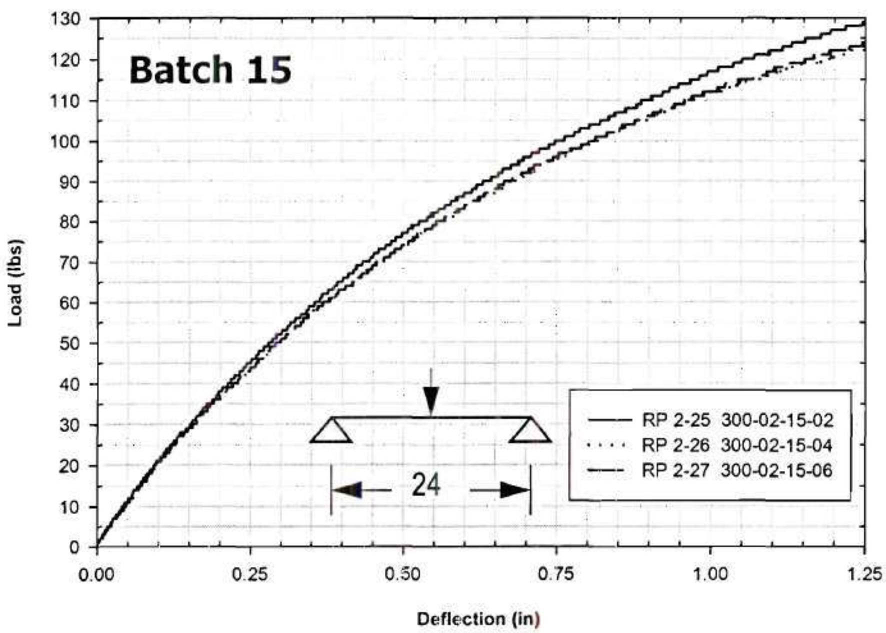

Figure B-10: Load - deflection curves for batch 15 specimens

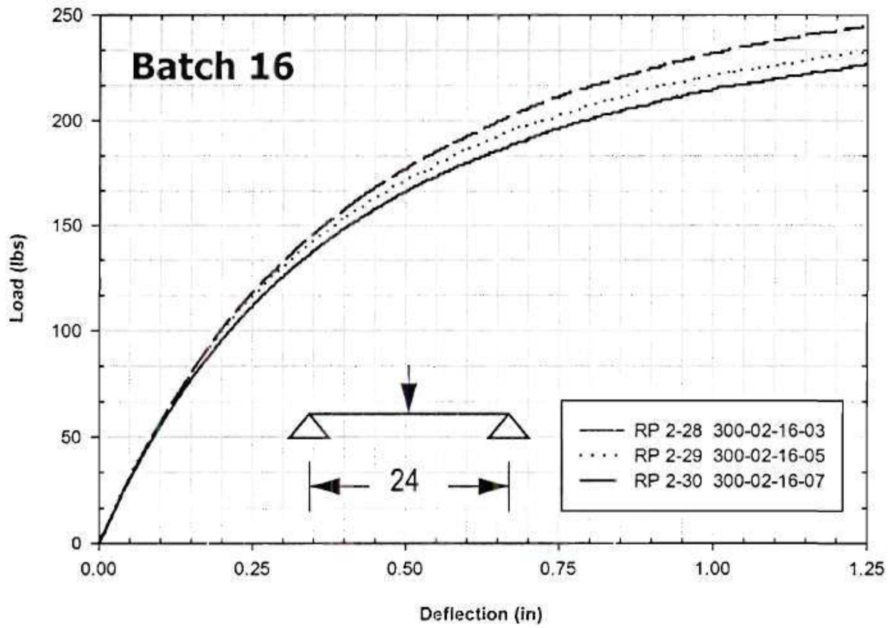

Figure B-11: Load - deflection curves for batch 16 specimens

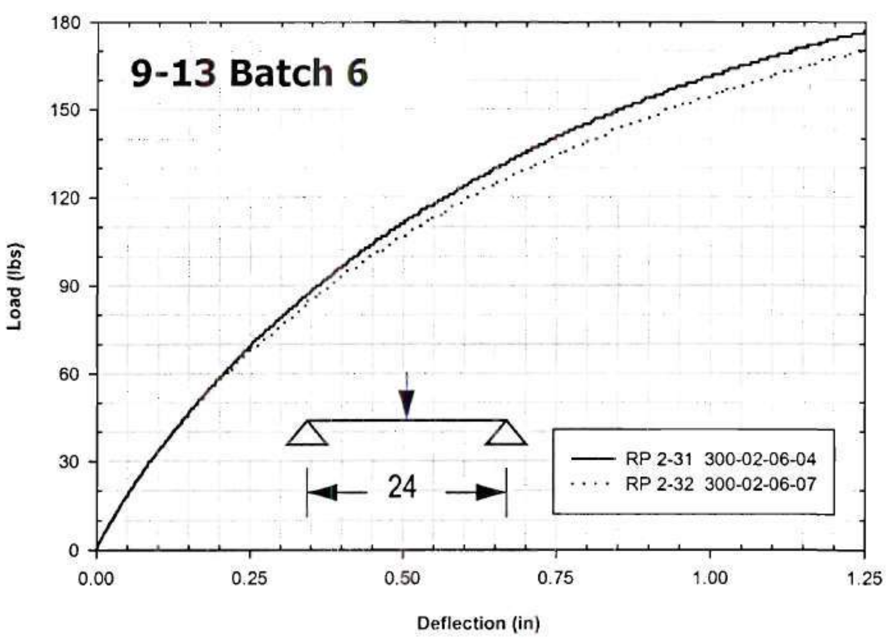

Figure B-12: Load - deflection curves for 9-13 batch 6 specimens

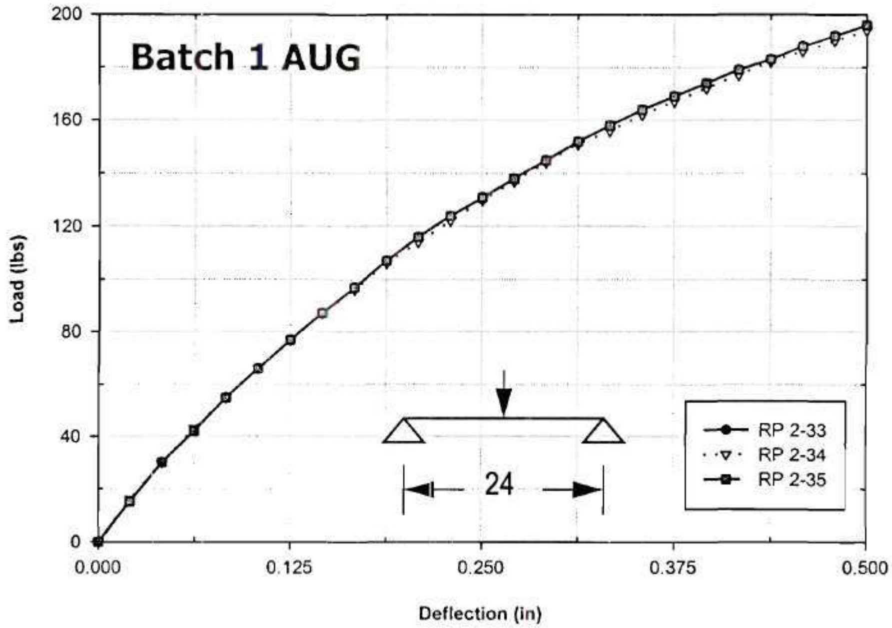

Figure B-13: Load - deflection curves for batch 1 AUG specimens

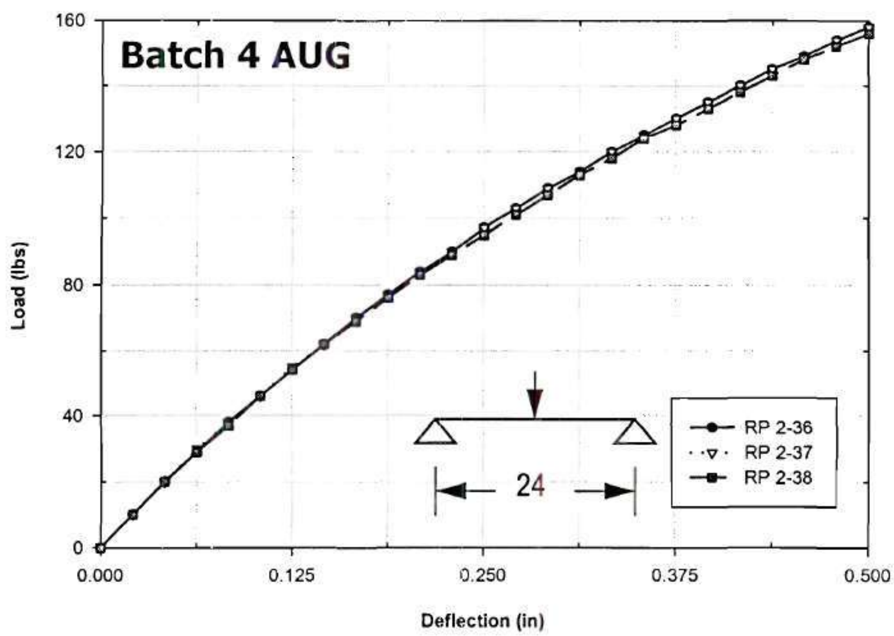

Figure B-14: Load - deflection curves for batch 4 AUG specimens

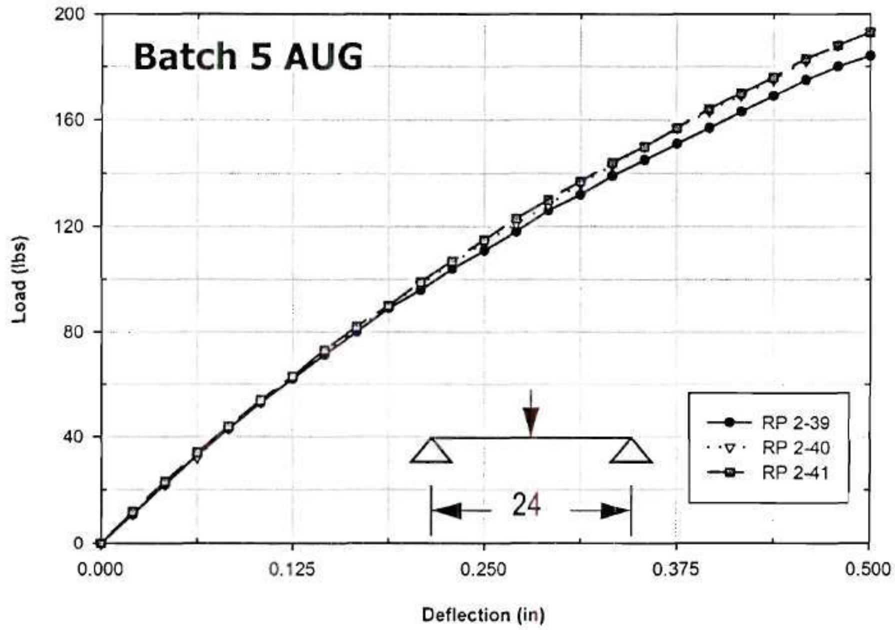

Figure B-15: Load - deflection curves for batch 5 AUG specimens

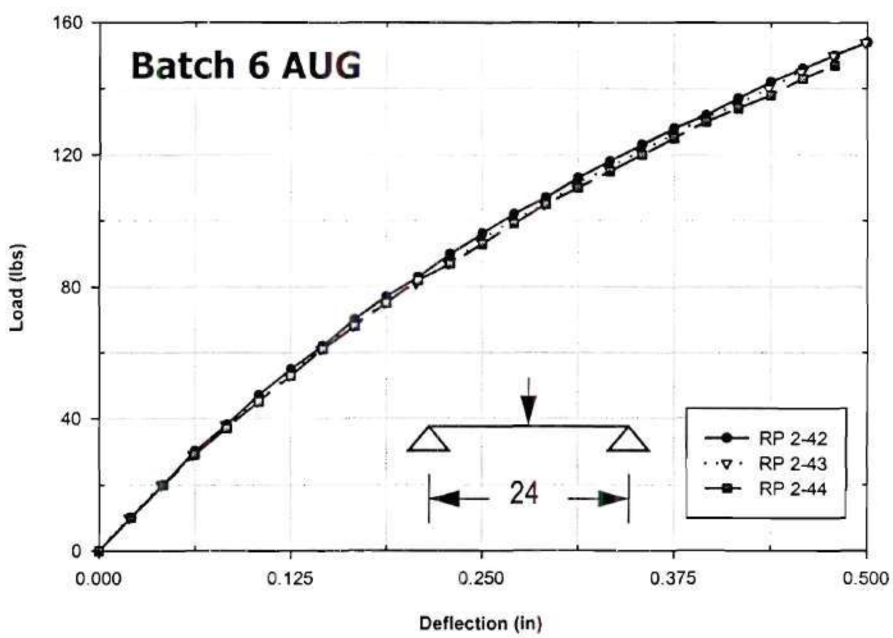

Figure B-16: Load - deflection curves for batch 6 AUG specimens

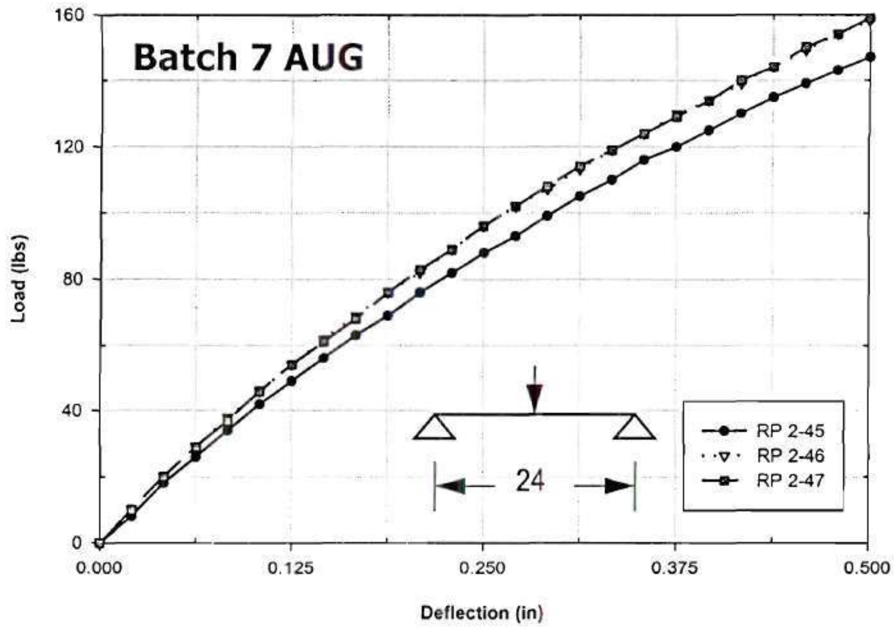

Figure B-17: Load - deflection curves for batch 7 AUG specimens

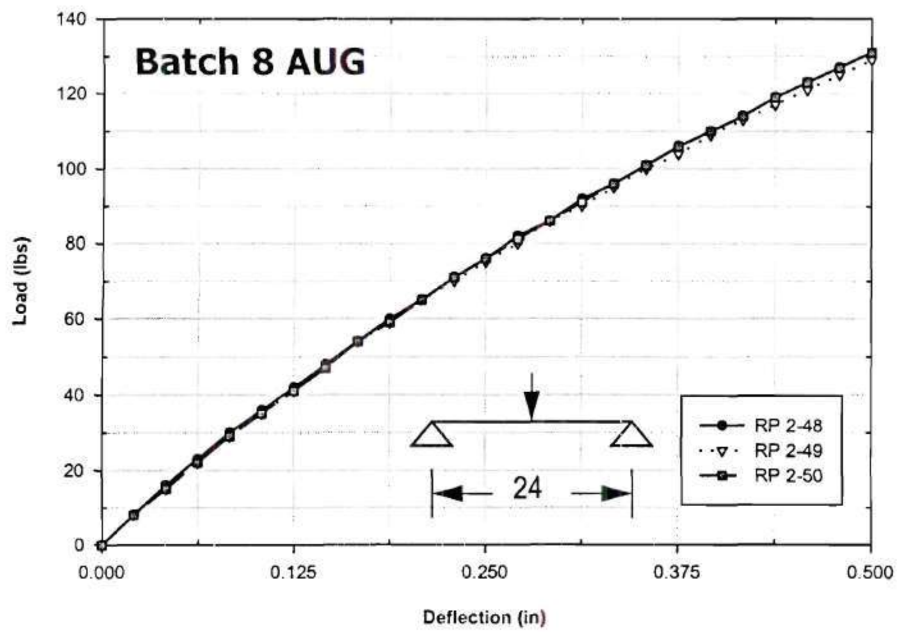

Figure B-18: Load - deflection curves for batch 8 AUG specimens

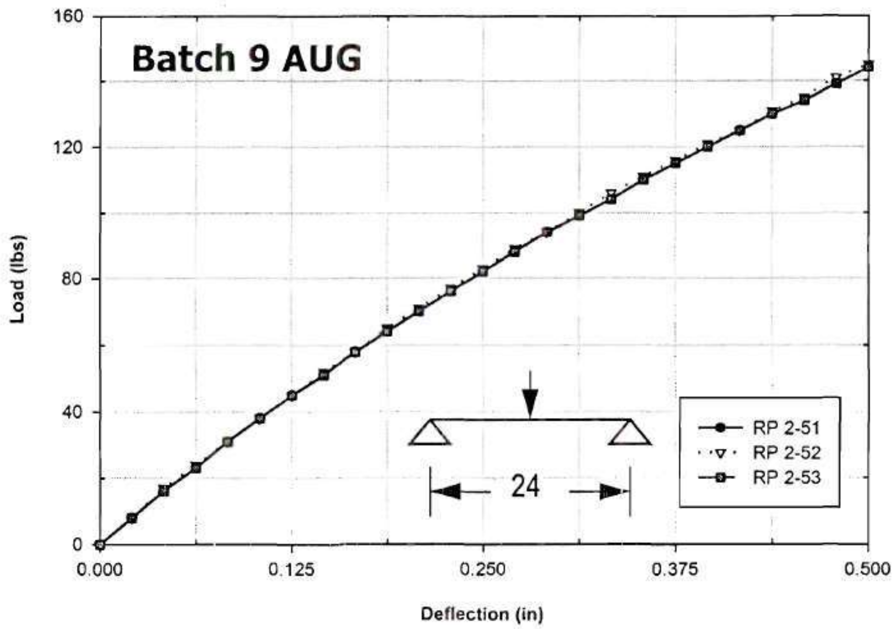

Figure B-19: Load - deflection curves for batch 9 AUG specimens

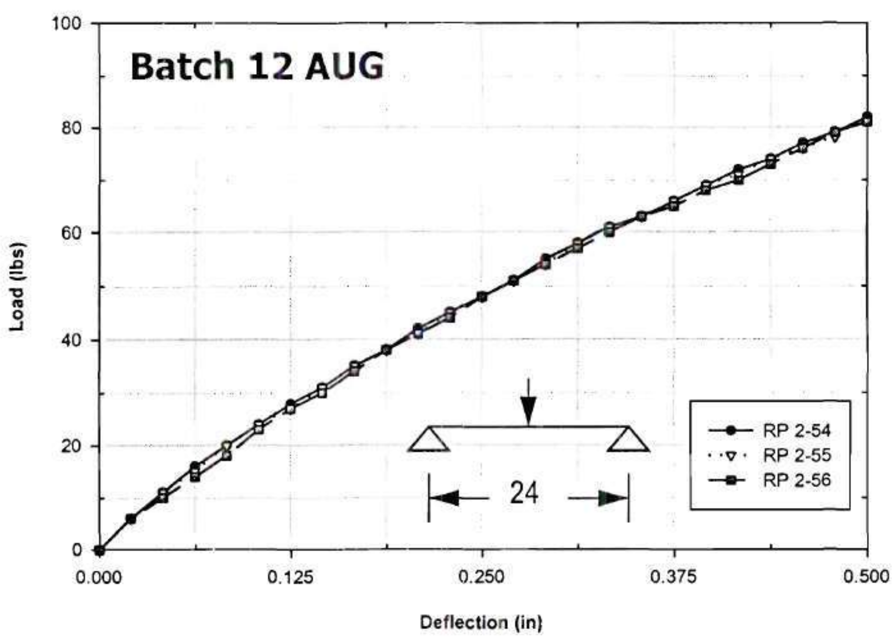

Figure B-20: Load - deflection curves for batch 12 AUG specimens

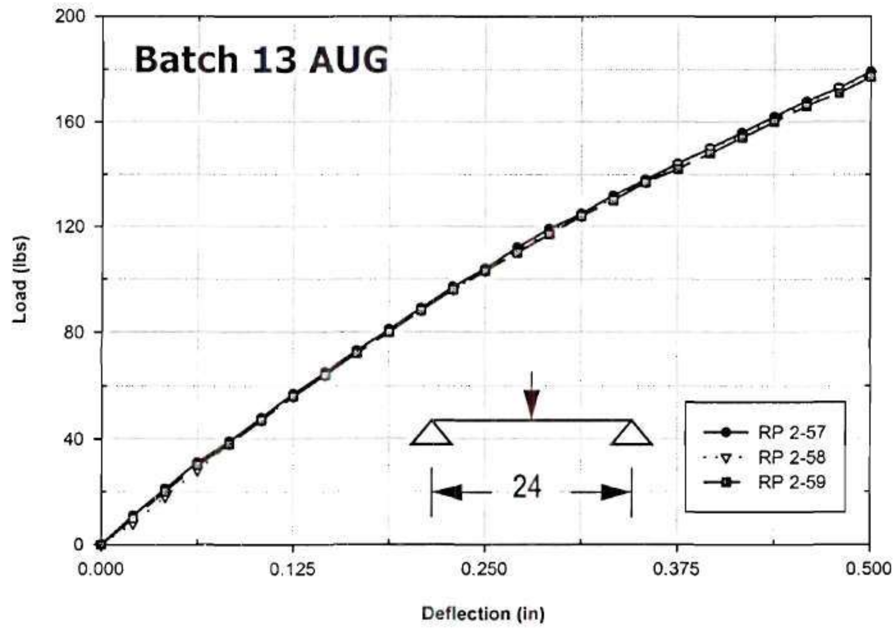

Figure B-21: Load - deflection curves for batch 13 AUG specimens

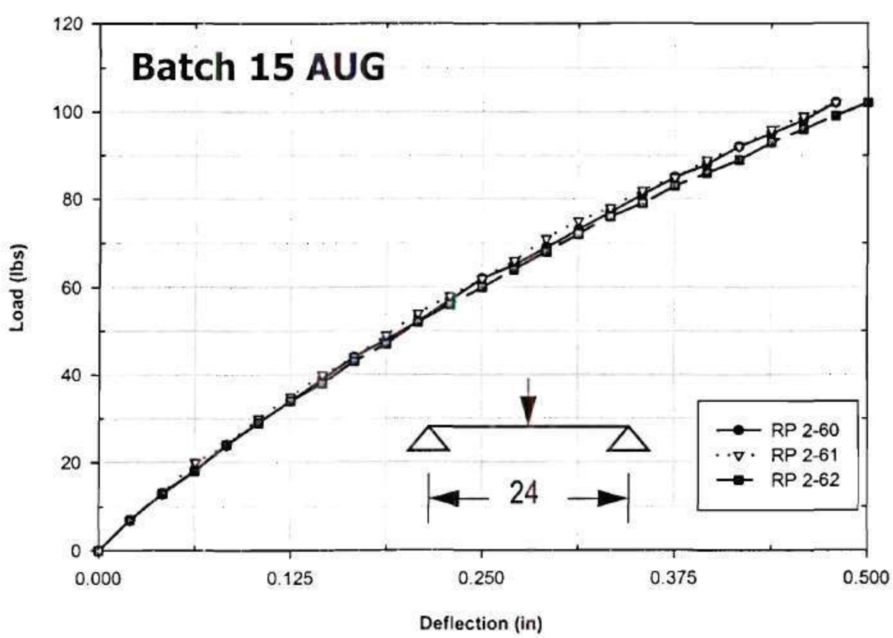

Figure B-22: Load - deflection curves for batch 15 AUG specimens

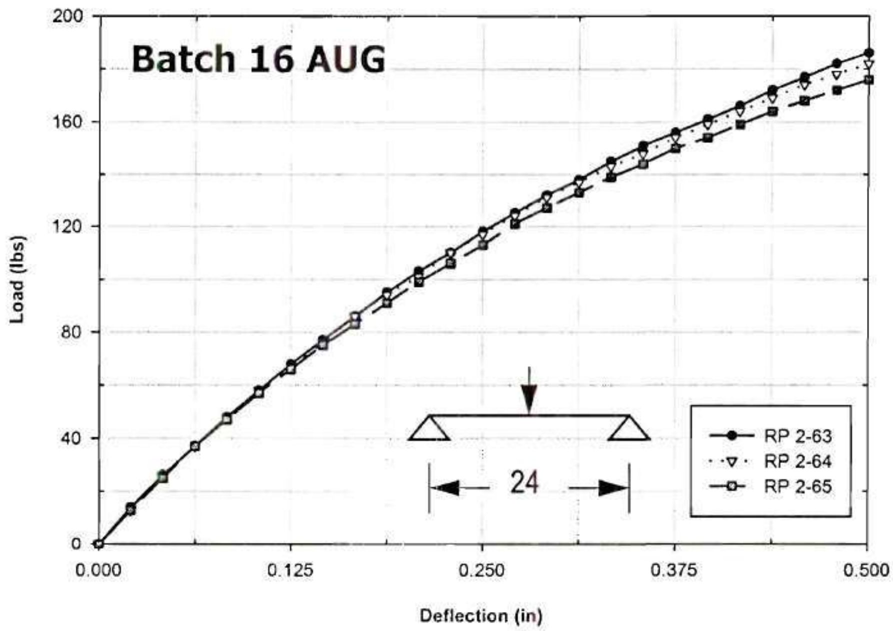

Figure B-23: Load - deflection curves for batch 16 AUG specimens

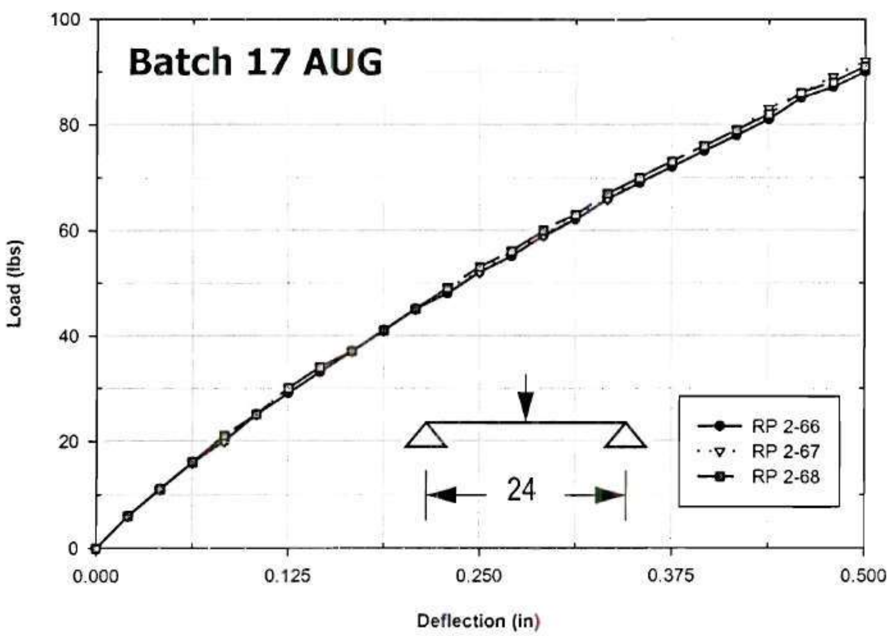

Figure B-24: Load - deflection curves for batch 17 AUG specimens

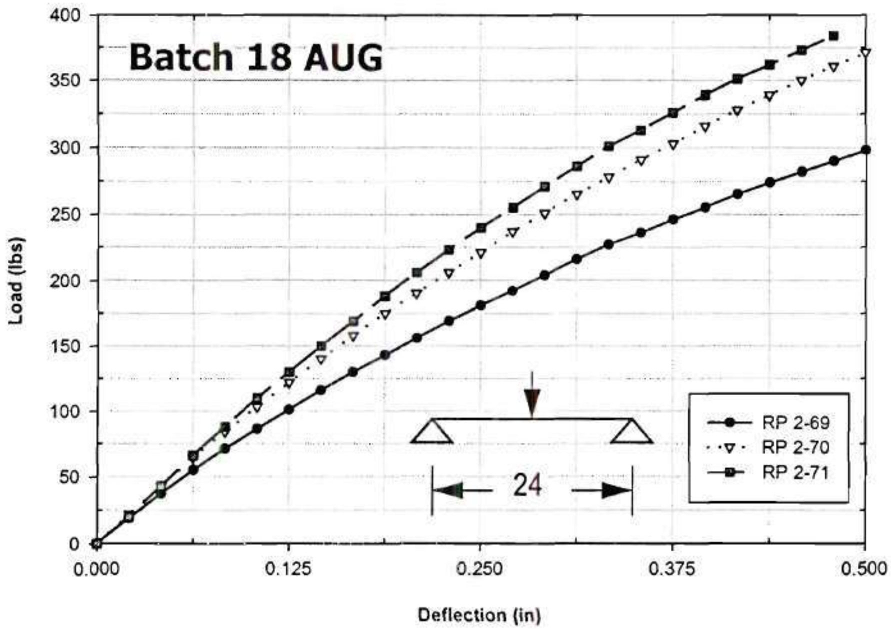

Figure B-25: Load - deflection curves for batch 18 AUG specimens

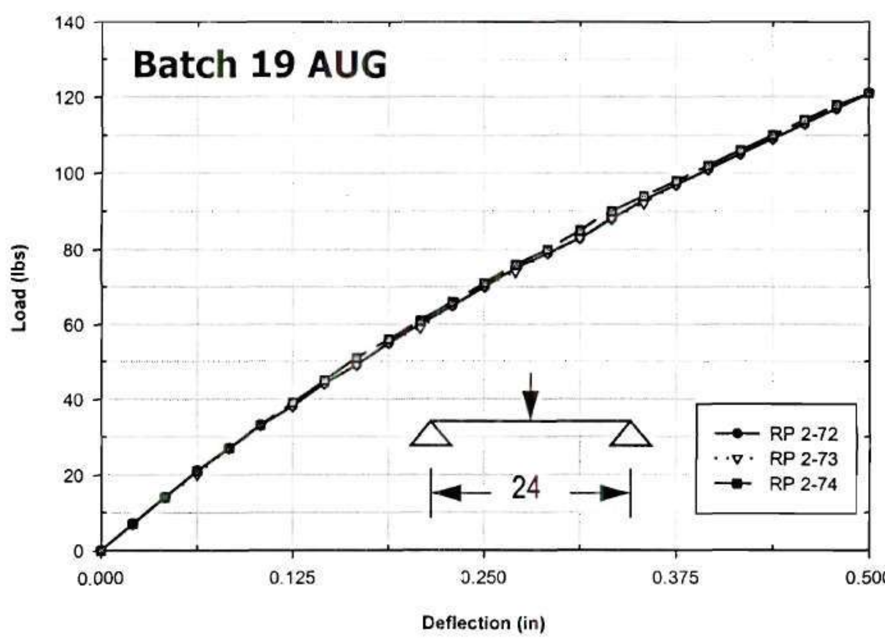

Figure B-26: Load - deflection curves for batch 19 AUG specimens

APPENDIX C

LOAD - APPARENT MODULUS CURVES OF RP2-1 THROUGH RP2-74

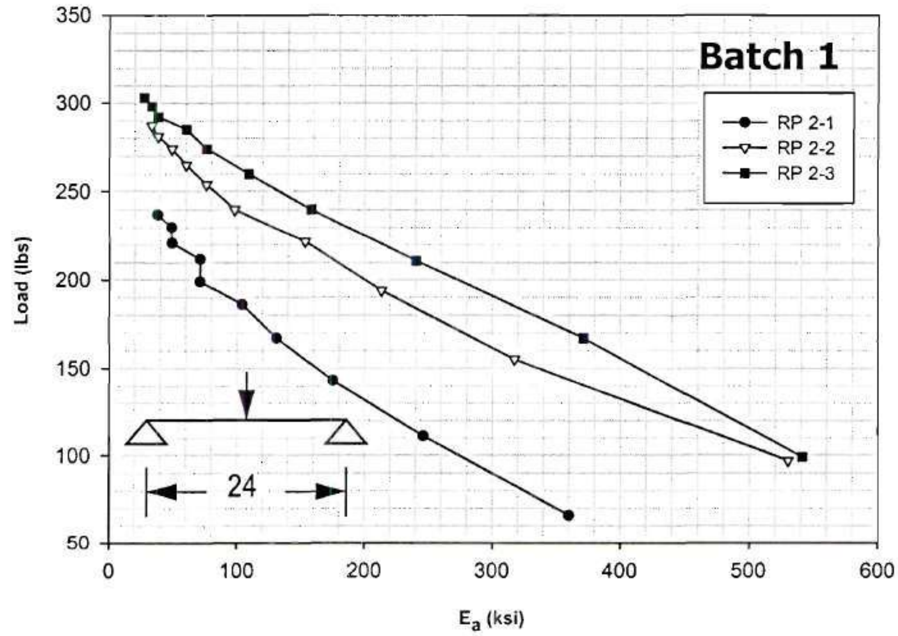

Figure C-1: Load - E_a curves data for batch 1 specimens

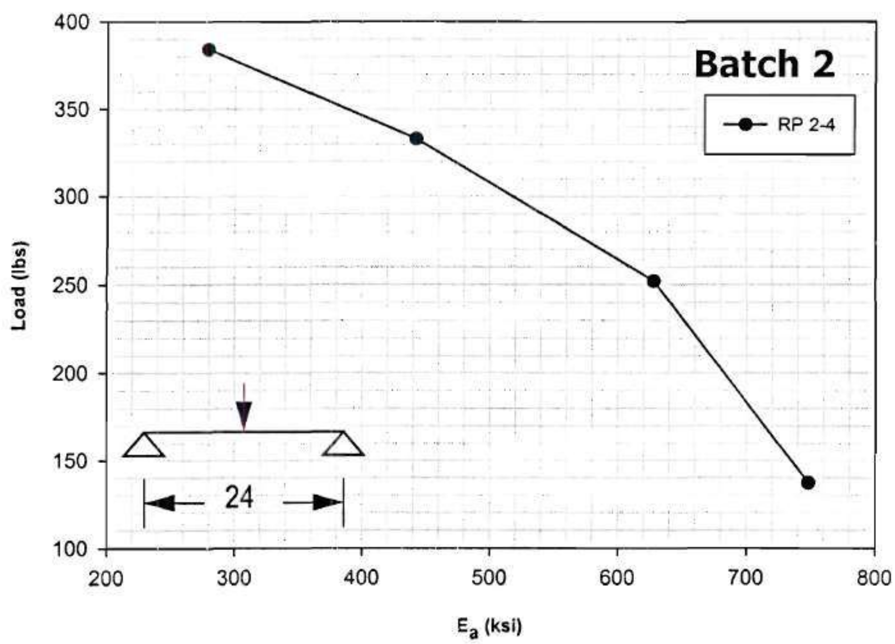

Figure C-2: Load - E_a curves data for batch 2 specimen

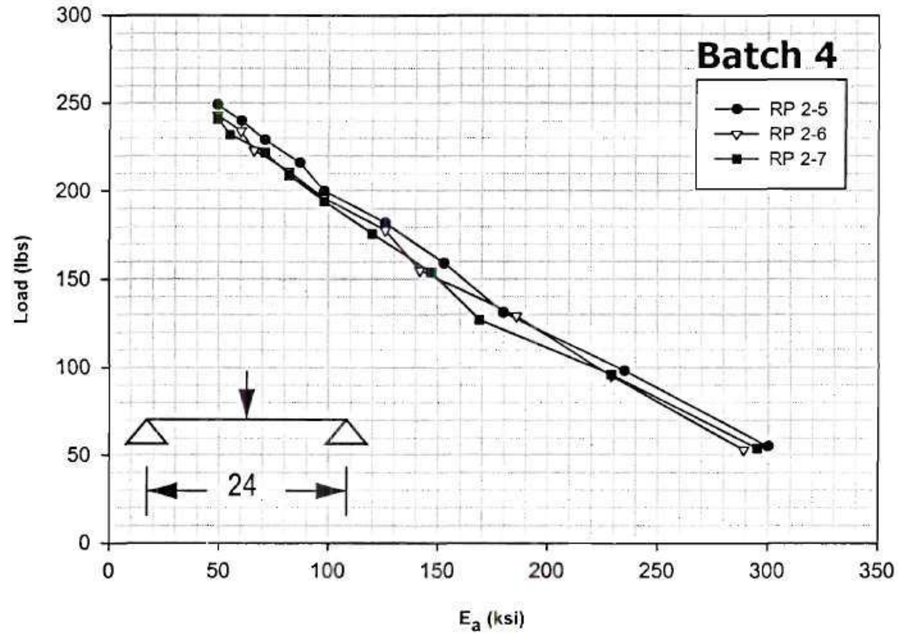

Figure C-3: Load - E_a curves data for batch 4 specimens

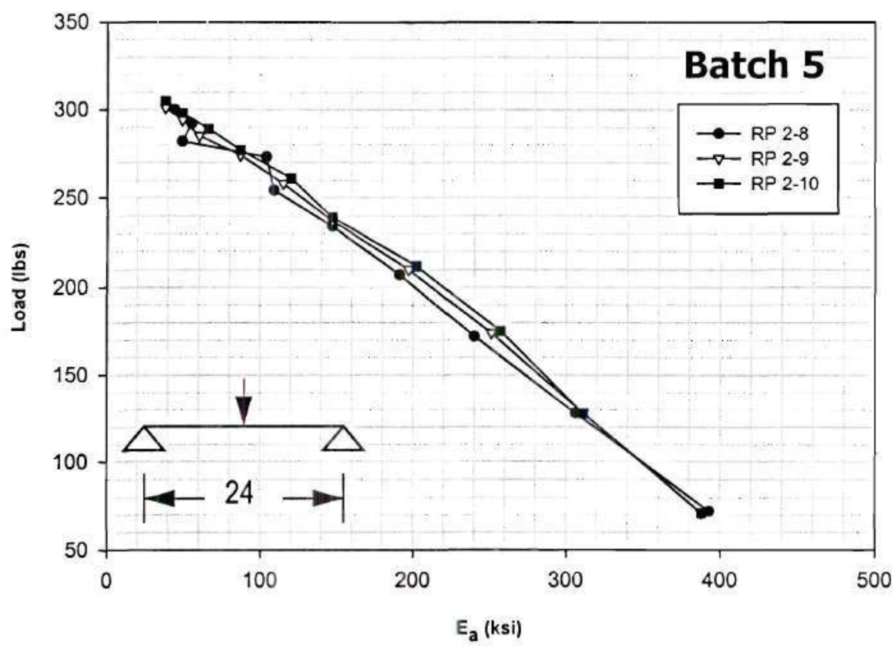

Figure C-4: Load - E_a curves data for batch 5 specimens

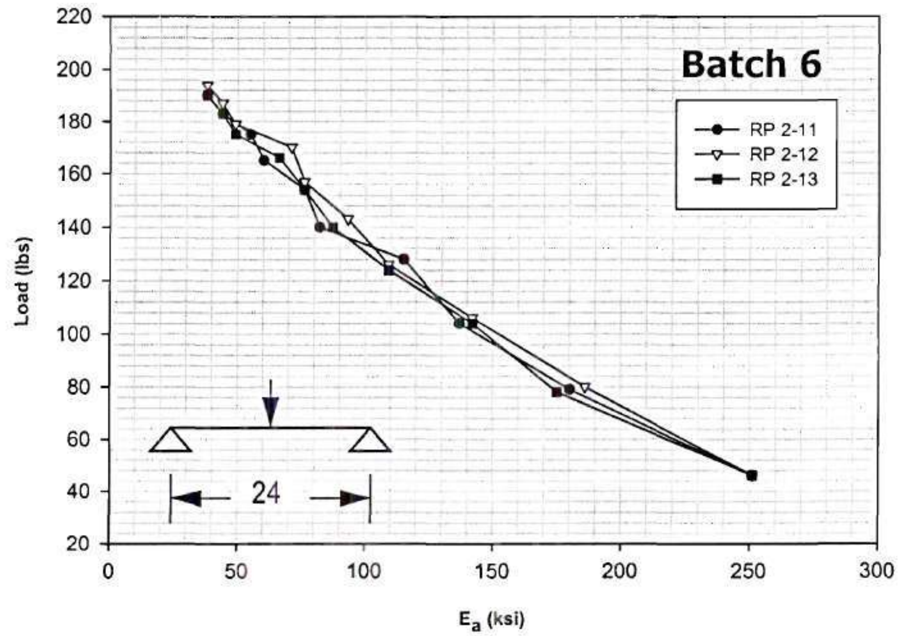

Figure C-5: Load - E_a curves data for batch 6 specimens

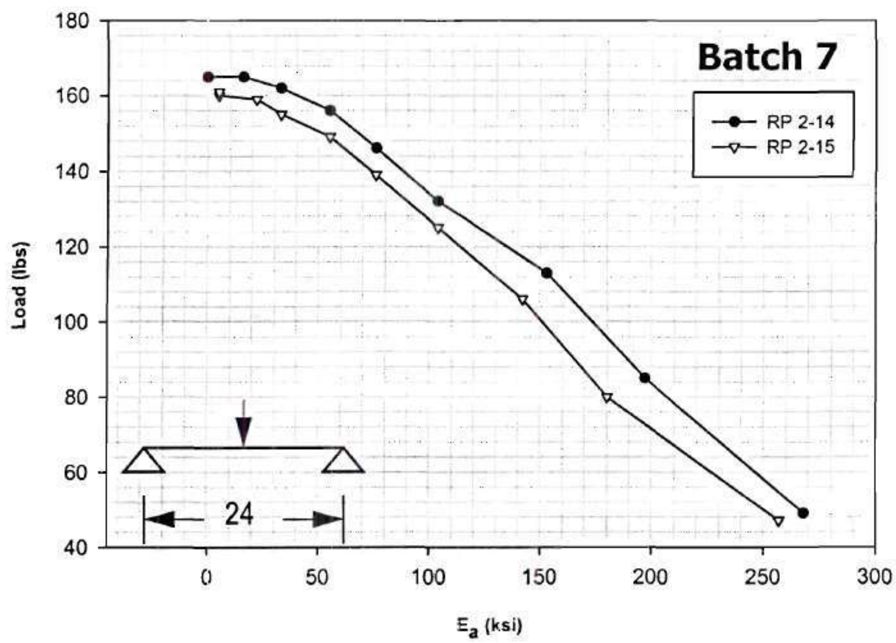

Figure C-6: Load - E_a curves data for batch 7 specimens

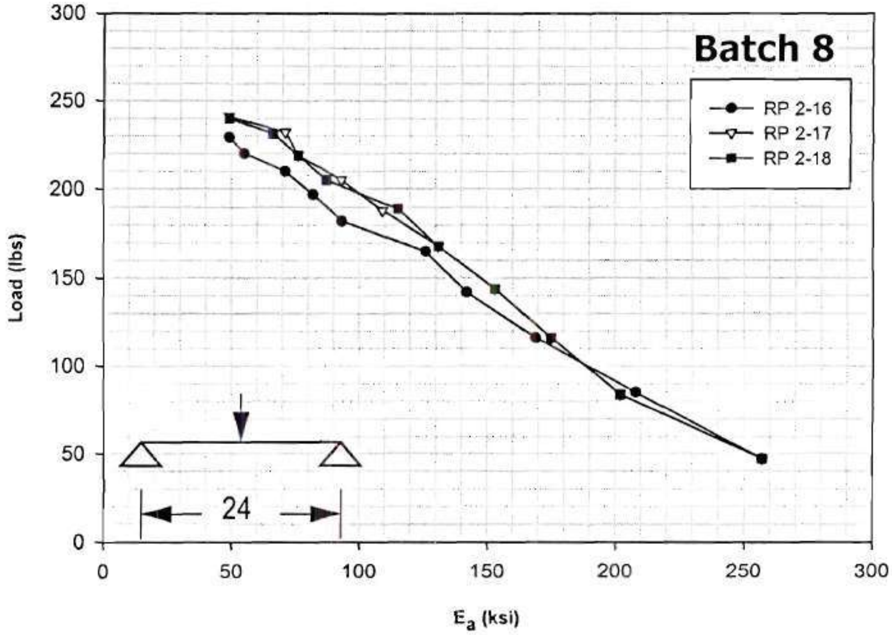

Figure C-7: Load - E_a curves data for batch 8 specimens

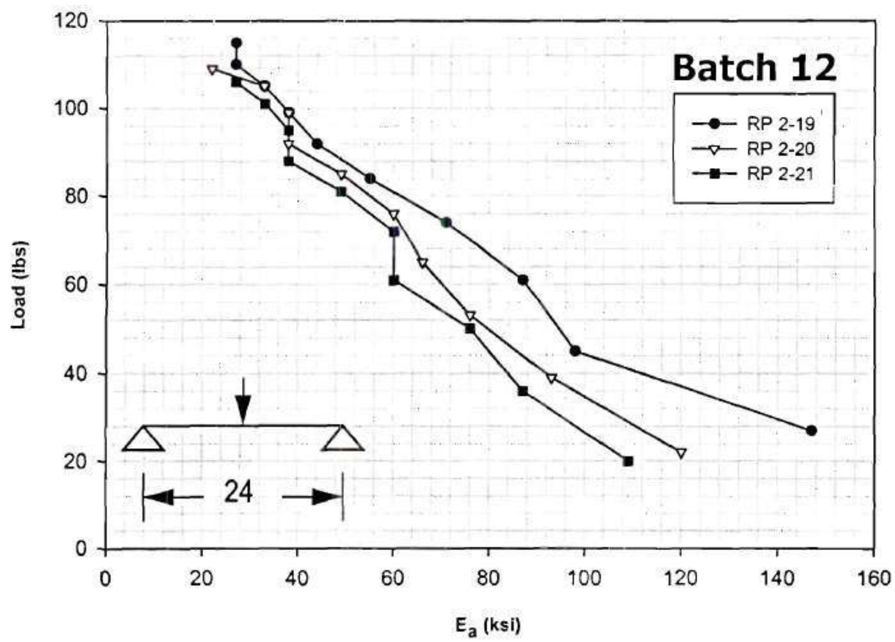

Figure C-8: Load - E_a curves data for batch 12 specimens

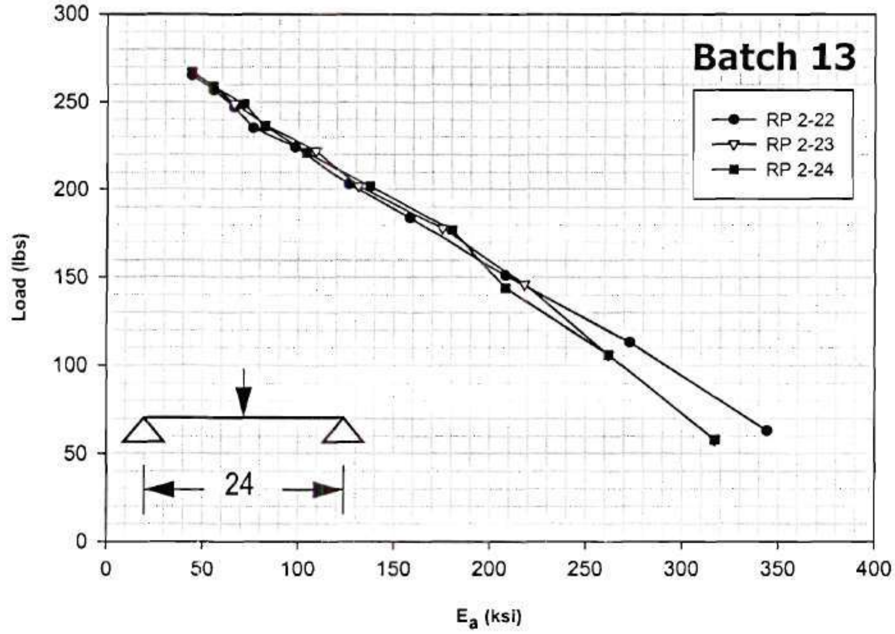

Figure C-9: Load - E_a curves data for batch 13 specimens

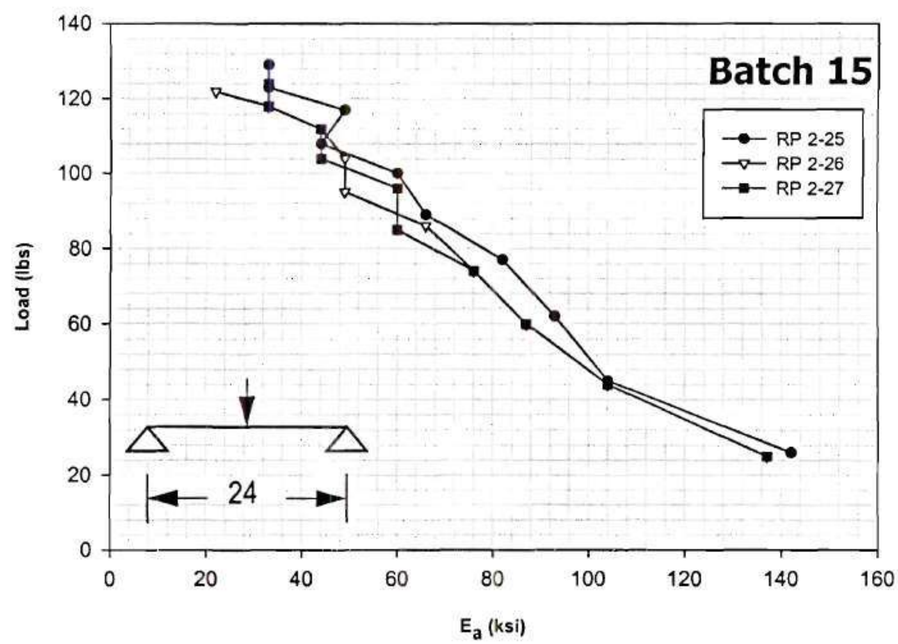

Figure C-10: Load - E_a curves data for batch 15 specimens

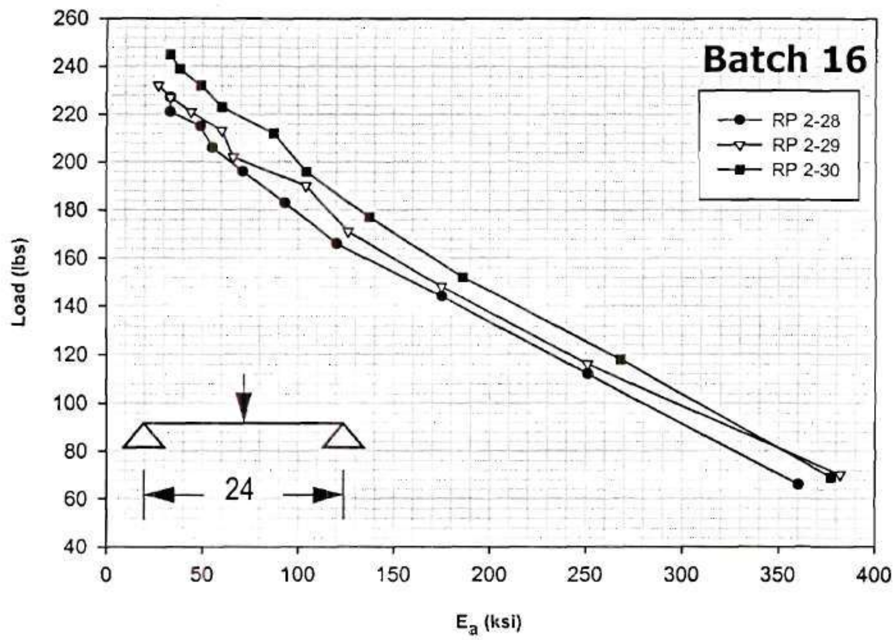

Figure C-11: Load - E_a curves data for batch 16 specimens

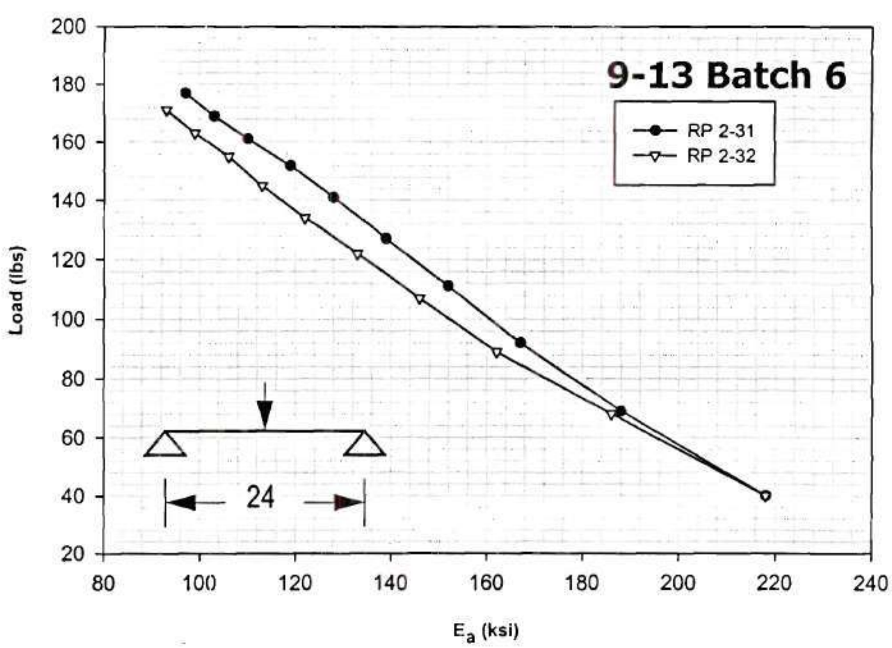

Figure C-12: Load - E_a curves data for 9-13 batch 6 specimens

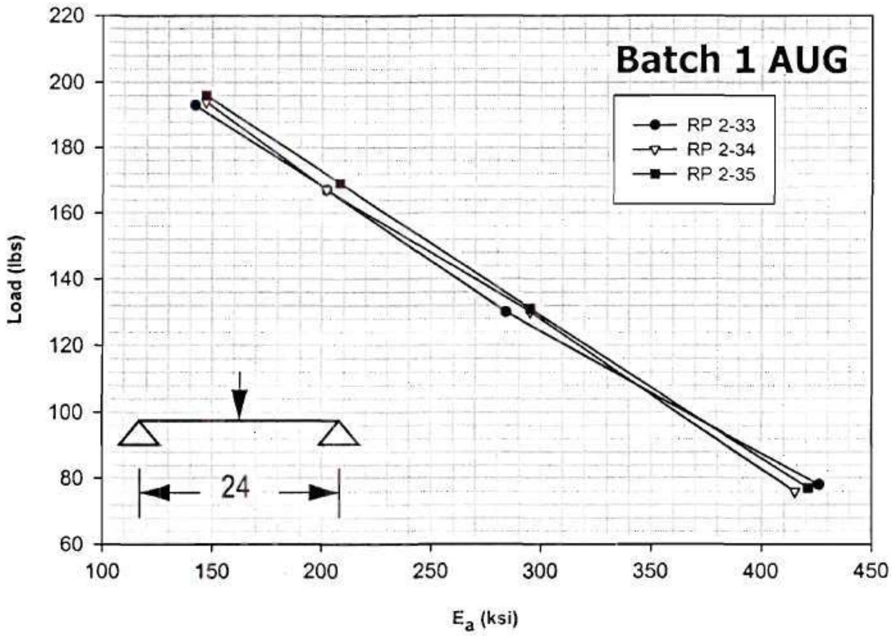

Figure C-13: Load - E_a curves data for batch 1 AUG specimens

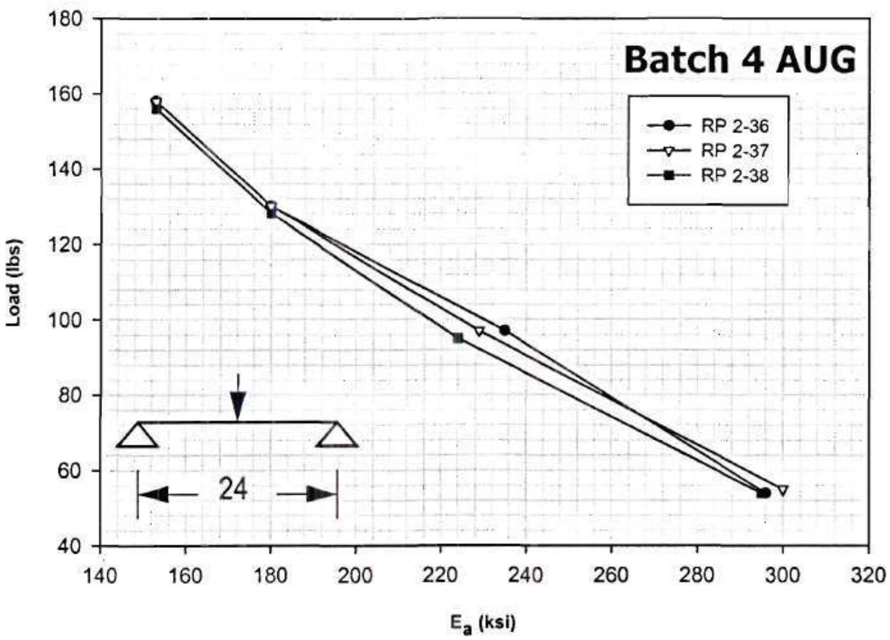

Figure C-14: Load - E_a curves data for batch 4 AUG specimens

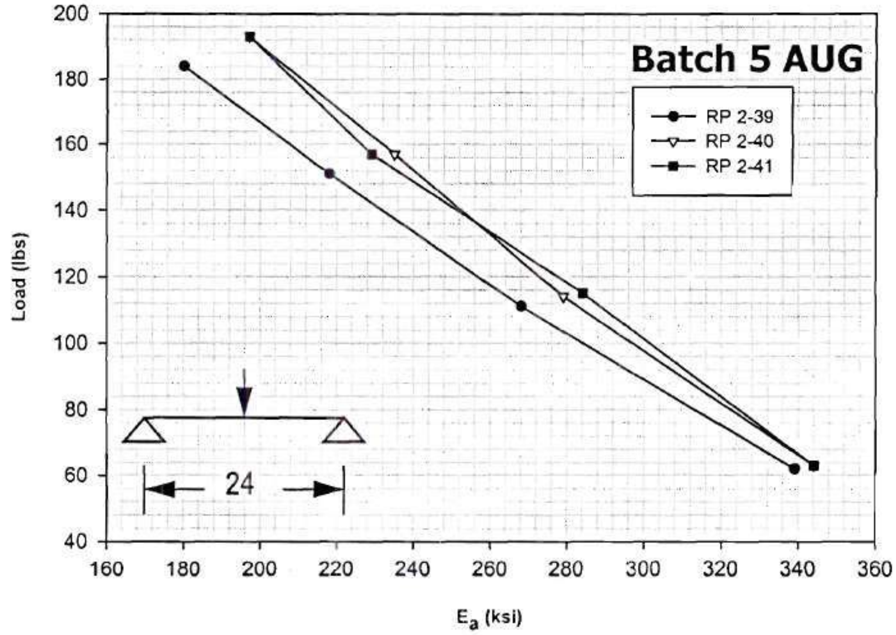

Figure C-15: Load - E_a curves data for batch 5 AUG specimens

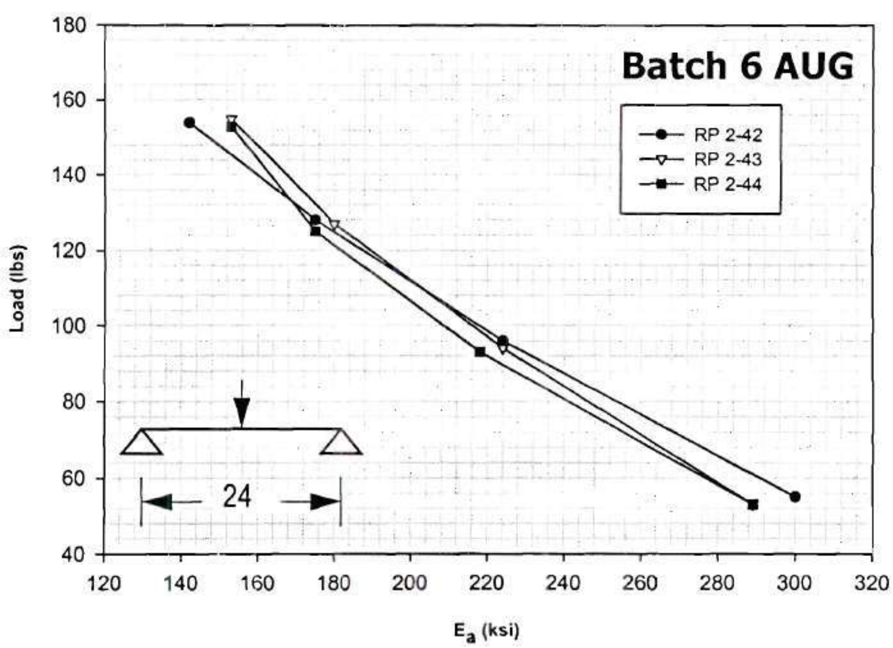

Figure C-16: Load - E_a curves data for batch 6 AUG specimens

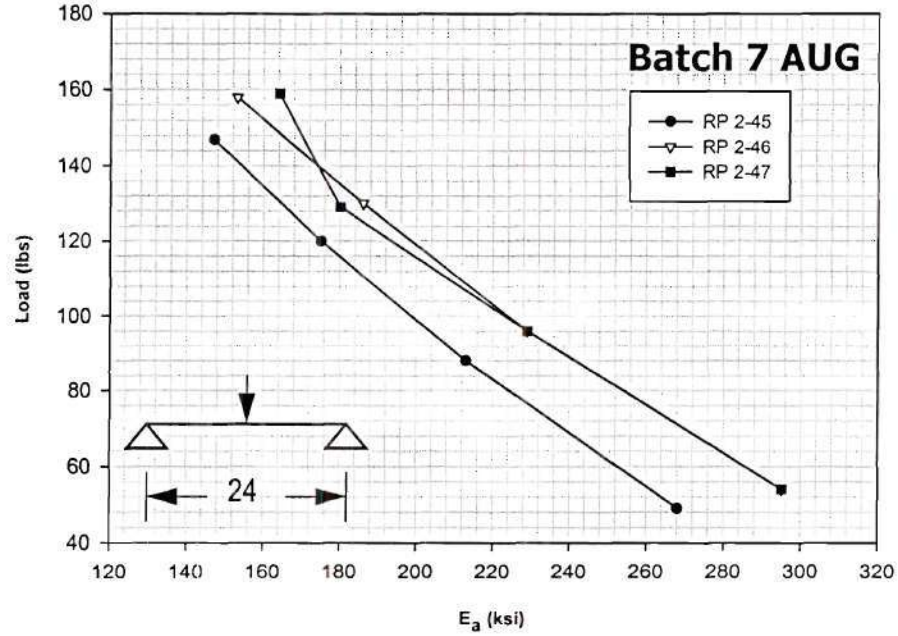

Figure C-17: Load - E_a curves data for batch 7 AUG specimens

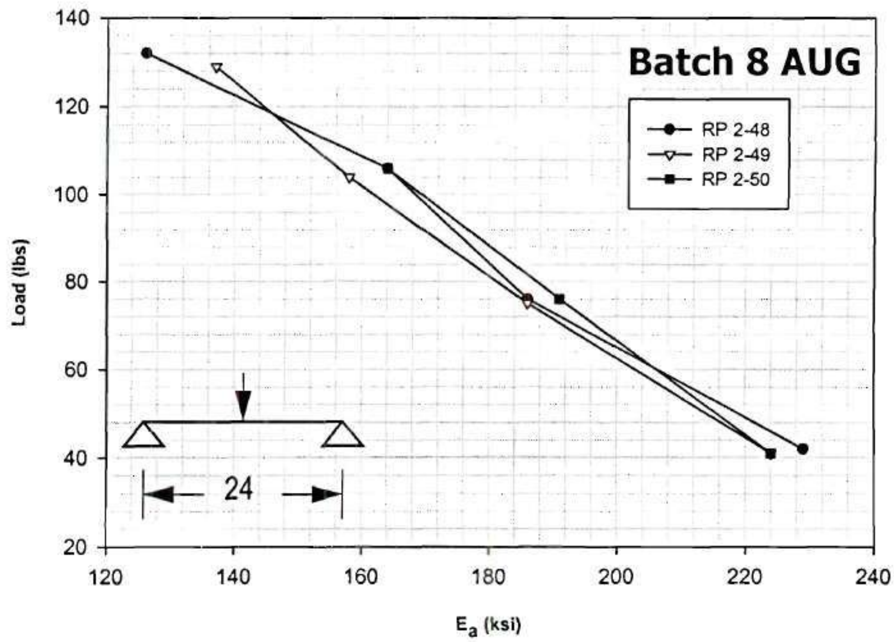

Figure C-18: Load - E_a curves data for batch 8 AUG specimens

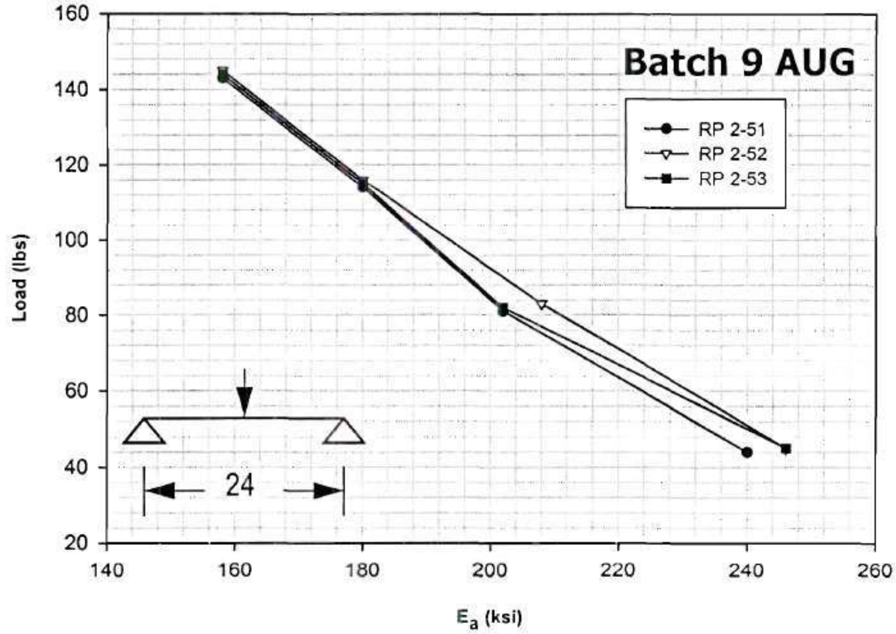

Figure C-19: Load - E_a curves data for batch 9 AUG specimens

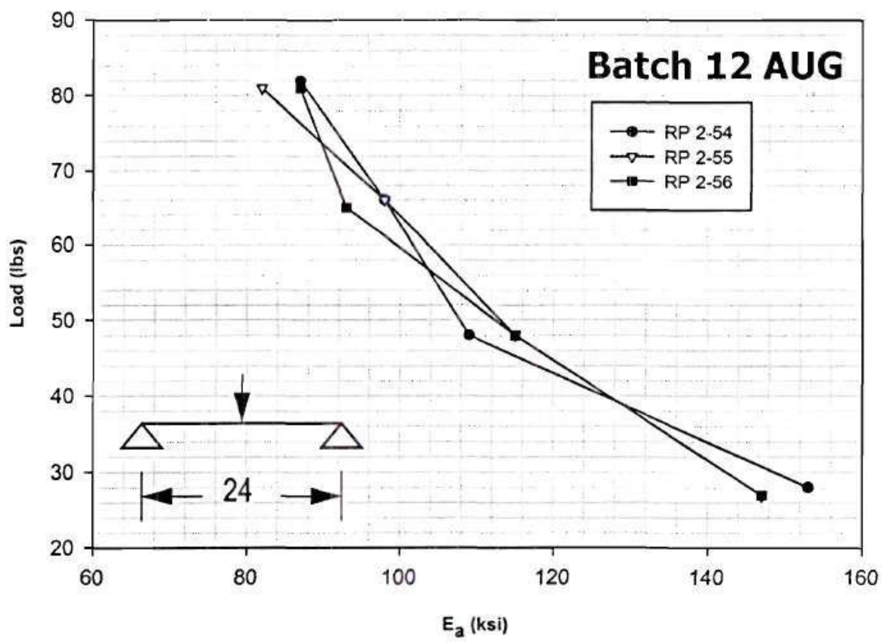

Figure C-20: Load - E_a curves data for batch 12 AUG specimens

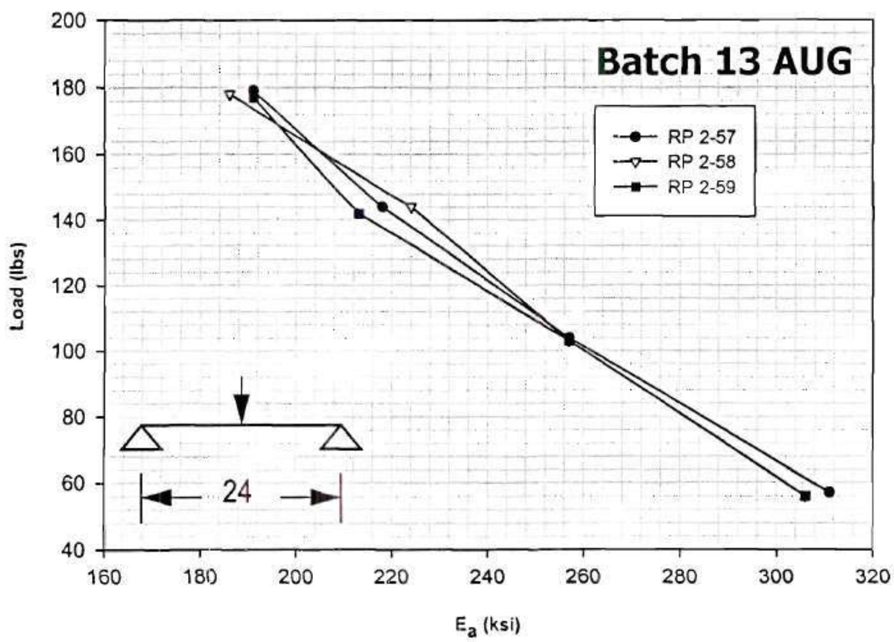

Figure C-21: Load - E_a curves data for batch 13 AUG specimens

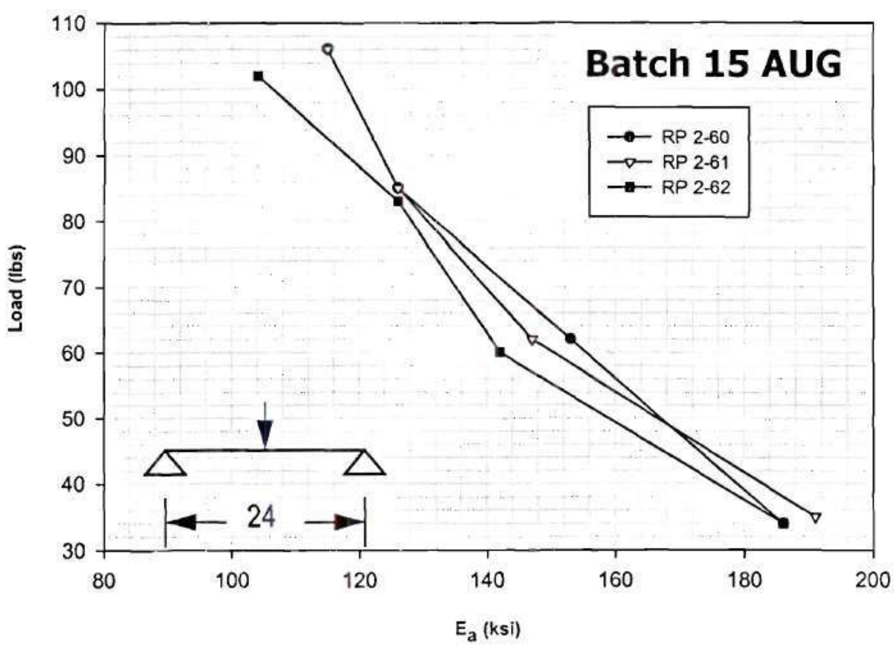

Figure C-22: Load - E_a curves data for batch 15 AUG specimens

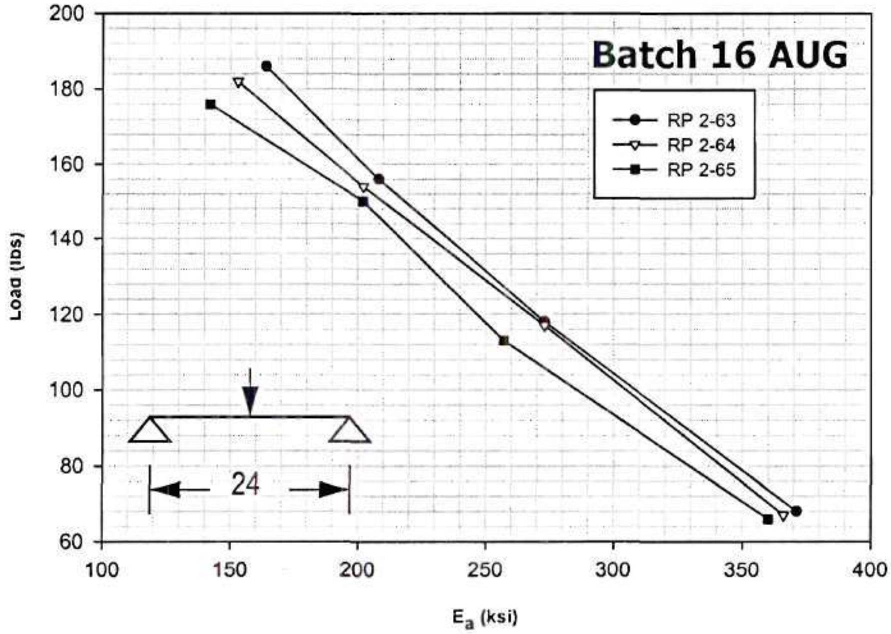

Figure C-23: Load - E_a curves data for batch 16 AUG specimens

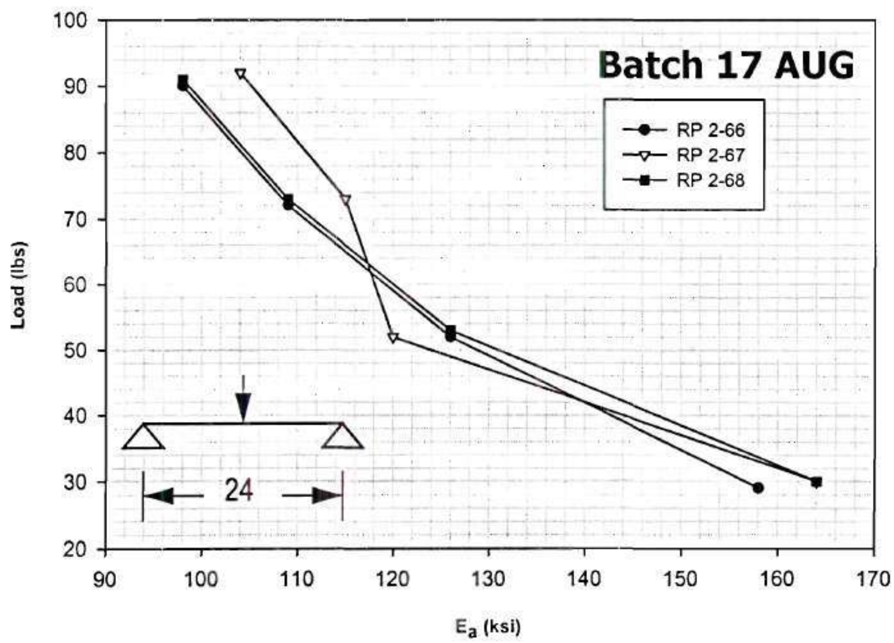

Figure C-24: Load - E_a curves data for batch 17 AUG specimens

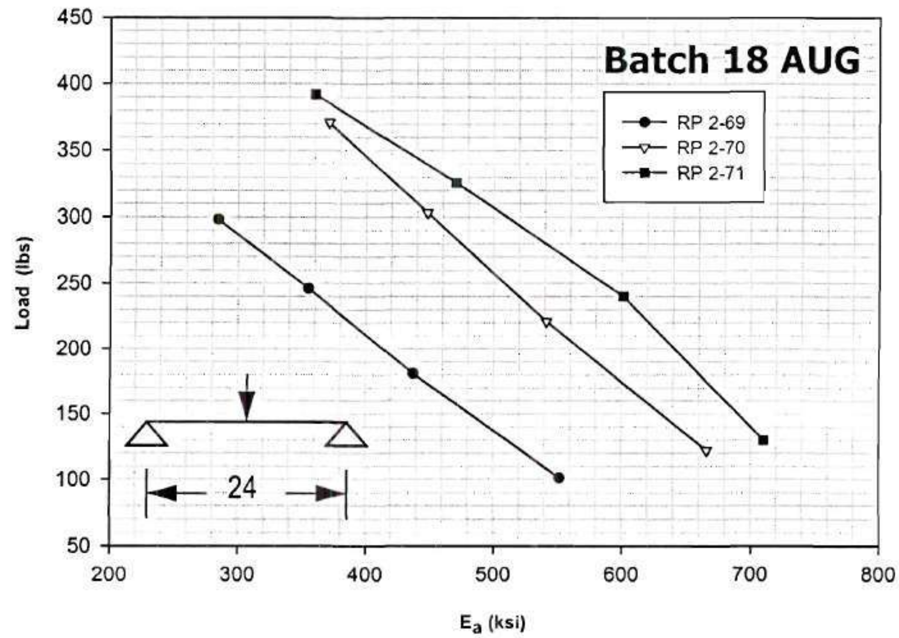

Figure C-25: Load - E_a curves data for batch 18 AUG specimens

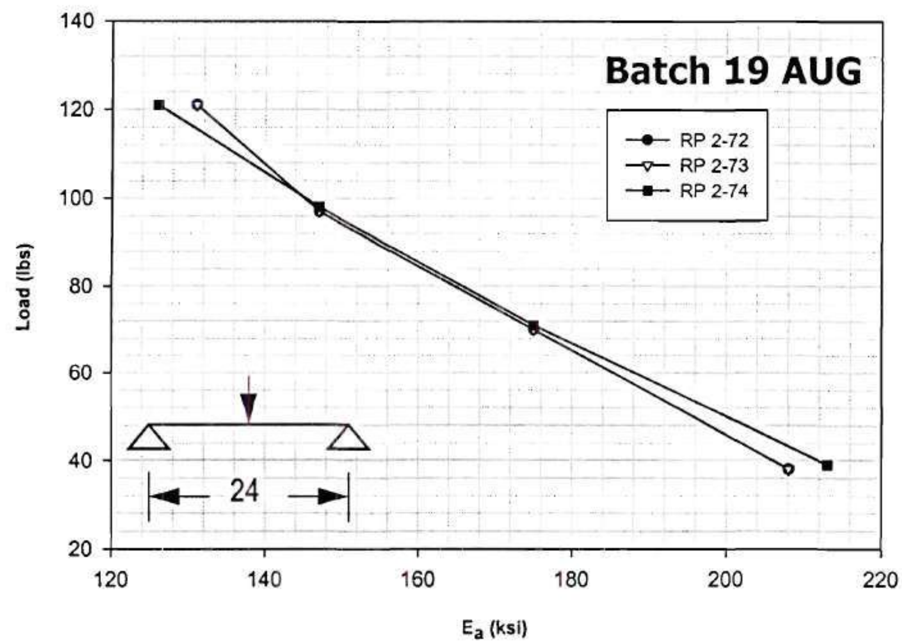

Figure C-26: Load - E_a curves data for batch 19 AUG specimens

REFERENCES

Anonymous. "Ames, Iowa: Tire Chips used to make environmentally safer rail-road ties" BioCycle J.G. Press Inc. December 1995: 20-.

Bonnett, Clifford F. Practrical Railway Engineering, London: Imperial College Press. 1996.

Chopin, D. "Track's wooden workhorse." Railway Track & Strucures August 1983: 33-35.

Davalos, Julio F.; Zipfel, Michael; Qiao, Pizhong. "Feasibility Study of Prototype GFRP-Reinforced Wood Railroad Crosstie." Journal of Composites for ConstructionMay 1999: 92-99.

Eastpoint Company. "Comparative Properties of Plastic Materials, Datasheets for 49 Generic Materials" plasticsusa.com http://www.e-composites.com/commonFiles/matlpropdb.asp (July, 2001).

Gillespie, Barry.; Lutz M.; Nosker T.; Plotkin D. "Development of a Recycled Plastic Composite Crosstie." American Railway Engineering Association (AREA) Bulletin No. 760, May 1997 Volume 78: 181-187.

Lampo, Richard G.; Nosker T.; Renfree R. "Design considerations for the Use of Plastic Lumber in Structural Applications." Materials for the New Millennium 199 , ASCE: 1492-1500.

NARSTCO. "Specification For Railway Steel Ties" specification sheets North American Railway Steel Tie Corporation, 1996.

NATK. North American Technologies Group, Inc. http://www.natk.com/TieTek1.html (April, 2001)

Nosker, Thomas.; Renfree R.; Lutz M.; Gillespie B.; Lampo R.; Van Ness K. E.; Lynch J. "A Performance-Based Approach to the Development of a Recycled Plastic/Composite Crosstie." Confrence Proceedings, April 1998, Proceedings of the 56th Annual Technical Confrence (ANTEC) / Society of Plastic Enfgineers: 2912-2914.

Trus Jois MacMillan®. (1998) "Parallam® PSL Ties and Timbers," Truss joist MacMillan. http://www.tjm.com/PDFFiles/3400.pdf (July 8, 1998).

Profillidis, V. A. Railway Engineering, Great Brittian: Avebury Technical, 1995.

Primix Corporation. "Primix Technical Specifications," Primix Corporation http://www.primixcorp.com/TecSpec.asp (April, 2001).

Roe, Andrew G. "New Materials Tie the Rails." ENR May 1996: 18-.

Sonti, Somnath S.; Davalos, Julio G.; Zipfel, Michael G.; GangRao, Hota V S. "A Review of Wood Crosstie Peformance. " Forest Products Journal September 1995: 55-.

Springfellow. Springfellow Lumber Company LLC http://www.azobe.com/facts.html April, 2001.

TTS. "Tie Specification for Steel Railroad Ties," specification sheets Tie & Track Systems, Inc December 28, 1994.

Zarembski, A. M. "Extending the Life of Wood Crossties." Railway Track & Strucures December 1989: 13-14.